The Dissertation Committee for Joseph Reuben Cook Certifies that this is the approved version of the following dissertation:

Fundamental Water and Ion Transport Characterization of Sulfonated Polysulfone Desalination Materials

Committee:

Benny Freeman, Supervisor

Don Paul

Isaac Sanchez

Mukul Sharma

Sue Mecham

Fundamental Water and Ion Transport Characterization of Sulfonated Polysulfone Desalination Materials

by

Joseph Reuben Cook, B.S. Chemical Engineering

Dissertation

Presented to the Faculty of the Graduate School of

The University of Texas at Austin

in Partial Fulfillment

of the Requirements

for the Degree of

Doctor of Philosophy

The University of Texas at Austin

August 2014

Dedication

For my mother, who taught me to learn.

Acknowledgements

Here at the end of my graduate studies, the phrase “no man is an island” rings particularly true to me, and while I alone will stand to defend the contents of this report, I could have never arrived here on my own. I would like to thank my advisor Dr. Benny Freeman for his guidance and experience, as well as Dr. Don Paul and Dr. James McGrath who were also instrumental in guiding me through this work.

I also owe a debt of gratitude to the members of the Freeman and McGrath research group who have worked with me and aided me during my studies: Dr. Bryan McCloskey, Dr. Ho Bum Park, Dr. Chang Hyun Lee, Dr. Kwansoo Lee, Dr. Dan Miller, Dr. Wei Xie, Dr. Hao Ju, Dr. Geoff Geise, Dr. Katrina Czencusch, Dr. Zach Smith, Hee Jeung Oh, Peach Kasemset, Ni Yan, Jovan Kamcev, Eui Seong Jang, and Ben Sundel. I would also like to thank the Freeman research group as a whole for the atmosphere of teamwork that they have fostered.

I would finally like to thank my family, friends, and church family for supporting me during this time. I couldn’t have done it without you.

Fundamental Water and Ion Transport Characterization of Sulfonated Polysulfone Desalination Materials

Joseph Reuben Cook, Ph.D.

The University of Texas at Austin, 2014

Supervisor: Benny Freeman

Sulfonated polysulfones BisAS and BPS were fabricated into dense polymer films, and their water and ion transport properties were systematically characterized. Fundamental NaCl and water transport properties were correlated with polymer chemistry, and water and NaCl permeability were found to increase with degree of sulfonation due to the increasing polymer water content. The BisAS backbone structure was found to result in greater water uptake, increasing water and salt permeability, though the polysulfones show evidence of sensitivity to the thermal casting process as well. Additionally, water and ion permeability and sorption values were determined for select polymers when exposed to a feed consisting of mixtures of monovalent and divalent cation salts. The divalent cations were found to sorb into the polymer much more favorably than the monovalent sodium, similarly to charged materials found in the literature. The sodium permeability of sulfonated polysulfones was found to increase in the presence of divalent cations by ratios of 2 to 5 times more than when exposed to an equivalent increase in feed charge concentration of monovalent cations. It has been hypothesized the more strongly charged divalent cations are neutralizing the sulfonate charges and suppressing Donnan exclusionary effects that reduce salt transport in charged polymers.

Table of Contents

List of Tables

List of Figures

1. Introduction.

THE GLOBAL WATER CHALLENGE

Availability of clean water is one of the greatest challenges facing the world in the 21st century. Currently, over one billion people live without access to clean drinking water, and 2.3 billion people live in areas that are water-stressed.[1] The rate of increasing water usage outstrips global population growth; between 1900 and 2000, the world population increased roughly four times, while water usage by volume increased roughly seven times.[2] Additionally, the use of water by industry and agriculture has increased dramatically and induced water stress in countries with rapidly developing economies, such as China.[2,3] As surface water availability is finite, desalination processes are increasingly being used to satisfy water demand.

DESALINATION TECHNOLOGY

The first widespread industrial water desalination technologies were based on thermal evaporation, and multi-stage flash distillation is still used in Middle Eastern countries due to the high salinity and temperature of the naturally available feed water, as well as the low cost of energy in this region.[4] However, thermal evaporation remains an energy intensive and expensive process that must usually be coupled with power generation to offset its energy consumption, limiting its use in most regions as a water purification process.[4] Reverse osmosis (RO) membranes are a widely used and efficient desalination method,[5–9] and current RO membranes typically employ crosslinked aromatic polyamides as the separation layer.[7–12] While these materials have commercially advantageous water flux and salt rejection properties,[6,7,10] they are prone to degradation by strongly oxidizing agents such as aqueous chlorine.[8,9,13,14] Chlorine containing compounds, such as sodium hypochlorite (NaOCl), are often used as disinfecting agents

in water purification systems to inhibit microbial growth that can lead to membrane biofouling.[13–15] Typically, the feed water to a desalination plant is first chlorinated to control biological activity, then dechlorinated to protect the RO membranes, desalinated, and finally rechlorinated prior to distribution.[15]

SULFONATED POLYSULFONES FOR DESALINATION

Polysulfones have been proposed as potential desalination materials,[11,13,14,16–20] in part because they are more chlorine tolerant than current polyamide membranes.[11,13,14,18,21] Aromatic polysulfones are generally hydrophobic materials that can be modified with charged moieties, such as sulfonate groups, to introduce hydrophilicity and control water and salt transport.[13,14,16–32] Sulfonate groups may be incorporated into the backbone of polysulfone either prior to or following polymerization; desalination properties of polysulfone materials sulfonated by both routes have been reported.[13,18–28] Sulfonated polysulfones prepared by randomly copolymerizing sulfonated and non-sulfonated polysulfone monomers[19,23,29–32] eliminate some undesirable side reactions that occur in the post-polymerization sulfonation process and generally allow more precise control of the degree of sulfonation than in post-polymerization sulfonated materials.[29–32]

Previously, sulfonated polysulfone materials synthesized from sulfonated monomers were prepared with a backbone containing biphenyl moieties, referred to as BPS-X (cf., Figure 1.A), and their water and salt transport properties have been reported.[13,19,22,23] To investigate the effect of backbone structure on water and salt transport properties, sulfonated polysulfones based on bisphenol A,[31] referred to as BisAS-X, are considered in this study.

One challenge presented by charged polymers is the dependence of their properties on the ionic composition of the solutions surrounding the polymer.[18,19,21,33–36] Because these polymers contain charged moieties bound to the polymer backbone, they are subject to effects, such as Donnan partitioning, that non-charged materials are not.[34–40] Furthermore, the greater ionic affinity between sulfonate groups and divalent cations, such as Mg^{++} and Ca^{++}, than monovalent Na^{+} has demonstrated a charge shielding effect, where the strong ion pairing decrease the effective charge density of the membrane, thus allowing greater monovalent salt passage.[9,18,21,35,39–41] Previous studies of sorption equilibria of mixtures of ions in negatively charged polymers have generally found more favorable sorption for divalent cations such as calcium than monovalent cations.[42–46] Consequently, the presence of divalent cations, such as calcium, in a largely sodium chloride feed results in higher passage of sodium chloride through negatively charged materials.[18,21] The presence of calcium and other divalent cations in seawater and other desalination feed sources[47–49] makes development of a thorough understanding of this effect of increasing salt passage in sulfonated polysulfones an important goal.

DISSERTATION OBJECTIVES AND ORGANIZATION

The motivation for this work is driven by both industrial and public health concerns; however to further improve the technology of productive membranes, it is necessary to perform fundamental material characterization on novel polymers. As discussed above, polyamide RO membranes are widely employed to address the water supply challenge, though they suffer from chlorine sensitivity. Thus it is one goal of this project to develop fundamental water and salt transport properties of chlorine resistant materials, in this case sulfonated polysulfones. Furthermore, this dissertation aims to characterize the effects that divalent cations have on the transport properties of negatively

charged polymers considered for desalination membranes, phenomena that have not been sufficiently explored in the literature.

The dissertation consists of seven chapters and one appendix, Chapter 1 being this introduction. Chapter 2 provides background information on relevant polymer transport phenomena to guide the reader. Chapter 3 details the materials and experimental methods used in this work. The results of the experimentation in pursuit of the goals outlined above are discussed in Chapters 4 through 6. Chapter 4 presents the fundamental water and salt (NaCl) transport properties in a novel sulfonated polysulfone as a function of variations of the polymer chemistry and compares these results to another previously characterized polysulfone to examine the effect of backbone structure on polymer transport properties. With basic transport properties having been developed, Chapter 5 examines the permeability properties of these two families of sulfonated polysulfones with desalination feeds consisting of aqueous mixtures of NaCl and divalent cation salts. Chapter 6 expands upon the knowledge of the polysulfone permeability properties in a mixed ionic environment with the development of the sorption and diffusion properties of sulfonated polysulfone in mixed ionic environments. Finally, Appendix A details the results of further mixed ion experiments performed on mixtures of NaCl with other species of monovalent cation salts, and Appendix B reports data comparisons between two salt permeability testing methods.

REFERENCES

1. R.F. Service. Desalination freshens up. *Science*. 313 (2006) 1099–1090.

2. K. Watkins, L. Carvajal, D. Coppard, R. Fuentes. *Human development report 2006*. Prepared for the United Nations Development Programme, New York, 2006.

3. X. Cai. Water stress, water transfer and social equity in northern China—implications for policy reforms. *Journal of Environmental Management*. 87 (2008) 14–25.

4. R. Borsani, S. Rebagliati. Fundamentals and costing of MSF desalination plants and comparison with other technologies. *Desalination*. 182 (2005) 29–37.

5. A. Burbano. The state of full-scale RO/NF desalination: Results from a worldwide survey. *Journal - American Waterworks Association*. 99 (2007) 116.

6. L.F. Greenlee, D.F. Lawler, B.D. Freeman, B. Marrot, P. Moulin. Reverse osmosis desalination: water sources, technology, and today's challenges. *Water Research*. 43 (2009) 2317–48.

7. G.M. Geise, H.-S. Lee, D.J. Miller, B.D. Freeman, J.E. McGrath, D.R. Paul. Water purification by membranes: the role of polymer science. *Journal of Polymer Science Part B: Polymer Physics*. 48 (2010) 1685–1718.

8. C. Fritzmann, J. Löwenberg, T. Wintgens, T. Melin. State-of-the-art of reverse osmosis desalination. *Desalination*. 216 (2007) 1–76.

9. K.P. Lee, T.C. Arnot, D. Mattia. A review of reverse osmosis membrane materials for desalination—Development to date and future potential. *Journal of Membrane Science*. 370 (2011) 1–22.

10. J.E. Cadotte. Interfacially synthesized reverse osmosis membrane. U.S. Patent Number 4,277,344. 1981.

11. R.J. Petersen. Composite reverse osmosis and nanofiltration membranes. *Journal of Membrane Science*. 83 (1993) 81–150.

12. D. Li, H. Wang. Recent developments in reverse osmosis desalination membranes. *Journal of Materials Chemistry*. 20 (2010) 4551–4566.

13. H.B. Park, B.D. Freeman, Z.-B. Zhang, M. Sankir, J.E. McGrath. Highly chlorine-tolerant polymers for desalination. *Angewandte Chemie (International Ed in English)*. 47 (2008) 6019–6024.

14. J. Glater, S.K. Hong, M. Elimelech. The search for a chlorine-resistant reverse osmosis membrane. *Desalination*. 95 (1994) 325–345.

15. S.P. Nunes, K. V. Peinemann, eds. *Membrane Technology in the Chemical Industry*. Wiley-VCH, Weinheim, 2006.

16. A. Noshay, L. Robeson. Sulfonated polysulfone. *Journal of Applied Polymer Science*. 20 (1976) 1885–1903.

17. C. Brousse, R. Chapurlat, J.P. Quentin. New membranes for reverse osmosis I. Characteristics of the base polymer: sulphonated polysulphones. *Desalination*. 18 (1976) 137–153.

18. P.L. Parise, A.E. Allegrezza Jr., B.S. Parekh. Reverse osmosis: Chlorine-resistant polysulfone reverse osmosis membrane and module. *Ultrapure Water*. (1987) 54–65.

19. W. Xie, J. Cook, H.B. Park, B.D. Freeman, C.H. Lee, J.E. McGrath. Fundamental salt and water transport properties in directly copolymerized disulfonated poly(arylene ether sulfone) random copolymers. *Polymer*. 52 (2011) 2032–2043.

20. M. Padaki, A.M. Isloor, P. Wanichapichart, A.F. Ismail. Preparation and characterization of sulfonated polysulfone and N-phthloyl chitosan blend composite cation-exchange membrane for desalination. *Desalination*. 298 (2012) 42–48.

21. A.E. Allegrezza Jr., B.S. Parekh, P.L. Parise, E.J. Swiniarski, J.L. White. Chlorine resistant polysulfone reverse osmosis modules. *Desalination*. 64 (1987) 285–304.

22. W. Xie, G.M. Geise, B.D. Freeman, C.H. Lee, J.E. McGrath. Influence of processing history on water and salt transport properties of disulfonated polysulfone random copolymers. *Polymer*. 53 (2012) 1581–1592.

23. C.H. Lee, D. VanHouten, O. Lane, J.E. McGrath, J. Hou, L.A. Madsen, J. Spano, S. Wi, J. Cook, W. Xie, H.J. Oh, G.M. Geise, B.D. Freeman. Disulfonated poly(arylene ether sulfone) random copolymer blends tuned for rapid water permeation via cation complexation with poly(ethylene glycol) oligomers. *Chemistry of Materials*. 23 (2011) 1039–1049.

24. S.G. Kimura. Reverse osmosis performance of sulfonated poly(2,6-dimethylphenylene ether) ion exchange membranes. *Industrial & Engineering Chemistry Product Research and Development*. 10 (1971) 335–339.

25. C. Friedrich, A. Driancourt, C. Noel, L. Monnerie. Asymmetric reverse osmosis and ultrafiltration membranes prepared from sulfonated polysulfone. *Desalination*. 36 (1981) 39–62.

26. J. Quentin. Sulfonated polyarylethersulfones. U.S. Patent Number 3,709,841. 1973.

27. A.F. Graefe, C.W. Saltonstall, W.J. Schell. Process for the preparation of a stable salt form of a sulfonated polyarylether sulfone. U.S. Patent Number 3,875,096. 1975.

28. A. Hamza, G. Chowdhury, T. Matsuura, S. Sourirajan. Sulphonated poly(2,6-dimethyl-1,4-phenylene oxide)-polyethersulphone composite membranes. Effects of composition of solvent system, used for preparing casting solution, on membrane-surface structure and reverse-osmosis performance. *Journal of Membrane Science*. 129 (1997) 55–64.

29. F. Wang, M. Hickner, Y.S. Kim, T.A. Zawodzinski, J.E. McGrath. Direct polymerization of sulfonated poly(arylene ether sulfone) random (statistical) copolymers: candidates for new proton exchange membranes. *Journal of Membrane Science*. 197 (2002) 231–242.

30. M.A. Hickner, H. Ghassemi, Y.S. Kim, B.R. Einsla, J.E. McGrath. Alternative polymer systems for proton exchange membranes (PEMs). *Chemical Reviews*. 104 (2004) 4587–4612.

31. W.L. Harrison, F. Wang, J.B. Mecham, V.A. Bhanu, M. Hill, Y.S. Kim, J.E. McGrath. Influence of the bisphenol structure on the direct synthesis of sulfonated poly(arylene ether) copolymers. I. *Journal of Polymer Science Part A: Polymer Chemistry*. 41 (2003) 2264–2276.

32. T. E. Long, Y. Li, F. Wang, J. Yang, D. Liu, A. Roy, S. Case, J. Lesko, J.E. McGrath. Synthesis and characterization of controlled molecular weight disulfonated poly(arylene ether sulfone) copolymers and their applications to proton exchange membranes. *Polymer*. 47 (2006) 4210–4217.

33. G.M. Geise, B.D. Freeman, D.R. Paul. Characterization of a sulfonated pentablock copolymer for desalination applications. *Polymer*. 51 (2010) 5815–5822.

34. G.M. Geise, L.P. Falcon, B.D. Freeman, D.R. Paul. Sodium chloride sorption in sulfonated polymers for membrane applications. *Journal of Membrane Science*. 423-424 (2012) 195–208.

35. G. Geise, B. Freeman, D. Paul. Comparison of the permeation of $MgCl_2$ versus NaCl in highly-charged sulfonated polymer membranes, in: I.C. Escobar, B. Van der Bruggen (Eds.), *Modern Applications in Membrane Science*. American Chemical Society, 2011: pp. 239–245.

36. E. Glueckauf. A new approach to ion exchange polymers. *Proceedings of the Royal Society A: Mathematical, Physical and Engineering Sciences*. 268 (1962) 350–370.

37. F.G. Donnan. The theory of membrane equilibria. *Chemical Reviews*. 1 (1924) 73–90.

38. F.G. Donnan. Theory of membrane equilibria and membrane potentials in the presence of non-dialysing electrolytes. A contribution to physical-chemical physiology. *Journal of Membrane Science*. 100 (1995) 45–55.

39. G. Geise, C. Willis, C. Doherty, A.J. Hill, T.J. Bastow, J. Ford, K.I. Winey, B.D. Freeman, D.R. Paul. Characterization of aluminum-neutralized sulfonated styrenic pentablock copolymer films. *Industrial & Engineering Chemistry Research*. 52 (2012) 1056–1068.

40. F. Helfferich. *Ion exchange*. Dover Publications, New York, 1962.

41. K.K. Pushpa, D. Nandan, R.M. Iyer. Thermodynamics of water sorption by perfluorosulphonate (Nafion-117) and polystyrene-divinylbenzene sulphonate (Dowex 50W) ion-exchange resins at 298±1 K. *Journal of the Chemical Society, Faraday Transactions 1: Physical Chemistry in Condensed Phases*. 84 (1988) 2047–2056.

42. M. Higa, A. Kira, A. Tanioka, K. Miyasaka. Ionic partition equilibrium in a charged membrane immersed in a mixed ionic solution. *Journal of the Chemical Society, Faraday Transactions*. 89 (1993) 3433–3435.

43. O.D. Bonner, L.L. Smith. A selectivity scale for some divalent cations on Dowex 50. *The Journal of Physical Chemistry*. 61 (1957) 326–329.

44. K.R. Franklin, R.P. Townsend. Multicomponent ion exchange in zeolites. *Journal of the Chemical Society, Faraday Transactions 1: Physical Chemistry in Condensed Phases*. 81 (1985) 1071–1086.

45. P.N. Pintauro, R. Tandon, L. Chao, W. Xu, R. Evilia. Equilbrium partitioning of monovalent/divalent cation-salt mixtures in Nafion cation-exchange membranes. *Journal of Physical Chemistry*. 99 (1995) 12915–12924.

46. R. Tandon, P.N. Pintauro. Divalent / monovalent cation uptake selectivity in a Nation cation-exchange membrane : Experimental and modeling studies. *Journal of Membrane Science*. 136 (1997) 207–219.

47. W.-Y. Shih, A. Rahardianto, R.-W. Lee, Y. Cohen. Morphometric characterization of calcium sulfate dihydrate (gypsum) scale on reverse osmosis membranes. *Journal of Membrane Science*. 252 (2005) 253–263.

48. *Analysis of water from four wells at the Brackish Groundwater National Desalination Research Facility*. Tetra Tech, Inc. for the Bureau of Reclamation, Alamogordo, Contract No. R10PC40009, 2011.

49. K.K. Turekian. *Oceans*. First Ed. Prentice Hall, Englewood Cliffs, 1968.

2. Background

THE SOLUTION-DIFFUSION MODEL

The transport of solutes through nonporous polymer membranes and films is governed by the solution-diffusion model, which states that solutes transport through a polymer membrane by first dissolving into membrane phase, diffusing through the polymer molecular structure, then desorbing from the downstream face of the membrane.[1,2] Figure 2.1 shows a diagram of the various transport gradients present in a typical RO process, where a pressurized salt water feed is in contact with the membrane, and salt and water transport across the membrane from the high salt concentration feed to the low salt concentration permeate. The hydrostatic pressure (p) through the membrane is equal to the feed pressure.[1–3] The higher feed pressure develops a water concentration (C_W) gradient across the membrane which drives the transport of water, while the salt transport is driven by the salt concentration (C_S) difference between the feed and the permeate.[1–3]

According to the solution diffusion model, the permeability (P) of a solute in the polymer material is dependent upon the partition coefficient (K), and the diffusion coefficient (D):[1,2]

$$P = D \cdot K \tag{2.1}$$

The use of permeability coefficients to calculate commercially valuable properties such as flux and rejection will be discussed in Chapter 3; generally, if all other variables are fixed, increased solute permeability will result in increased flux of that solute.

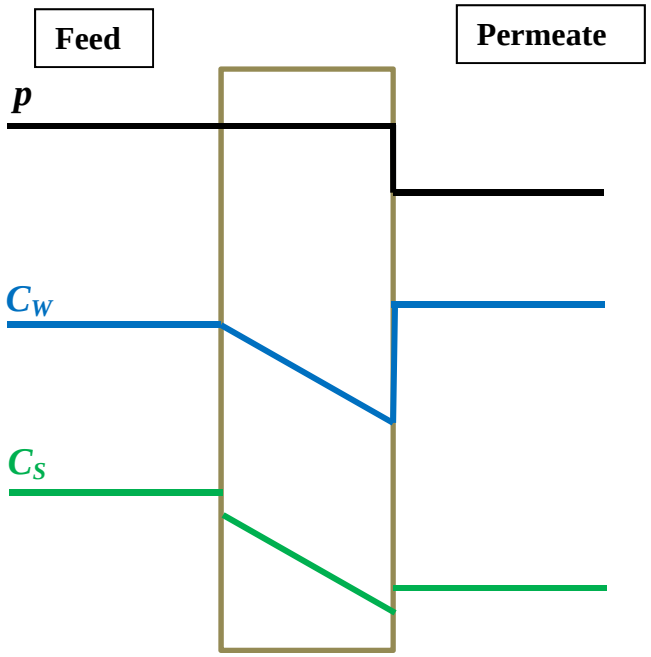

Figure 2.1. Pressure (p), water concentration (C_W) and salt concentration (C_S) across a reverse osmosis membrane.

FREE VOLUME THEORY

In previously studied desalination materials, a tradeoff between water permeability and water/salt permeability selectivity has been observed, as shown in Figure 2.2.[4–10] Similar tradeoff relationships can be found between diffusivity and diffusivity selectivity, and solubility and solubility selectivity. [4–10] From the free volume theory model presented by Yasuda et al.,[11] the free volume in a hydrated polymer is proportional to the water partition coefficient. This trend is obeyed in the BPS system, where increases in free volume element size, as determined by positron annihilation lifetime spectroscopy (PALS),[12] occur as water partition coefficient increases. In both charged materials, such as the BPS series,[4] and uncharged materials, such as poly

(ethylene glycol) (PEG) based hydrogels,[9] both water and salt solubility and diffusivity generally increase as water uptake increases. However, since hydrated sodium and chloride ions are larger than water molecules, they receive greater benefit from increased free volume, so salt permeability increases more with increasing water uptake than water permeability, driving down the water/salt selectivity and thus decreasing salt rejection.[4,13] Yasuda et al. proposed a free-volume based model relating salt diffusivity and water partition coefficient:[11]

$$\ln D_S = \ln D_0 - B\left(\frac{1}{K_W} - 1\right) \tag{2.3}$$

where D_0 is the salt diffusivity in water, K_W is the water partition coefficient, and B is an adjustable parameter dependent on the characteristic volume required for a solute to transport through the polymer.

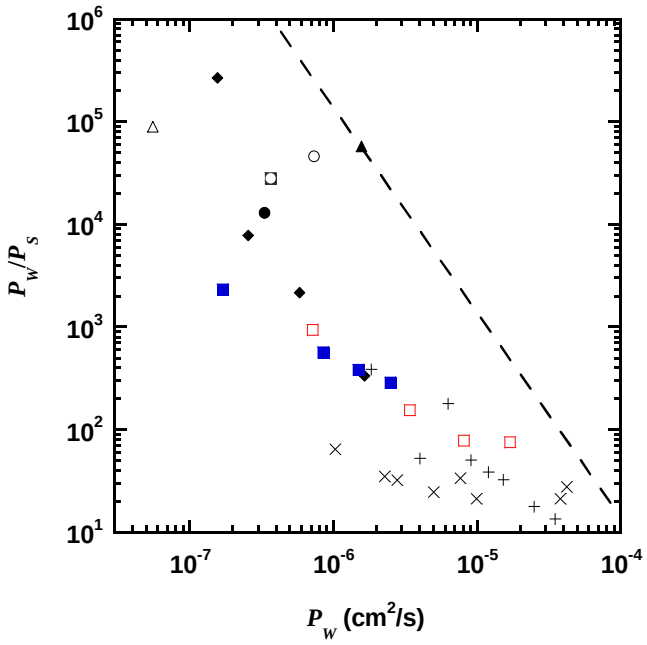

Figure 2.2. Water/NaCl permeability selectivity tradeoff. (■) = BPS,[4] (□) = BPSH,[4] (●) = Aromatic Polyamide,[5] (△) = Polyimide,[5] (◣) = PAH, [5] (◪) = BPS materials from the literature,[6,7] (+) = Cellulose Acetate,[8] (▲) = PBP,[5] (×) = PEG,[9] (○) = Aromatic Polyamide.[10] The dashed line represents the tradeoff upper bound from the literature.[7] Subscript "W" indicates water, and subscript "S" indicates salt, which was NaCl in this case.

MEMBRANE CHARGE EFFECTS ON WATER AND SALT TRANSPORT

In charged materials, salt sorption and transport can also be influenced by Donnan partitioning.[14–18] In polymers with covalently bound anionic groups (e.g., sulfonate groups in the case of the BPS and BisA materials), these charged groups limit the sorption of free anions from the feed solution, which can limit overall salt transport.[14,15,17] For NaCl partitioning between an aqueous solution and a polymer according to Donnan, the presence of an anionic species bound to a polymer backbone leads to an equilibrium

concentration balance of mobile ions between the polymer phase (1) and the aqueous feed phase (2) as follows:[14]

$$\frac{[Na^+]_2}{[Na^+]_1} = \frac{[Cl^-]_1}{[Cl^-]_2} \tag{2.4}$$

where the brackets indicate molar ion concentrations (note that later work has corrected this equation for the changes of ion activity coefficients between phases, along with other thermodynamic and electrochemical corrections).[16] This leads to a partitioning phenomenon where, in equilibrating solutions with low salt concentrations, the presence of sulfonate groups on the polymer backbone decreases the sorption of salt in the polymer compared to an uncharged polymer of similar water uptake.[14] However, as salt concentration in the equilibrating solution increases, the salt sorption of the sulfonated polymer increases and behaves more closely to that of an uncharged polymer.[14] This has been experimentally demonstrated in sulfonated polysulfone as shown in Figure 2.3.[17] This effect is important in testing and analysis of these materials, since the salt sorption coefficient will change with salt concentration,[17] and thus at higher salt concentration salt permeability can increase, which reduces salt rejection.[2,19] A detailed model of salt partitioning in charged polymers based on Donnan theory has been developed by Geise et al., shown here:[17]

$$K_S = f_D\left[\left(\frac{1}{4}\left(\frac{C_A^m}{C_S^S}\right)^2 + (K_\infty)^2\right)^{1/2} - \frac{C_A^m}{2C_S^S}\right] + (1 - f_D)K_\infty \tag{2.5}$$

where f_D is the fraction of the polymer that acts as an ideal Donnan exclusion material (i.e. f_D = 1 corresponds to a material following ideal Donnan exclusion, and f_D = 0

corresponds to salt partitioning in an ideal uncharged material), C^m_A is the concentration of fixed charged groups in the material (i.e., sulfonate groups), C^S_S is the concentration of salt in the external solution, and K_∞ is the salt partition coefficient of an uncharged material with equal water uptake to the material in question.[17] In many ion exchange materials, the distribution of electrical potential is not uniform throughout the material, and this model, which takes into account the existence of incomplete Donnan behavior in the material, can be used to model salt sorption behavior in charged and uncharged materials.[17]

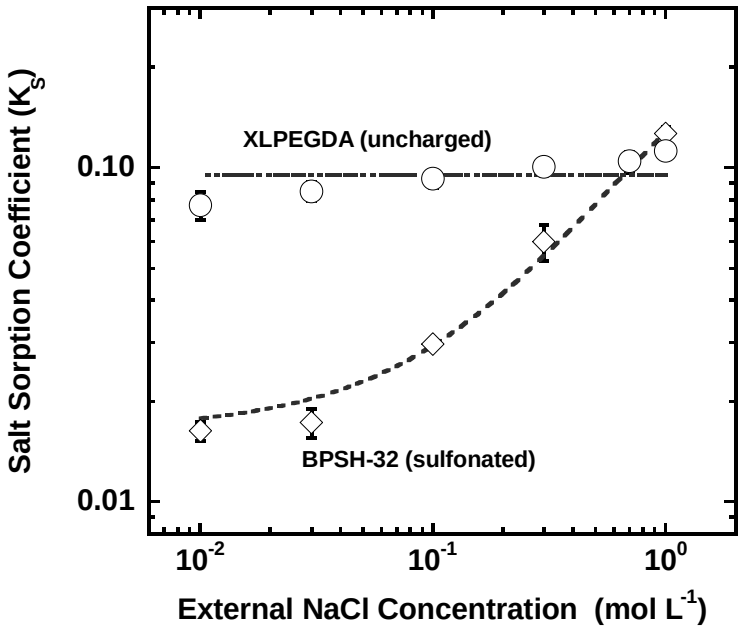

Figure 2.3. Salt sorption in charged and uncharged polymers.[17] (○) = XLPEGDA, crosslinked PEG, (◇) = BPSH-32. Samples were equilibrated in NaCl solutions as shown and their salt was sorption measured.

Donnan theory has been extended to describe ion partitioning in a system with a mixture of monovalent and divalent ions (such as sodium and calcium chloride), where two monovalent ions must equilibrate between phases for each divalent ion to maintain electroneutrality.[15] The Donnan model for equilibrium cation partitioning is given in Equation 2.6,[15] where the ratio of the concentrations of divalent cations between the contiguous aqueous phase (2) and the polymer phase (1) is equal to the square of the ratio of monovalent cations:[15]

$$\left(\frac{[Na^+]_2}{[Na^+]_1}\right)^2 = \frac{[Ca^{++}]_2}{[Ca^{++}]_1} \tag{2.4}$$

Salt diffusivity has also been shown to increase in sulfonated polymers with increasing salt concentration while it remains relatively constant in uncharged polymers, though the mechanism for this is not well understood.[18] With an increase in both K_S and D_S with increasing external salt solution concentration, P_S must increase with increasing salt concentration in such materials.[4,19] The dependence of transport properties on salt concentration in charged polymers is important to characterize. Since water treatment and other industrial membrane separation processes face a wide range of salt concentrations, the performance of a charged material could change significantly when filtering feed streams of different salt concentrations.

REFERENCES

1. J.G. Wijmans, R.W. Baker. The solution-diffusion model: a review. *J. Memb. Sci.* 107 (1995) 1–21.

2. D.R. Paul. Reformulation of the solution-diffusion theory of reverse osmosis. *J. Memb. Sci.* 241 (2004) 371–386.

3. G.M. Geise, H.-S. Lee, D.J. Miller, B.D. Freeman, J.E. McGrath, D.R. Paul. Water purification by membranes: the role of polymer science. *J. Polym. Sci. Part B Polym. Phys.* 48 (2010) 1685–1718.

4. W. Xie, J. Cook, H.B. Park, B.D. Freeman, C.H. Lee, J.E. McGrath. Fundamental salt and water transport properties in directly copolymerized disulfonated poly(arylene ether sulfone) random copolymers. *Polymer (Guildf).* 52 (2011) 2032–2043.

5. W.J. Koros, G.K. Fleming, S.M. Jordan, T.H. Kim, H.H. Hoehn. Polymeric membrane materials for solution-diffusion based permeation separations. *Prog. Polym. Sci.* 13 (1988) 339–401.

6. H.B. Park, B.D. Freeman, Z.-B. Zhang, M. Sankir, J.E. McGrath. Highly chlorine-tolerant polymers for desalination. *Angew. Chem. Int. Ed. Engl.* 47 (2008) 6019–6024.

7. G.M. Geise, H.B. Park, A.C. Sagle, B.D. Freeman, J.E. McGrath. Water permeability and water/salt selectivity tradeoff in polymers for desalination. *J. Memb. Sci.* 369 (2011) 130–138.

8. H.K. Lonsdale, U. Merten, R.L. Riley. Transport properties of cellulose acetate osmotic membranes. *J. Appl. Polym. Sci.* 9 (1965) 1341–1362.

9. H. Ju, A.C. Sagle, B.D. Freeman, J.I. Mardel, A.J. Hill. Characterization of sodium chloride and water transport in crosslinked poly(ethylene oxide) hydrogels. *J. Memb. Sci.* 358 (2010) 131–141.

10. M.A. Frommer, J.S. Murday, R.M. Messalem. Solubility and diffusivity of water and of salts in an aromatic polyamide film. *Eur. Polym. J.* 9 (1973) 367–373.

11. H. Yasuda, C.E. Lamaze, L.D. Ikenberry. Permeability of solutes through hydrated polymer membranes, Part 1. Diffusion of sodium chloride. *Die Makromol. Chemie*. 118 (1968) 19–35.

12. W. Xie, H. Ju, G.M. Geise, B.D. Freeman, J.I. Mardel, A.J. Hill, J.E. McGrath. Effect of free volume on water and salt transport properties in directly copolymerized disulfonated poly(arylene ether sulfone) random copolymers. *Macromolecules*. 44 (2011) 4428–4438.

13. H. Yasuda, C.E. Lamaze, A. Peterlin. Diffusive and hydraulic permeabilities of water in water-swollen polymer membranes. *J. Polym. Sci. Part A Polym. Chem.* 9 (1971) 1117–1131.

14. F.G. Donnan. Theory of membrane equilibria and membrane potentials in the presence of non-dialysing electrolytes. A contribution to physical-chemical physiology. *J. Memb. Sci.* 100 (1995) 45–55.

15. F.G. Donnan. The theory of membrane equilibria. *Chem. Rev.* 1 (1924) 73–90.

16. F. Helfferich. *Ion exchange*. Dover Publications, New York, 1962.

17. G.M. Geise, L.P. Falcon, B.D. Freeman, D.R. Paul. Sodium chloride sorption in sulfonated polymers for membrane applications. *J. Memb. Sci.* 423-424 (2012) 195–208.

18. G.M. Geise, B.D. Freeman, D.R. Paul. Sodium chloride diffusion in sulfonated polymers for membrane applications. *J. Memb. Sci.* 427 (2013) 186–196.

19. G.M. Geise, B.D. Freeman, D.R. Paul. Characterization of a sulfonated pentablock copolymer for desalination applications. *Polymer (Guildf).* 51 (2010) 5815–5822.

3. Experimental Procedures

MATERIALS

Sulfonated Polysulfones

The BisAS and BPS series chemical structures are shown in Figure 3.1. The BisAS series of polymers was synthesized in the potassium ion form from nonsulfonated and disulfonated monomers as described previously[1] by Dr. James McGrath's polymer research group at Virginia Tech, with 20, 25, 30, 35, and 40 mol% disulfonated monomer, as well as BPS-26. In addition, BisAS-35, and BPS-20 and 32 were supplied by Akron Polymer Systems (Akron, Ohio, U.S.).

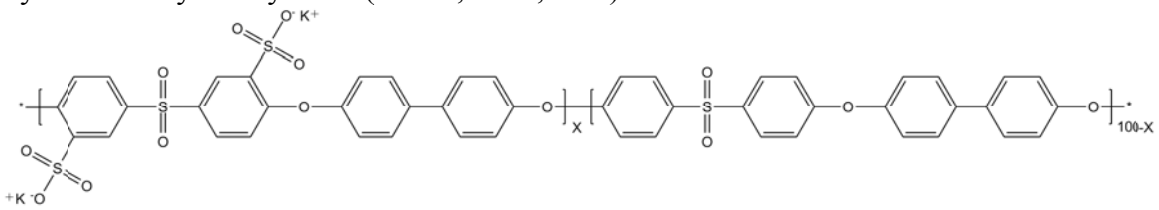

(A) BPS-X Series

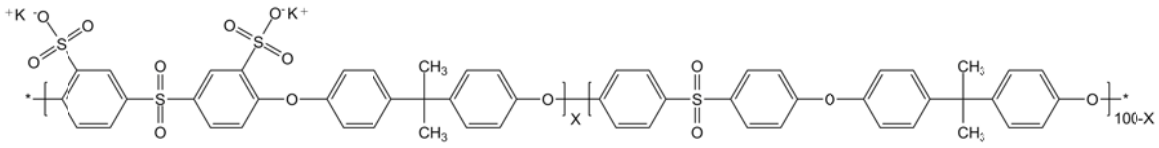

(B) BisAS-X Series

Figure 3.1. Chemical structures of sulfonated polysulfone random copolymers. X = the degree of sulfonation, i.e., the mol% of repeat units containing disulfonated monomer (0 < X < 100).

Sample Fabrication

Freestanding, dense, defect-free films were prepared using methods based on the method of Lee et al.[2] Glass casting plates were pretreated by soaking them in an approximately 20 g/L solution of potassium hydroxide in isopropanol at ambient conditions for at least 4 h. The polymer was dissolved in *N,N*-dimethylacetamide (DMAc) at a concentration of 0.1 g polymer/mL solvent, then filtered through a 0.45 µm

glass microfiber syringe filter. To remove air bubbles, the solution was allowed to stand at ambient conditions for at least 1 h, after which it was then poured onto a casting plate. Solvent was partially removed from the BPS polymer films by drying in an oven at 60 °C for 8 h in air, followed by drying at 120 °C for 12 h under vacuum. In BisAS materials, this process annealed the films, resulting in a decrease in permeability. Thus, all BisAS samples, and some samples of BPS-32, for comparison, were subjected to more moderate drying conditions of 60 °C for 48 hours at ambient pressure. The films were then soaked in deionized water for approximately 24 h to remove any remaining solvent and to fully hydrate them before testing.

Salts and Reagents

N,N-dimethylacetamide (DMAc) was purchased from Sigma-Aldrich (U.S.) for use in dense film fabrication. Potassium hydroxide (KOH) (Avatar Performance Materials, U.S.) and isopropyl alcohol (C_3H_7OH) (Fisher Scientific, U.S.) were purchased and used for glass plate pretreatment. 1 Molar standard solutions of sodium chloride (NaCl) from Sigma-Aldrich were used for the fundamental permeability and desorption studies described below. Sodium bicarbonate ($NaHCO_3$) was purchased from Fisher Scientific for use in pH control of the crossflow feed. Several salts were obtained for use permeability and sorption studies: sodium chloride (Fisher Scientific), calcium chloride ($CaCl_2$) (Sigma Aldrich), magnesium chloride ($MgCl_2$) (Amresco, U.S.), lithium chloride (LiCl) (Sigma Aldrich), potassium chloride (KCl) (Fisher Scientific), and cesium chloride (CsCl) (Sigma Aldrich)

POLYMER IEC ANALYSIS

The degrees of sulfonation of the polymers were determined by ^{1}H NMR spectroscopy at Virginia Tech as described previously.[1] Ion exchange capacity (IEC,

meq/g), a measurement of the density of charged groups in the polymer, was calculated from the degree of sulfonation (X) as follows:

$$IEC = \frac{2 \cdot X/100}{(X/100)(MW_S) + (1 - X/100)(MW_n)} \tag{3.1}$$

where MW_S and MW_n are the molecular weights of the sulfonated and non-sulfonated repeat groups, respectively. Additionally, non-aqueous potentiometric titration was performed at Virginia Tech on BPS-32 as described in the literature.[1,3]

ELEMENTAL ANALYSIS

While conductivity was sometimes used to determine salt concentration in water solutions as described below, conductivity is unable to differentiate between different species of ions. Thus elemental analysis was performed on aqueous solutions containing multiple species of salt, on solutions of single salts that were being compared to multi-salt solutions to maintain analytical consistency, as well as on some low-concentration samples of a single salt to obtain greater accuracy than conductivity measurements.

The cation concentrations of salt solution samples were determined by a Varian AA140 atomic absorption spectrophotometer (Varian Inc., U.S.). Sodium concentrations were determined with an air/acetylene flame, while magnesium and calcium concentrations were determined with an NO_2/acetylene flame. All samples and calibration solutions were prepared in an approximately 2% nitric acid/deionized water solution. Calibration solutions were prepared at compositions that were similar to that of the samples that were being tested, e.g., samples with mixtures of NaCl and $CaCl_2$ were calibrated with solutions of NaCl and $CaCl_2$ in roughly similar concentrations. Calibration details are listed for each test.

Anion concentrations were determined with a Dionex ICS-2100 ion chromatograph (Thermo Scientific, U.S.). In the case of NaCl only solutions, the

concentration of chloride anions could be used to measure the concentration of the NaCl salt, since electroneutrality requires one sodium cation to be present for each chloride anion. All salt samples and calibrations were aqueous solutions. Measurements of mixtures of competing anions, i.e., chloride and sulfate, were calibrated with mixtures of NaCl and Na_2SO_4; all other anion measurements were only to detect the chloride anion, and they were calibrated with aqueous solutions of NaCl, listed below.

TRANSPORT PROPERTY CHARACTERIZATION

Water Sorption

Water uptake, w_W, was determined as follows by measuring the hydrated mass, m_h, and dry mass, m_d, of the polymer:[4]

$$w_W = \frac{m_h - m_d}{m_d} \tag{3.2}$$

The polymer sample was soaked in deionized water at room temperature for at least 24 hours, removed and blotted dry with clean paper wipes, and then immediately weighed; this process was repeated until the film hydrated mass was constant. To obtain the dry mass, the film was dried under vacuum at 100 °C for at least 24 h, then removed from the oven and weighed; this process was repeated until the film attained a constant dry mass.

The water partition coefficient, K_W, is the ratio of the water concentration in the polymer, $C_{W,P}$, to the concentration of pure water, C_W (1 g/cm^3), as shown:[5,6]

$$K_W = \frac{C_{W,P}}{C_W} \tag{3.3}$$

If the partial molar volume of water in the polymer is equal to the molar volume of pure water, the water partition coefficient is equal to the volume fraction of water in the polymer, allowing K_W values to be calculated from hydrated and dry masses of the polymer sample as follows:[7]

$$K_W = \frac{V_{W,P}}{V_P + V_{W,P}} = \frac{(m_h - m_d)/\rho_W}{m_d/\rho_P + (m_h - m_d)/\rho_W} \tag{3.4}$$

where $V_{W,P}$ is the volume of water dissolved in the hydrated polymer, V_P is the dry polymer volume, ρ_W is the density of water, and ρ_P is the dry polymer density. Polymer density was calculated at Virginia Tech from the mass and volume of polymer samples, determined by measuring their physical dimensions. Sample thickness was determined using a Mitutoyo Absolute micrometer (Mitutoyo, Japan), and the area of a film sample was determined with a ruler. From the IEC and water uptake data, the hydrated charge concentration may be calculated as follows:

$$\text{Hydrated Charge Concentration} = \frac{IEC}{1/\rho_P + w_W/\rho_W} \tag{3.5}$$

Water Permeability and Diffusivity

Steady state pure water permeability was measured by dead end permeation[2] at room temperature in a Sterlitech HP4750 stirred cell (Sterlitech Co., USA), operated at a feed pressure of 400 psig (27.6 barg) using deionized water as the feed; the permeate pressure was atmospheric. The volume of permeate was measured as a function of time and used to calculate the water flux, J_W, as shown below:[8]

$$J_W = \frac{\Delta V}{A \cdot \Delta t} \tag{3.6}$$

where ΔV is the change in permeate volume during a time interval Δt, and A is the area of the film available for mass transfer. The hydraulic water permeability, $P_{W,H}$ (L μm/(m^2 h bar)), is the steady state water flux normalized by the sample thickness and net driving force:[9,10]

$$P_{W,H} = \frac{J_W \cdot l}{\Delta p - \Delta \pi} \tag{3.7}$$

where l is the average hydrated film thickness, Δp is the hydrostatic pressure difference, and $\Delta\pi$ is the osmotic pressure difference due to any salt concentration difference between the feed and permeate solutions; $\Delta\pi$ is zero in pure water permeation experiments. The measured hydraulic water permeability cannot be used to directly calculate water diffusivity in highly water-swollen polymer films, since the transport of water in the film is caused by both diffusive transport and convective flow;[11] there is also a thermodynamic correction factor that enters the flux expression for highly water swollen films.[5,11,12] If the Flory-Huggins model can be used to describe the thermodynamic correction factor, then the relationship between $P_{W,H}$ and the diffusive water permeability, P_W (cm^2/s), is given by the following: [7,12]

$$P_W = D_W \cdot K_W = P_{W,H} \cdot \frac{RT}{\overline{V_W}}\left[(1-K_W)^2(1-2\chi \cdot K_W)\right] \tag{3.8}$$

where R is the ideal gas constant, T is absolute temperature, K_W is the water partition coefficient defined in Equation 3.3, and $\overline{V_W}$ is the molar volume of water. If $(1\text{-}K_W)^2(1\text{-}2\chi\cdot K_W)$ is approximately 1, then Equation 3.8 simply acts to convert the units of hydraulic water permeability to cm^2/s. The χ parameter can be estimated from the Flory-Huggins theory as follows:[13,14]

$$\chi = -\left[\frac{\ln K_W + (1-K_W)}{(1-K_W)^2}\right] \tag{3.9}$$

The effective, average water diffusivity, D_W, was calculated from P_W and K_W using the solution diffusion model:[5]

$$D_W = P_W / K_W \tag{3.10}$$

Salt Permeability

Steady state salt permeability, P_S, through a polymer film was measured in glass diffusion cells[7] (Permegear, USA), where two water-jacketed cells held at a temperature of 25 °C were separated by a polymer film. The donor cell was filled with a salt solution having a concentration of, for example, 1 M sodium chloride, while the receiver cell was filled with deionized water. The conductivity in the receiver cell was measured as a function of time with a Cond 7300 conductivity meter (WTW, Germany) to determine the concentration change of sodium chloride over time as salt permeated through the film. Within the concentration range considered, the conductivity was linear with respect to salt concentration, and the conductivity meter was calibrated by measuring the conductivity of sodium chloride solutions at concentrations ranging from 2.8×10^{-6} to 8.0×10^{-4} mol/L. The salt permeability, P_S, in this experiment was calculated from:[15]

$$\ln\left[1-2\frac{C_R(t)}{C_D(t_0)}\right]\left[-\frac{V\cdot l}{2A}\right]=P_S\cdot t \tag{3.11}$$

where t is time, $C_R(t)$ is the salt concentration in the receiver cell as a function of time, $C_D(t_0)$ is the initial salt concentration in the donor cell, V is the donor and receiver cell volumes, and A is the area of the polymer film exposed to the donor and receiver solutions.

Salt Diffusion and Sorption Coefficients

The salt partition coefficient, K_S, was determined by desorption,[16] where a circular polymer film sample was equilibrated in, for example, a 1 M sodium chloride solution. The volume of the hydrated polymer sample was determined by measuring the radius of a circular film sample using Fowler Pro-Max digital calipers (Fowler, USA), and the thickness was measured using the micrometer mentioned previously; care was taken to ensure that the sample did not dry out during these measurements. The sample was

blotted dry to remove any salt solution on its surface, then placed in an extraction bath containing a known amount (e.g., 50 mL) of deionized water in a stirred, water-jacketed cell at a constant temperature of 25 °C. The cell was sealed with paraffin wax film (i.e., Parafilm), and sodium chloride was allowed to desorb for approximately 24 h. The concentration of desorbed salt was measured with the ion chromatograph described above, which was calibrated with standards ranging from 0.1 to 10 mg/L sodium chloride. The mass of salt (m_S) extracted from the film into the water was used to calculate the salt partition coefficient:[16,17]

$$K_S = \frac{m_S / V_{P,eq}}{C_{S,eq}} \tag{3.12}$$

where $V_{P,eq}$ is the volume of the polymer film when equilibrated with the salt solution, and $C_{S,eq}$ is the salt concentration of the equilibration solution. From P_S and K_S values, the average salt diffusion coefficient, D_S, was calculated as follows:[5]

$$D_S = P_S / K_S \tag{3.13}$$

Mixed Ion Sorption

Ion sorption measurements were also performed using equilibration mixtures of salts. After fabrication and deionized water soaking, circular samples of BPS-32 (cast using the high-temperature vacuum drying conditions described above) were cut with dies ranging from 2 to 3.4 cm in diameter. Samples were equilibrated for at least 48 h in the target salt solutions.

Desalination feed sources may have a wide range of saline compositions. For example, calcium and magnesium are present in seawater at 411 ppm (7 mM) and 1,290 ppm (53 mM) for seawater at 3.5% salinity (35,000 ppm total dissolved solids).[18] Additionally, groundwater feeds may have varying compositions; for example, analysis

of groundwater wells in the Alamogordo region of New Mexico reveal groundwater concentrations ranging from 310 to 720 ppm sodium (i.e., 13 to 31 mM sodium), 49 to 550 ppm calcium (i.e., 1.2 to 13 mM calcium) and 13 to 340 ppm magnesium (i.e., 0.5 to 14 mM magnesium).[19] The crossflow permeation tests described below were performed with feed solutions using NaCl concentrations that are generally representative of brackish water levels, with smaller amounts of $CaCl_2$ and $MgCl_2$ added to investigate the effects of relatively low concentrations of divalent cation in a mostly NaCl environment on the polymer transport properties. The target concentrations for the mixed ion permeability tests and the concentrations used for the mixed ion sorption tests are listed in Table 3.1.

Test	Salt Species	Crossflow Test Target Feed Concentrations (mM)	Crossflow Test Target Feed Concentrations (ppm)	Sorption Test Equilibration Solution Concentrations (mM)	Sorption Test Equilibration Solution Concentrations (ppm)
NaCl Only	NaCl	16; 28; 34; 40; 48	940; 1600; 2000; 2300; 2800	28; 32; 34; 40	1600; 1850; 2000; 2300
NaCl + $CaCl_2$	NaCl	34	2000	34	2000
	$CaCl_2$	0.4; 1.0; 1.4; 2.4; 3.4	40; 110; 160; 270; 380	0.4; 1.4; 3.4; 34	40; 160; 380; 3800
NaCl + $MgCl_2$	NaCl	34	2000	34	2000
	$MgCl_2$	0.3; 0.5; 1.5; 2.4; 3.8; 6.6	30; 50; 140; 230; 360; 630	0.3; 2.4; 6.6; 34	30; 230; 630; 3200
NaCl + Na_2SO_4	NaCl	34	2000	n/a	n/a
	Na_2SO_4	0.4; 1.5; 2.5; 4.0; 6.9	60; 210; 360; 570; 980	n/a	n/a

Table 3.1. Feed and equilibration solution concentrations for mixed ion crossflow and sorption testing

For the mixed ion sorption testing, NaCl solutions were prepared in 28, 32, 34, and 40 mM (i.e., 1600, 1850, 2000, and 2300 ppm) concentrations; mixed NaCl and $CaCl_2$ solutions were prepared using 34 mM (2000 ppm) NaCl mixed with 0.4, 1.4, 3.4, and 34 mM (44, 160, 380, and 3800 ppm) $CaCl_2$; mixed NaCl and $MgCl_2$ solutions were prepared using 34 mM (2000 ppm) NaCl mixed with 0.3, 2.4, 6.6, and 34 mM (28, 230, 630, and 3200 ppm) $MgCl_2$. These compositions were chosen to match the compositions used in the mixed ion crossflow tests described below, as well as to include one test of equal molar amounts of NaCl and the divalent cation salt.

After equilibration in the salt solutions, water, cation, and anion sorption values were determined from the polymer samples using methods described by Geise et al.[16] The physical dimensions of samples for anion sorption were measured with the micrometer and calipers described above. The samples were then gently patted dry and immersed in deionized water as described above, and they were allowed to desorb for at least 24 h. Aliquots of the desorption solution were then analyzed by ion chromatography as described above, to determine their chloride concentration, using calibration solutions containing 0.01 to 1.0 ppm NaCl. The concentration of chloride anions in the polymer, $C_{Cl,P}$ was calculated as follows:[16]

$$C_{Cl,P} = \frac{C_{Cl,s} V_s}{V_{P,eq}} \tag{3.14}$$

where $C_{Cl,s}$ is the chloride concentration in the desorption solution, and V_s is the volume of the desorption solution. The sorption coefficient of the chloride anion is defined as the ratio of the concentration of chloride in the polymer to that in the equilibration solution:[16,17]

$$K_{Cl} = \frac{C_{Cl,P}}{C_{Cl,eq}} \tag{3.15}$$

The wet mass values of samples used for cation sorption and water sorption were recorded using the method described above. After the final wet mass measurement, the samples were dried under vacuum at ambient conditions, and the dry mass was measured until it was constant. The water uptake and water partition coefficient were determined with Equations 3.2 and 3.3. The dried films were then ashed in a furnace at 700 °C for 3 hours. The ash was dissolved with 15 mL of 2% nitric acid solution and mixed by drawing and returning 5 mL of the solution by pipette twenty times. The cation content of the ash was then analyzed by flame AA as described above. NaCl samples were calibrated with NaCl solutions ranging from 0.25 to 2.0 ppm. Samples equilibrated in mixed NaCl/$CaCl_2$ solutions were calibrated for sodium detection using solutions ranging from 0.25 to 2.0 ppm NaCl with equal amounts of $CaCl_2$, and they were calibrated for calcium detection using solutions ranging from 0.1 to 5.0 ppm $CaCl_2$ with equal amounts of NaCl. Samples equilibrated in mixed NaCl/$MgCl_2$ solutions were calibrated for sodium detection using solutions ranging from 0.25 to 2.0 ppm NaCl with equal amounts of $MgCl_2$, and they were calibrated for magnesium detection using solutions ranging from 0.1 to 0.8 ppm $MgCl_2$ with equal amounts of NaCl. The cation concentration in the polymer, $C_{M,P}$ was determined by:[16]

$$C_{M,P} = \frac{C_{M,ash} \cdot V_{ash}}{V_{P,eq}} \tag{3.16}$$

where $C_{M,ash}$ is the concentration of the cation M in the ash solution, and V_{ash} is the volume of the ash solution (i.e., 15 mL). From the polymer density and water uptake measurements, the equilibrated polymer volume of the cation sorption samples was determined using the denominator from Equation 3.4:

$$V_{P,eq} = V_P + V_{W,P} = m_d / \rho_P + (m_h - m_d) / \rho_W \tag{3.17}$$

The ion exchange capacity (IEC), measured as the mass concentration of fixed charged groups on the polymer backbone and expressed as milliequivalents/gram of dry polymer, determines the number of charged sites available for cation exchange in the polymer.[16] For comparison, the concentration of charges, C_{meq} (meq/g), of each species of cation in the polymer was calculated as follows:

$$C_{meq} = \frac{C_{M,ash} \cdot V_{ash} \cdot z_M}{m_d} \tag{3.18}$$

where z_M is the number of charges on the cation M (e.g., $z_M = 1$ for Na^+ and 2 for Ca^{++}).

Crossflow Characterization

Salt permeability and water permeability were also determined, along with salt rejection, in crossflow filtration using techniques employed by Van Wagner et al.[20] Polymer samples were loaded into CF042 crossflow cells (Sterlitech Co., U.S.) that were connected to a high-pressure feed solution recirculating system. To protect the samples, filter paper was placed between the polymer films and the cell's porous metal plate backing. Feed water maintained at 25 °C was circulated at a constant flow rate of approximately 1 gallon per minute (3.8 L/min) over the surface of the polymer samples in the cells, with a feed velocity of 0.6 m/s and a Reynolds number of 3070 at the sample surface. As the feed solution permeated through the film, permeate was collected from the downstream side of the cell. The mass of permeate produced over time was recorded to determine the volume of permeate (assuming that the permeate density is that of water at room temperature). The ionic compositions of the permeate samples and samples taken from the feed were determined using either flame AA or ion chromatography, as is noted for each set of tests.

To examine the effect of feed composition on polymer transport properties, crossflow characterization was performed on samples of BPS-32 (prepared at the high-

temperature vacuum drying conditions) and BisAS-35 (prepared at the low-temperature atmospheric conditions) using a sodium chloride feed with a competing salt introduced into the feed solution in discrete steps. A schematic of the testing procedure is presented in Figure 3.2. Initially, deionized water was circulated to flush the system. Then a control test was performed using a feed composition of nominally 34 mM NaCl (2000 mg/L) to establish the baseline water and salt permeability for a brackish water feed. The permeate was collected during the 34 mM NaCl initial portion of the experiment to permit calculation of water permeability, salt rejection and, in turn, salt permeability. These calculations are described in more detail below. Then, calcium chloride was added to the feed to achieve a concentration of 34 mM NaCl and 0.4 mM $CaCl_2$ (i.e., 40 ppm $CaCl_2$). The crossflow test was allowed to reach steady-state, and the permeate and feed samples were collected for measurement. Steady-state conditions were verified by successive measurements of the permeate conductivity over time using an Oakton 100 portable conductivity meter (Oakton, U.S.), and steady state was achieved once the conductivity measurements were constant (steady-state conditions were confirmed after salt permeability calculation, as the time allowed for steady state for each test was greater than the calculated l^2/P_S value). The process of adding $CaCl_2$ to the feed, allowing the crossflow to come to steady state, and collecting the permeate for analysis was repeated several times, until the total $CaCl_2$ concentration in the feed solution was approximately 3.4 mM (i.e., 380 ppm $CaCl_2$). After the final permeation test using the last mixture of NaCl and $CaCl_2$, the crossflow system was flushed with deionized water for at least 24 hours. Then a nominally 34 mM NaCl solution was fed to the membranes for at least 24 hours to verify that the samples maintained the baseline water and salt permeability properties. Then $MgCl_2$ was added to the feed in increasing, discreet steps beginning with 0.3 mM (i.e., 30 ppm $MgCl_2$) up to 6.6 mM (i.e., 630 ppm $MgCl_2$), and permeate and

feed samples were collected at each step (note that the sorption tests described above include these concentrations, as well as one further test at equimolar NaCl and divalent ion salt). The system was again rinsed with deionized water for 24 hours, and the crossflow process was repeated using a 34 mM NaCl feed with increasing concentrations of Na_2SO_4, ranging from 0.4 mM (i.e., 60 ppm Na_2SO_4) to 6.9 mM (i.e., 1000 ppm Na_2SO_4). Finally, after flushing the crossflow system with deionized water for 24 hours, crossflow testing was performed using a 16 mM (940 ppm) NaCl feed, with increasing amounts of NaCl added in discreet steps up to 48 mM (2800 ppm) to bracket the range of cation and anion charge concentrations in the mixed salt tests and compare the effect of increasing concentrations of NaCl on the polymer properties.

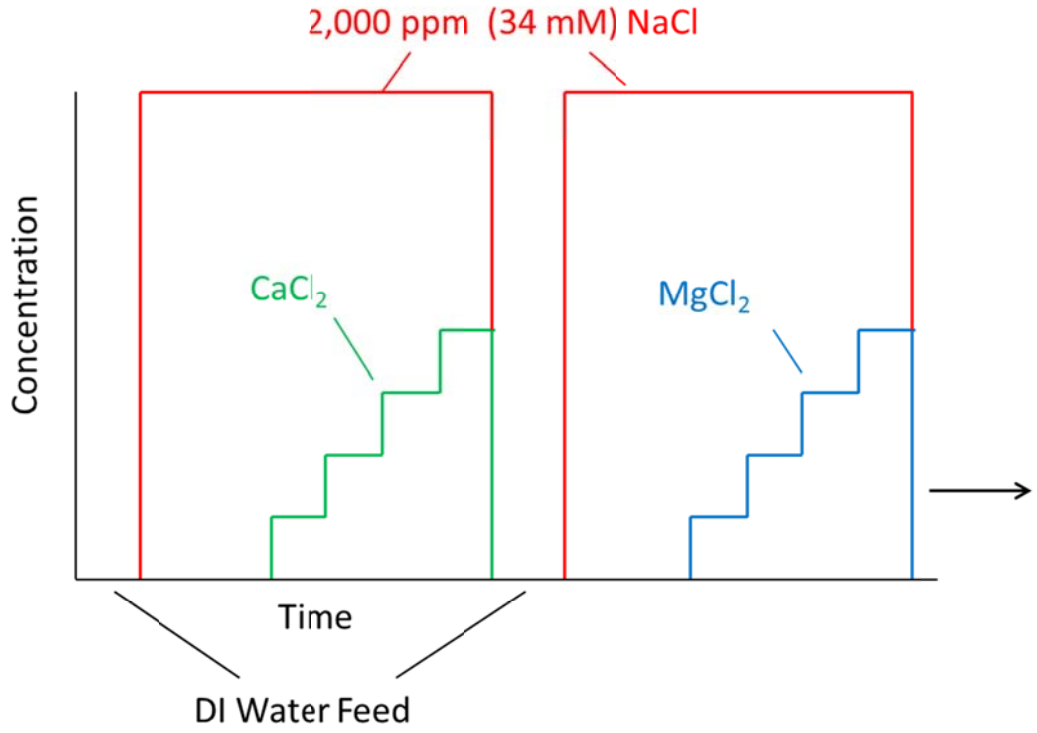

Figure 3.2. Crossflow testing procedure. $P_{W,H}$ and P_S for each salt (e.g., P_{NaCl} and P_{CaCl2}) were measured at each concentration step.

The J_W and $P_{W,H}$ values of each sample were determined from the permeate volume as per Equations 3.6 and 3.7. At the low concentrations of salt present in the permeate in this study, the contribution of the salt content to the total permeate flux is negligible, and the total permeate flux is essentially equal to the water flux. The osmotic pressure change is calculated from the total permeate salt concentrations ($C_{S,f}$ and $C_{S,p}$, respectively) as follows:[21]

$$\Delta\pi = RT(C_{S,f} - C_{S,p}) \tag{3.19}$$

The cation concentrations of diluted feed and permeate samples were determined by flame AA as described above. Sodium concentration measurements were calibrated using sodium chloride solutions ranging from 0.25 to 2.0 mg/L Na^+; calibrations for permeate and feed samples from mixed ion tests included the competing divalent salt (i.e., magnesium chloride or calcium chloride) such that the mass concentration of the divalent cation was 10% of the concentration of the sodium cation, so that the calibration solutions would have similar concentration ratios as the feed solutions. For the tests using NaCl only, no other salts were added to the calibrations. Magnesium calibration standards were prepared by dissolving $MgCl_2$ in the nitric acid matrix at concentrations of 0.1 to 1.0 mg/L Mg^{++}, while calcium calibration standards were prepared from $CaCl_2$ in nitric acid solutions ranging from 0.5 to 4 mg/L Ca^{++}. Both magnesium and calcium calibration standards had sodium chloride added to achieve 10× the concentration of Na^+ as the divalent cation to maintain similarity to the feed sample solutions.

Anion concentrations from the tests using mixtures of NaCl and Na_2SO_4 were determined using the ion chromatograph as described above. Both chloride and sulfate concentrations were determined using calibration solutions prepared from mixtures of

sodium sulfate and sodium chloride in deionized water ranging from 0.5 mg/L Na_2SO_4 and 5 mg/L NaCl to 7.5 mg/L Na_2SO_4 and 75 mg/L NaCl.

The elemental analysis of the feed and permeate ion concentrations allows the calculation of permeability coefficients (P_X, X indicating the species of ion) of ions in the polymer:[9]

$$P_X = \frac{J_X \cdot l}{C_{X,f} - C_{X,p}} \tag{3.20}$$

where $C_{X,f}$ and $C_{X,p}$ are the feed and permeate ion concentrations, respectively, and J_X is flux of the ion across the film, determined as follows:[20]

$$J_X = C_{X,p} \cdot J_W \tag{3.21}$$

To maintain electroneutrality in the experiments involving chloride as the anion, every cation that permeates the polymer film is accompanied by a number of chloride anions equal to the cation valent charges. Thus, the permeation of one mol of sodium cations requires the permeation of one mol of chloride anions, and the permeation of one mol of calcium or magnesium requires the permeation of two mols of chloride. Similar principles apply to the divalent anion considered, e.g., sulfate. For this reason the permeability coefficient of the cation is equal to the permeability coefficient of the salt of that cation in tests using a mixed cation feed, i.e., $P_{Na+} = P_{NaCl}$, and $P_{Ca++} = P_{CaCl2}$ in the $NaCl/CaCl_2$ mixed feed test. Conversely, the permeability coefficient of an anion is equal to the permeability coefficient of the salt of that anion in tests using the mixed anion feed, i.e., $P_{Cl-} = P_{NaCl}$, and $P_{SO4--} = P_{Na2SO4}$ in the $NaCl/Na_2SO_4$ mixed feed test.

The same principle applies to rejection as well, that is $R_{Na+} = R_{NaCl}$ and $R_{Ca++} = R_{CaCl2}$ in the $NaCl/CaCl_2$ mixed feed test, while $R_{Cl-} = R_{NaCl}$ and $R_{SO4--} = R_{Na2SO4}$ in the $NaCl/Na_2SO_4$ mixed feed test. The ion rejection was determined from the feed and permeate ion concentrations:[22]

$$R(\%) = 100 \cdot \left(1 - \frac{C_{X,p}}{C_{X,f}} \right) \tag{3.22}$$

The ion or salt rejection may also be expressed as ion or salt passage, where passage = 100 – R(%).

REFERENCES

1. W.L. Harrison, F. Wang, J.B. Mecham, V.A. Bhanu, M. Hill, Y.S. Kim, J.E. McGrath. Influence of the bisphenol structure on the direct synthesis of sulfonated poly(arylene ether) copolymers. I. *Journal of Polymer Science Part A: Polymer Chemistry*. 41 (2003) 2264–2276.

2. C.H. Lee, D. VanHouten, O. Lane, J.E. McGrath, J. Hou, L.A. Madsen, J. Spano, S. Wi, J. Cook, W. Xie, H.J. Oh, G.M. Geise, B.D. Freeman. Disulfonated poly(arylene ether sulfone) random copolymer blends tuned for rapid water permeation via cation complexation with poly(ethylene glycol) oligomers. *Chemistry of Materials*. 23 (2011) 1039–1049.

3. F. Wang, M. Hickner, Y.S. Kim, T.A. Zawodzinski, J.E. McGrath. Direct polymerization of sulfonated poly(arylene ether sulfone) random (statistical) copolymers: candidates for new proton exchange membranes. *Journal of Membrane Science*. 197 (2002) 231–242.

4. T.A. Zawodzinski, T.E. Springer, J. Davey, R. Jestel, C. Lopez, J. Valerio, S. Gottesfeld. A comparative study of water uptake by and transport through ionomeric fuel cell membranes. *Journal of The Electrochemical Society*. 140 (1993) 1981.

5. J.G. Wijmans, R.W. Baker. The solution-diffusion model: a review. *Journal of Membrane Science*. 107 (1995) 1–21.

6. U. Merten, ed. *Desalination by Reverse Osmosis*. MIT Press, Cambridge, Massachusetts, 1966.

7. W. Xie, J. Cook, H.B. Park, B.D. Freeman, C.H. Lee, J.E. McGrath. Fundamental salt and water transport properties in directly copolymerized disulfonated poly(arylene ether sulfone) random copolymers. *Polymer*. 52 (2011) 2032–2043.

8. W. Xie, G.M. Geise, B.D. Freeman, H.-S. Lee, G. Byun, J.E. McGrath. Polyamide interfacial composite membranes prepared from m-phenylene diamine, trimesoyl

chloride and a new disulfonated diamine. *Journal of Membrane Science*. 403-404 (2012) 152–161.

9. D.R. Paul. Reformulation of the solution-diffusion theory of reverse osmosis. *Journal of Membrane Science*. 241 (2004) 371–386.

10. H.K. Lonsdale, U. Merten, R.L. Riley. Transport properties of cellulose acetate osmotic membranes. *Journal of Applied Polymer Science*. 9 (1965) 1341–1362.

11. H. Yasuda, C.E. Lamaze, A. Peterlin. Diffusive and hydraulic permeabilities of water in water-swollen polymer membranes. *Journal of Polymer Science Part A: Polymer Chemistry*. 9 (1971) 1117–1131.

12. D.R. Paul. Relation between hydraulic permeability and diffusion in homogeneous swollen membranes. *Journal of Polymer Science Part B: Polymer Physics*. 11 (1973) 289–296.

13. P. Flory. Thermodynamics of high polymer solutions. *The Journal of Chemical Physics*. 9 (1941) 660.

14. M.L. Huggins. Solutions of long chain compounds. *The Journal of Chemical Physics*. 9 (1941) 440.

15. Y.S. Kim, F. Wang, M. Hickner, S. McCartney, Y.T. Hong, W. Harrison, T.A. Zawodzinski, J.E. Mcgrath. Effect of acidification treatment and morphological stability of sulfonated poly(arylene ether sulfone) copolymer proton-exchange membranes for fuel-cell use above 100 °C. *Journal of Polymer Science Part B: Polymer Physics*. 41 (2003) 2816–2828.

16. G.M. Geise, L.P. Falcon, B.D. Freeman, D.R. Paul. Sodium chloride sorption in sulfonated polymers for membrane applications. *Journal of Membrane Science*. 423-424 (2012) 195–208.

17. W. Pusch. Measurement techniques of transport through membranes. *Desalination*. 59 (1986) 105–198.

18. K.K. Turekian. *Oceans*. First Ed. Prentice Hall, Englewood Cliffs, 1968.

19. *Analysis of water from four wells at the Brackish Groundwater National Desalination Research Facility*. Tetra Tech, Inc. for the Bureau of Reclamation, Alamogordo, Contract No. R10PC40009, 2011.

20. E.M. Van Wagner, A.C. Sagle, M.M. Sharma, B.D. Freeman. Effect of crossflow testing conditions, including feed pH and continuous feed filtration, on commercial reverse osmosis membrane performance. *Journal of Membrane Science*. 345 (2009) 97–109.

21. B.D. Freeman. Osmosis, in: *Encyclopedia of Applied Polymer Physics*. 1995: pp. 59–71.

22. R. Baker. *Membrane technology and applications*. 1st ed. John Wiley & Sons, 1995.

4. Characterization of Bisphenol-A based Sulfonated Polysulfone

ABSTRACT

The salt and water transport properties of a sulfonated polysulfone with a bisphenol-A based backbone (BisAS) were determined at varying degrees of sulfonation. The BisAS materials have lower dry and hydrated densities than a biphenyl-based sulfonated polysulfone backbone (BPS) analogs, possibly due to the bulky isopropylidene unit in BisAS, and resulting in greater water sorption. The BisAS materials demonstrate increasing water and salt permeability, diffusivity, and solubility as a function of increasing degree of sulfonation, consistent with other sulfonated polymers. The BisAS materials generally exhibit greater salt and water transport properties than the BPS materials due to their higher water uptake, and display selectivity trends that are consistent with previously investigated free volume effects. However, these materials are sensitive to their thermal processing history, and this effect was not widely investigated in this study, so the preceding conclusion should be regarded as speculative.

RESULTS AND DISCUSSION

The water and salt transport properties of the BisAS series of polymers were characterized as a function of the degree of sulfonation, and the results are recorded in Table 4.1. The water uptake and water and salt permeabilities increase with increasing degree of sulfonation, and water/salt selectivity decreases. These trends are consistent with those observed in BPS polymers.[1] Thus, the inclusion of highly hydrophilic sulfonate groups into BisAS materials has qualitatively similar effects as when they are incorporated into other polymer backbones.[1–27] Table 4.2 lists the dry IEC values of the polymers investigated as determined by ^{1}H NMR, as well as the concentrations of fixed charged groups in the hydrated polymer, calculated from the dry IEC and water uptake

values where both measurements were available. Although BisAS-40 has a higher dry IEC than BPS-32, the higher water uptake of BisAS-40 effectively dilutes the concentration of sulfonate groups, and as a result the BisAS-40 has a lower hydrated concentration of charges than BPS-32.

Sample	$P_{W,H}$ (L μm /(m^2 h bar))	P_W (cm^2/s) · 10^7	K_W	D_W (cm^2/s) · 10^6	P_S (cm^2/s) · 10^9	K_S	D_S (cm^2/s) · 10^7
BisAS 20	0.13 ± 0.01	2.1 ± 0.2	0.15 ± 0.01	1.5 ± 0.2	0.72 ± 0.11	0.030 ± 0.001	0.24 ± 0.01
BisAS 30	0.46 ± 0.02	4.5 ± 0.2	0.24 ± 0.01	1.9 ± 0.1	9.0 ± 0.3	0.056 ± 0.007	1.6 ± 0.2
BisAS 40	1.53 ± 0.23	8.9 ± 1.3	0.34 ± 0.01	2.6 ± 0.2	53 ± 4	0.080 ± 0.005	6.6 ± 0.5
BPS 32	0.55 ± 0.12	6.2 ± 1.3	0.22 ± 0.01	2.8 ± 0.6	10.8 ± 4		

Table 4.1. Summary of water and salt transport properties in BisAS and BPS polymers.

Polymer	K^+ form IEC (meq/g of dry polymer)	K^+ form hydrated charge concentration (meq/mL of hydrated polymer)
BisAS-20	0.82	0.87
BisAS-25	1.00	
BisAS-30	1.13	1.06
BisAS-35	1.30	
BisAS-40	1.49	1.31
BPS-20	0.92	
BPS-26	1.11	
BPS-32	1.34	1.41

Table 4.2. IEC and charge concentrations of BisAS and BPS polymers.

Polymer Density and Water Transport

The dry and hydrated density values for BisAS-20, 25, 30, 35, and 40, and BPS-20, 26, and 32 were measured at Virginia Tech using 5 cm × 5 cm samples of each polymer film, and the results are presented in Figure 4.1. Density increases in both dry and wet samples as the degree of sulfonation increases, which is consistent with previously reported results on BPS.[28] Part of this increase in the dry polymer density is due to the addition of heavier sulfur atoms to the structure, while some loss in free volume may result from the stronger cohesion between polymer chains due to the favorable molecular interactions between the sulfonate groups and other polar moieties in the surrounding polymer chains.[28] Of course, the sorption of water into the polymer reduces the density, due to the lower density of water relative to that of polymer and due to water's ability to disrupt polymer-polymer interactions present in the dry polymer.[28] Additionally, the BisAS polymers have lower density than the BPS polymers at similar degrees of sulfonation, potentially due to less efficient chain packing in the BisAS materials arising from the bulky isopropylidene units in its backbone structure. The density values of the BisAS and BPS materials cast into films at 60 °C in air for 48 h are compared against density values measured from BisAS and BPS materials dried at 60 °C for 48 h, followed by drying under vacuum at 150 °C for 48 h; within the experimental error range, there is little change in polymer density at these two drying conditions.

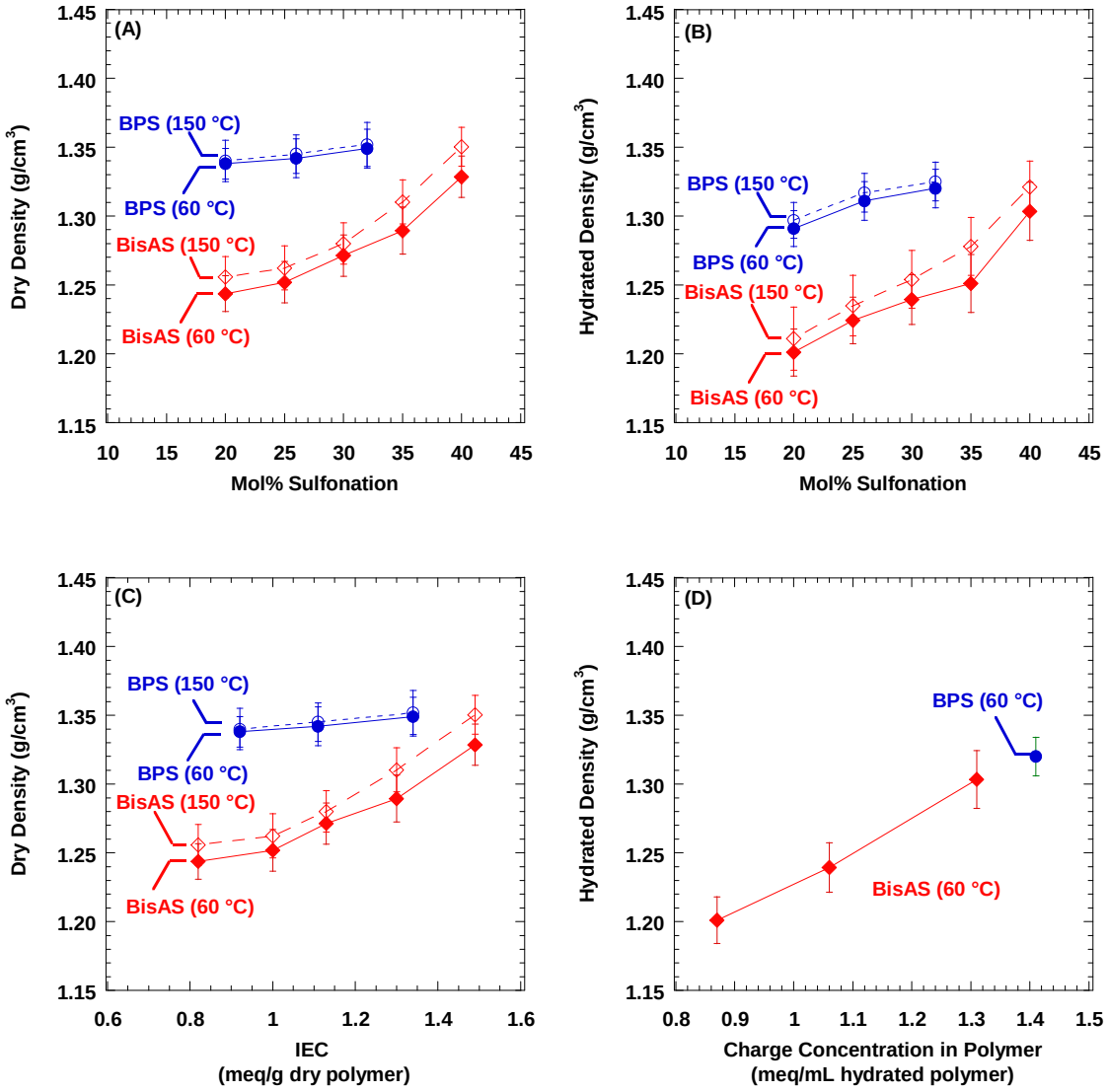

Figure 4.1. Dry (A) and hydrated (B) density values of BisAS and BPS as a function of degree of sulfonation, and dry (C) and hydrated (D) density values of BisAS and BPS as a function of IEC and hydrated charge concentration, respectively. (●) = BPS cast at 60 °C, (○) = BPS cast at 60 °C then 150 °C with vacuum, (◆) = BisAS cast at 60 °C, (◇) BisAS cast at 60 °C then 150 °C with vacuum. The lines are drawn to guide the eye.

The water partition coefficients, K_W, in BisAS 20, 30, and 40 were determined from pure water uptake measurements and the dry polymer density using Equation 3.4. In

Figure 4.2, these values are compared to those from BPS materials reported previously at casting conditions of IR lamp drying for 24 h followed by 48 h of vacuum drying at 120 °C,[2] IR lamp drying for 8 h followed by 6 h of vacuum drying at 150 °C,[9] and oven drying at atmospheric pressure and 80 °C for 24 h followed by 48 h of vacuum drying at 110 °C.[9] In the case of data from Park et al.,[2] values of K_W were calculated from reported values of w_W and polymer density. The BisAS materials have higher water solubility than the BPS materials at similar degrees of sulfonation, which is consistent with the trend of lower density in the BisAS polymers. All materials show an increase in K_W with increasing degree of sulfonation, due to increasing polymer hydrophilicity introduced by the presence of more sulfonate groups at higher degrees of sulfonation. Figure 4.2 (B) shows the trends of K_W as a function of hydrated charge concentration, calculated from Equation 3.5 using the reported IEC, polymer density, and water content values.[1,2,9,28] The hydrated charge concentration of the polymers is a useful point of comparison, as it provides an alternative characterization of the transport environment encountered by ions and water molecules, as opposed to degree of sulfonation alone.

Yasuda et al.[29,30] correlated water and salt transport properties with water uptake in the polymer, and they hypothesized that K_W was proportional to the free volume available for water and ion transport in hydrated polymers. Measurements of free volume element size by positron annihilation lifetime spectroscopy have shown a correlation between free volume and K_W in BPS polymers[28] and in uncharged materials such as crosslinked poly(ethylene glycol).[31] These composite results suggest higher free volume in the more highly hydrated samples, which is at least qualitatively consistent with higher solute transport in BisAS materials than in BPS materials at similar degrees of sulfonation.

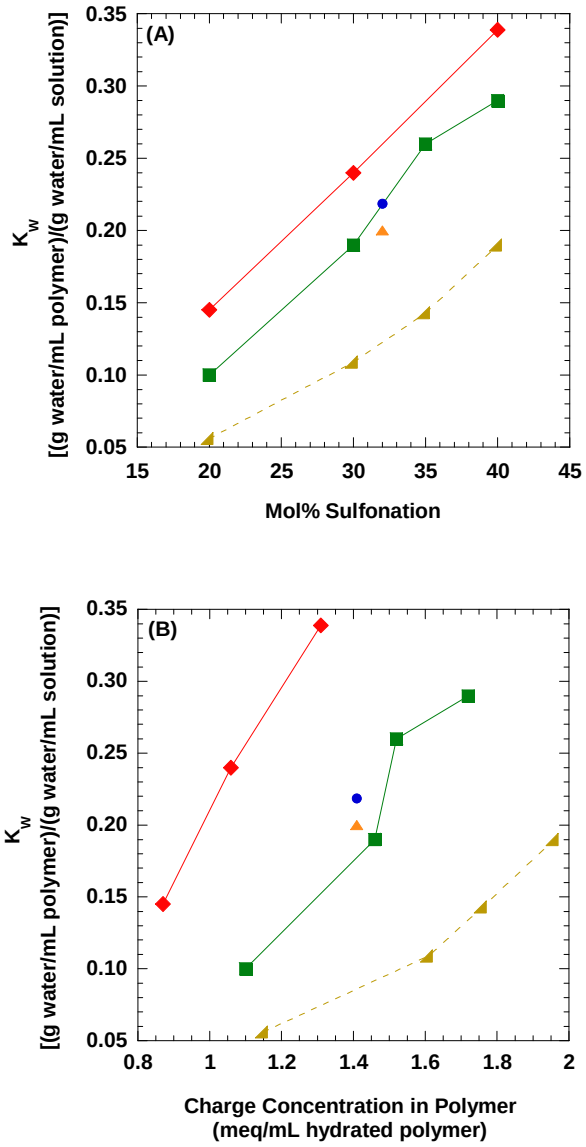

Figure 4.2. Water solubility coefficient (K_W) in as a function of composition (A) and hydrated charge concentration (B). (●) = BPS cast at 60 °C, (◆) = BisAS cast at 60 °C, (■) = BPS cast at 60 °C then 110 °C with vacuum,[1] (▲) = BPS cast under IR lamp then 150 °C with vacuum,[9] (◢) = BPS cast under IR lamp then 120 °C with vacuum.[2] The lines are drawn to guide the eye.

Hydraulic and diffusive water permeability coefficients, $P_{W,H}$ and P_W, were determined from dead end permeation experiments using pure water, and the results are

presented in Figure 4.3. Water diffusivity values were calculated from P_W and K_W and are presented in Figure 4.4. In the BisAS series, the water permeability increases with increasing degree of sulfonation, similar to the previously reported trends in the BPS series.[1] Free volume theory predicts greater solute permeability when K_W is higher,[29,30] so the BisAS materials should exhibit increasing water permeability with increasing degree of sulfonation. The BPS-32 material cast at 60 °C shows similar water permeability as the BisAS materials cast at 60 °C on the basis of degree of sulfonation, indicating that the thermal casting conditions can affect the transport properties, as evidenced by their sensitivity to processing history;[9] however, when viewed on the basis of charge concentration, the effect of backbone structure may still be observed, with the BisAS materials displaying higher water permeability than the BPS materials at similar charge concentrations due to their higher water uptake, which likely results from higher hydrated free volume due to less efficient chain packing in the BisAS materials. Both families of materials show an approximately exponential increase in water permeability as the degree of sulfonation, and thus K_W, increases. This rise in permeability results mainly from the increase in water diffusivity with increased water sorption, as seen in Figure 4.4. The diffusive water permeability does not show as strong an increase with degree of sulfonation as the hydraulic water permeability, which is reasonable considering that the calculation for P_W expressed in Equation 3.8 attempts to correct for the bulk water flow in water-swollen polymer films, which is greater as water sorption increases.

The BPS-32 material cast at 60 °C demonstrates similar values of water content as the BPS materials cast at 110 °C; this is consistent with the similar densities of BPS polymers at different casting conditions shown in Figure 4.1. As discussed above, the water permeability of the BPS-32 material cast at 60 °C is higher than that of the BPS materials cast at 110 °C, even though they have similar water sorption values. This

results in a higher calculated value of D_W in the BPS-32 polymer cast at 60 °C than in the BPS cast at 110 °C or even the BisAS samples cast at 60 °C, though the mechanism for this is not clear. In fact, this result is contradictory to the arguments advanced above regarding the effect of water uptake on small molecule transport in hydrated polymers. As a result, these experimental results should be viewed with great caution until and unless a rational explanation for these trends is proposed. In Figure 4.4 (A), the hollow symbols represent attempts during this study to replicate previously published results on polymers cast at maximum temperatures of 110 °C[1] and 150 °C[9] using both BPS-32 and BPS-35. These literature repeat samples showed higher water permeability than exhibited in previous studies; the thermal sensitivity of these materials in an aqueous environment has been explored,[9] and it is possible slight differences in the casting conditions could have contributed to the higher reading of permeability, though the cause is not clear at this time.

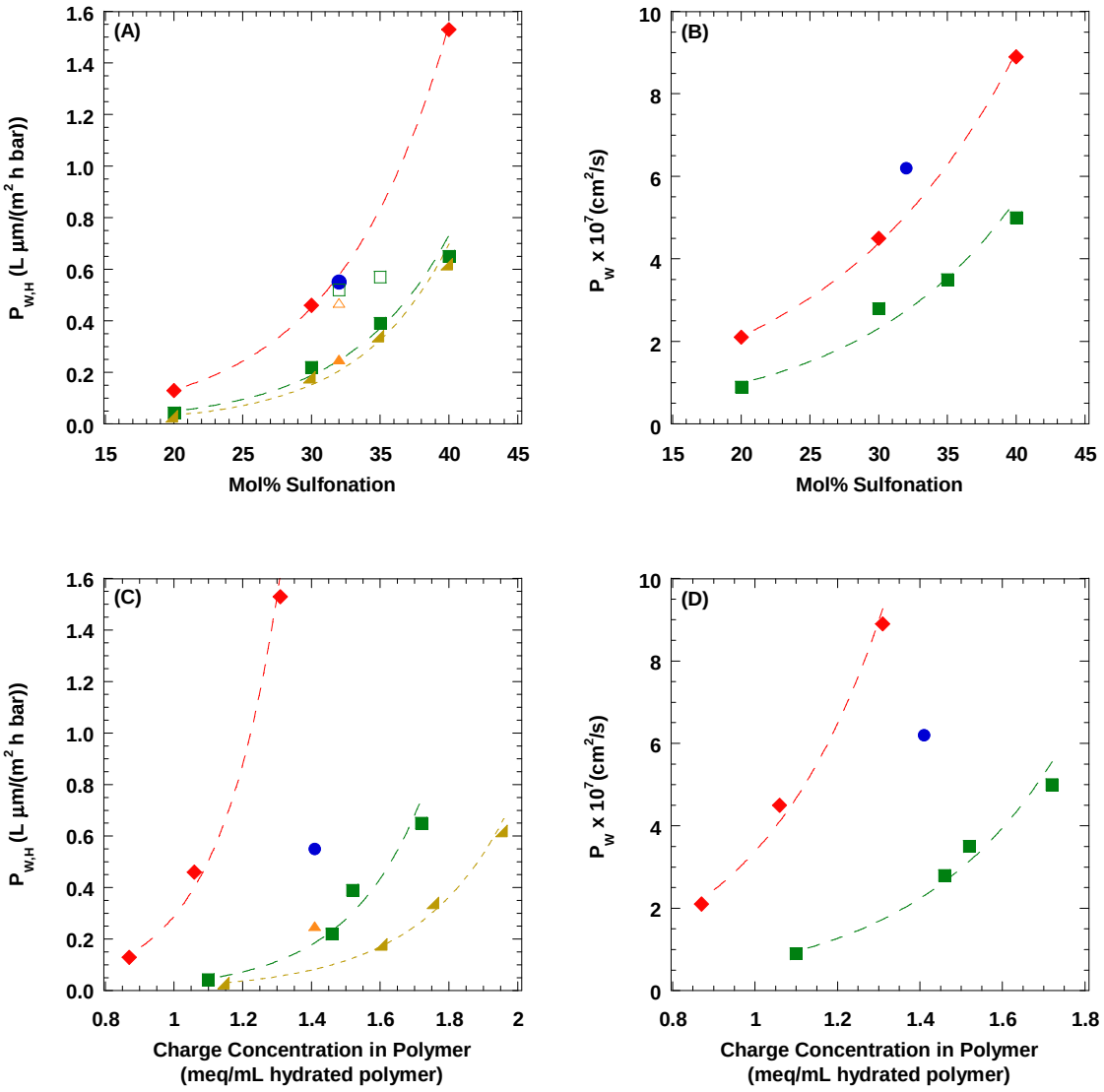

Figure 4.3. Hydraulic (A) and diffusive (B) water permeability as a function of polymer composition, and hydraulic (C) and diffusive (D) water permeability as a function of hydrated charge concentration. (●) = BPS cast at 60 °C, (◆) = BisAS cast at 60 °C, (■) = BPS cast at 60 °C then 110 °C with vacuum,[1] (□) = repeated samples of BPS cast at 60 °C then 110 °C with vacuum, (▲) = BPS cast under IR lamp then 150 °C with vacuum,[9] (△) = repeated samples of BPS cast under IR lamp then 150 °C with vacuum, (◢) = BPS cast under IR lamp then 120 °C with vacuum.[2] The lines are drawn to guide the eye.

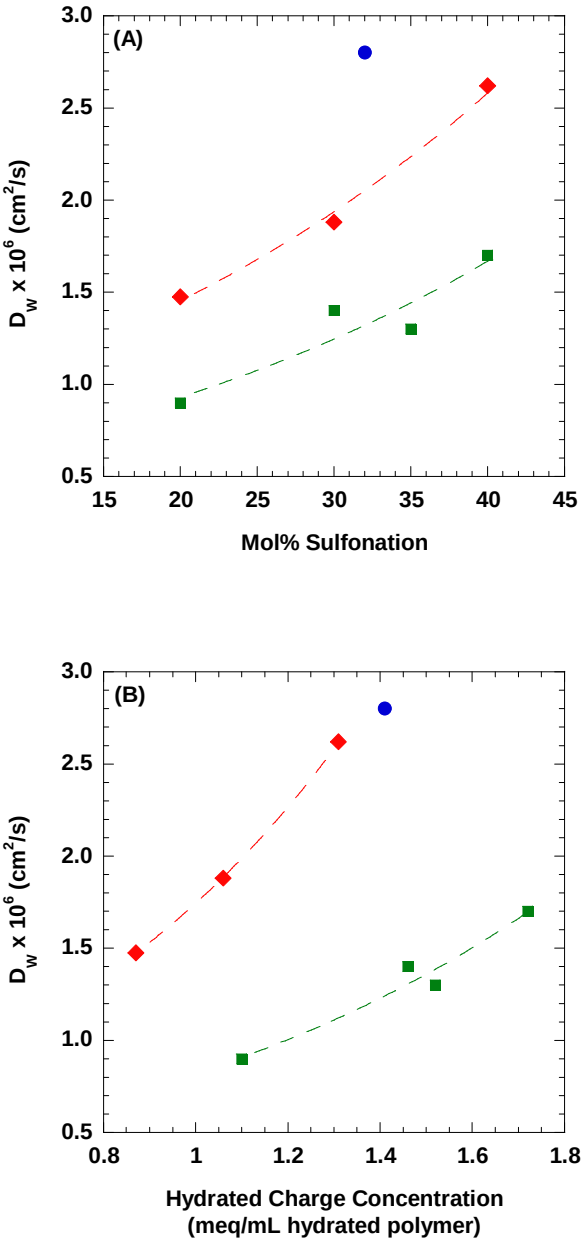

Figure 4.4. Water diffusivity as a function of polymer composition (A) and charge concentration (B). (●) = BPS cast at 60 °C, (◆) = BisAS cast at 60 °C, (■) = BPS cast at 60 °C then 110 °C with vacuum.[1] The lines are drawn to guide the eye.

Salt Transport Properties

Measurements of salt permeability in the BisAS materials were also performed in direct permeation cells using a 1 M sodium chloride solution in the donor cell; the results are reported in Figure 4.5. The BisAS series shows an increase in salt permeability as a function of increasing degree of sulfonation, which is consistent with the findings in the BPS series[1,2] and in other sulfonated polymers.[5,26,32] The BisAS materials also show higher salt permeability than the BPS materials from the literature[1,2,9] at similar degrees of sulfonation, and they show higher salt permeability than all BPS materials when considered on the basis of hydrated charge concentration. This phenomenon is to be expected, with the higher water uptake in the BisAS materials allowing faster transport of the sorbed ions through the polymer, as predicted by free volume theory.[29,30] Although the sulfonated polysulfones are subject to Donnan effects as demonstrated previously,[1,33] the increase in the concentration of fixed charged groups does not result in a net decrease in the salt permeability of the polymer, presumably because the higher water uptake at higher degrees of sulfonation more than offsets any potential reduction in permeability due to charge effects. The greater salt permeability in the BPS-32 material cast at 60 °C than the literature examples of BPS samples cast at higher temperatures[1,2,9] is consistent with the higher water permeability found in the BPS-32 material cast at 60 °C, though the greater salt permeability is not explained by water content effects. In Figure 4.5 (B), the BisAS materials demonstrate higher salt permeability than the BPS materials at similar charge concentrations, perhaps because the BisAS materials have, at comparable hydrated charge concentrations, higher water uptake than the BPS materials. Samples of BPS-32 and BPS-35 were prepared in accordance with the casting procedures published for the 110 °C vacuum dried samples,[1] which showed somewhat higher permeability than the literature examples, the cause of which has not been determined at this time.

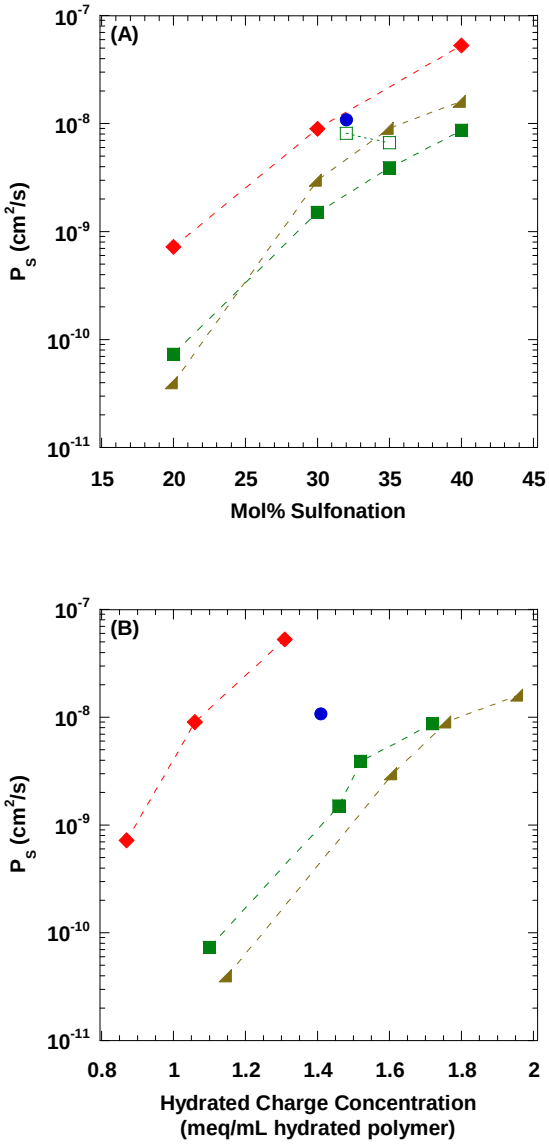

Figure 4.5. Salt Permeability as a function of polymer composition (A) and hydrated charge concentration (B). (●) = BPS cast at 60 °C, (◆) = BisAS cast at 60 °C, (■) = BPS cast at 60 °C then 110 °C with vacuum,[1] (□) = repeated samples of BPS cast at 60 °C then 110 °C with vacuum (water uptake data was not available, and these points are not shown in (B)), (◢) = BPS cast under IR lamp then 120 °C with vacuum.[2] The lines are drawn to guide the eye.

The effects of the composition of the polymer on the salt sorption coefficients of the BisAS materials can be seen in Figure 4.6. K_S was determined by desorption after equilibration in a solution of 1 M sodium chloride, and the BisAS and BPS materials show an increase in K_S with increasing degree of sulfonation. The Donnan effect would act to depress mobile salt concentration as the concentration of charged groups increased, all other factors being equal.[34,35] However, in BisAS and BPS[1] the increasing degree of sulfonation leads to an increase in water content which may contribute to higher salt sorption. The sorption of salt into non-ideal Donnan materials like these sulfonated polysulfones has been modeled by Geise et al., where the sorption of salt into the polymer is driven down by an increasing number of charged groups, but is driven up as the polymer's water uptake increases, resulting in a net increase of salt sorption with increasing sulfonate group concentration in the materials that have been studied so far.[33]

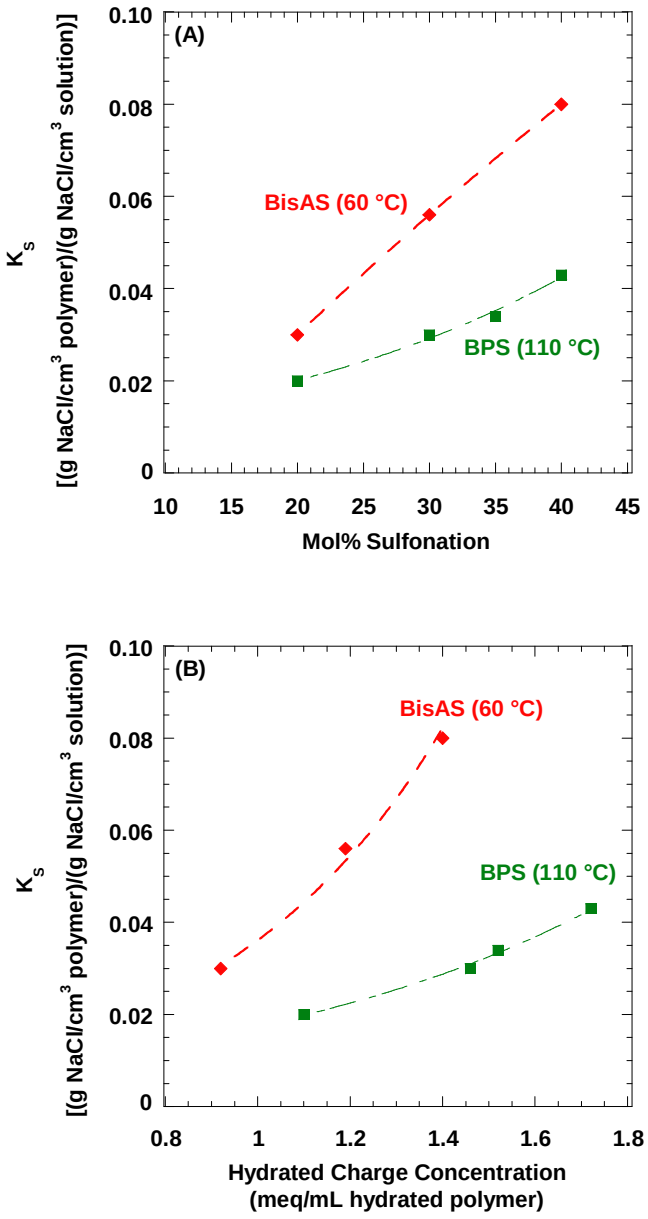

Figure 4.6. Salt sorption coefficient at 1 M NaCl as a function of composition (A) and hydrated charge concentration (B). (◆) = BisAS cast at 60 °C, (■) = BPS cast at 60 °C then 110 °C with vacuum.[1] The lines are drawn to guide the eye.

The salt sorption coefficients of the BisAS materials are plotted as a function of water sorption and compared to data from the literature collected on various uncharged materials[30] in Figure 4.7. One limit of the relation between salt and water sorption in a polymer is represented by the solid line in Figure 4.7.[30] In this limit, the salt is dissolved in the water in the polymer at the same concentration as in the external solution. However, even in uncharged materials, interactions between the polymer and sorbed ions reduce the concentration of salt in the polymer driving the K_S values below the plotted parity line.[30] The effect of Donnan exclusion can be seen in the BisAS and BPS materials, which are the only charged materials in this figure, where the K_S values of these charged materials are lower than those of uncharged polymers with similar K_W values, suggesting that Donnan exclusion is acting to reduce salt sorption. However, other phenomena, such as dielectric exclusion, may also be active and have not been considered in this study.

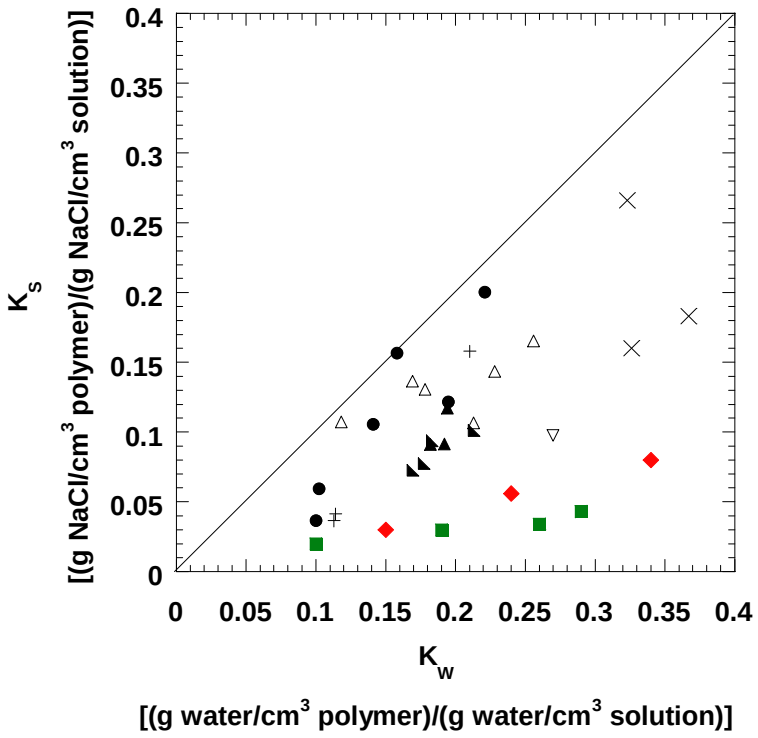

Figure 4.7. Salt sorption coefficient as a function of water sorption coefficient. (♦) = BisAS cast at 60 °C, (■) = BPS cast at 60 °C then 110 °C with vacuum,[1] (●) = methyl methacrylate - glycerol methacrylate (MMA/GMA),[30] (△) = hydroxypropyl methacrylate - methyl methacrylate (HPMA/MMA),[30] (◣) = HPMA,[30] (▽) = hydroxypropyl methacrylate - glycidyl methacrylate (HPMA/GdMA),[30] (+) = Cellulose Acetate,[30] (▲) = hydroxyethyl methacrylate - methyl methacrylate (HEMA/MMA),[30] (×) = HEMA,[30] (○) = hydroxypropyl methacrylate - glycerol methacrylate (HPMA/GMA).[30] The parity line represents a hypothetical material with equal K_W and K_S.

The polymer salt diffusivity coefficients were calculated from P_S and K_S using Equation 3.13, and are presented in Figure 4.8. The behavior of salt diffusivity in the BisAS and BPS[1] polymers as a function of degree of sulfonation is consistent with water and salt transport properties described thus far, where the increasing water content in the polymer as the degree of sulfonation increases leads to increasing salt diffusivity. The

BisAS materials also show higher salt diffusivity than BPS materials at similar degrees of sulfonation, potentially related to the BisAS series' higher water content. It is notable that while the salt sorption increases by roughly a factor of 3 from BisAS-20 to BisAS-40, the salt diffusivity increases by over an order of magnitude. This demonstrates that the diffusivity is more sensitive than the sorption to changes in water content, and that the increase in salt diffusivity is the primary factor for the increase in salt permeability with increasing degree of sulfonation.

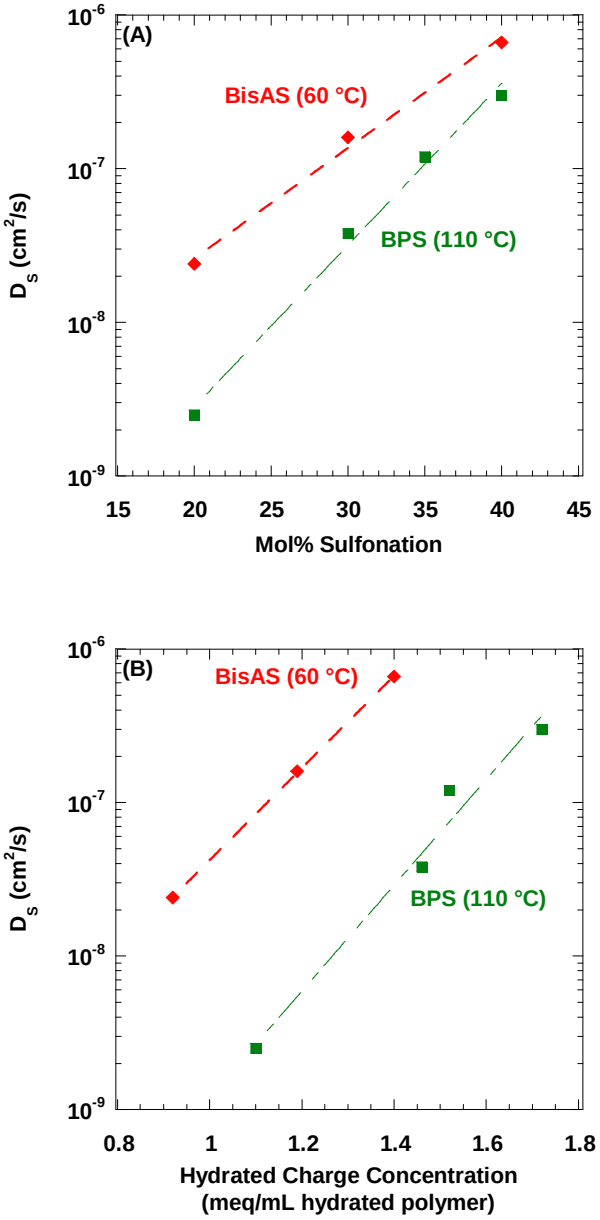

Figure 4.8. Salt diffusivity in sulfonated polysulfones as a function of composition (A) and hydrated charge concentration (B). (◆) = BisAS cast at 60 °C, (■) = BPS cast at 60 °C then 110 °C with vacuum.[1] Lines are drawn to guide the eye.

Free Volume Effects on Water/Salt Selectivity

As a polymer's water content changes, salt diffusivity in a polymer often changes more than that of water, presumably due, in part to, the larger size of hydrated ions relative to water molecules.[1] This effect is demonstrated in Figure 4.9, where the water and salt permeability coefficients and water and salt diffusivity coefficients reported above are plotted against the reciprocal of the water partition coefficient of the BisAS polymers. Figure 4.9 (B) demonstrates that while the water diffusivity decreases by roughly a factor of 2 as water content increases, the salt diffusivity decreases by roughly a factor of 27. Yasuda et al. relate the salt diffusivity to the water partition coefficient through the model presented in Equation 2.2:[30]

$$\ln D_S = \ln D_0 - B\left(\frac{1}{K_W} - 1\right) \tag{2.2}$$

where the constant D_0 is the diffusion coefficient of salt in water and B is a fitting parameter dependent on the characteristic volume for transport of the ionic solute in the polymer. Equation 2.2 shows that ln D_S is proportional to -1/K_W, which is consistent with the relationship shown in Figure 4.9 (B), where on a logarithmic scale the salt diffusivity shows a proportional decrease with increasing 1/K_W. As stated previously, the change in salt permeability is strongly driven by the changes in salt diffusivity, which is reflected in Figure 4.9 (A), where the salt permeability decreases as a function of 1/K_W to a greater extent than does the water permeability. The salt permeability and salt diffusivity of BisAS are presented in Figure 4.10 (A) and (B), respectively, in comparison to the values for the BPS series[1] and the uncharged polymers studied by Yasuda et al.[30] The dashed lines[1,32] represent a fit of the literature data to Equation 2.2 developed previously[1], and both the charged and uncharged materials show a reasonable conformation to these

trends, demonstrating that the transport properties of these materials are in agreement with free volume theory.

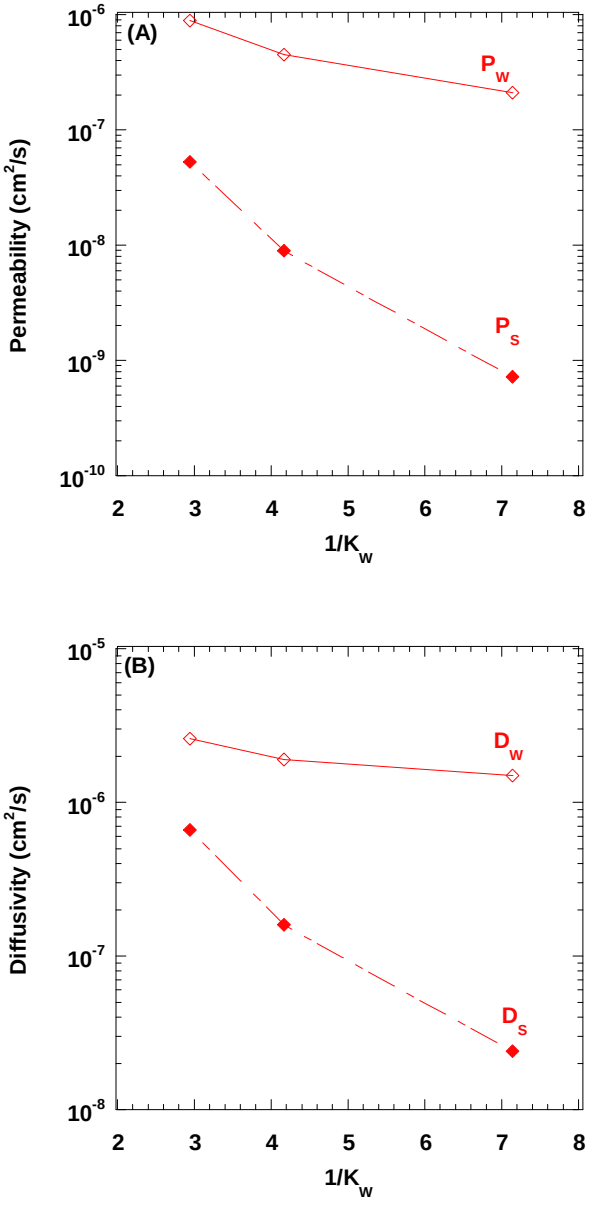

Figure 4.9. Changes in water and salt permeability (A) and diffusivity (B) of BisAS as a function of $1/K_W$.

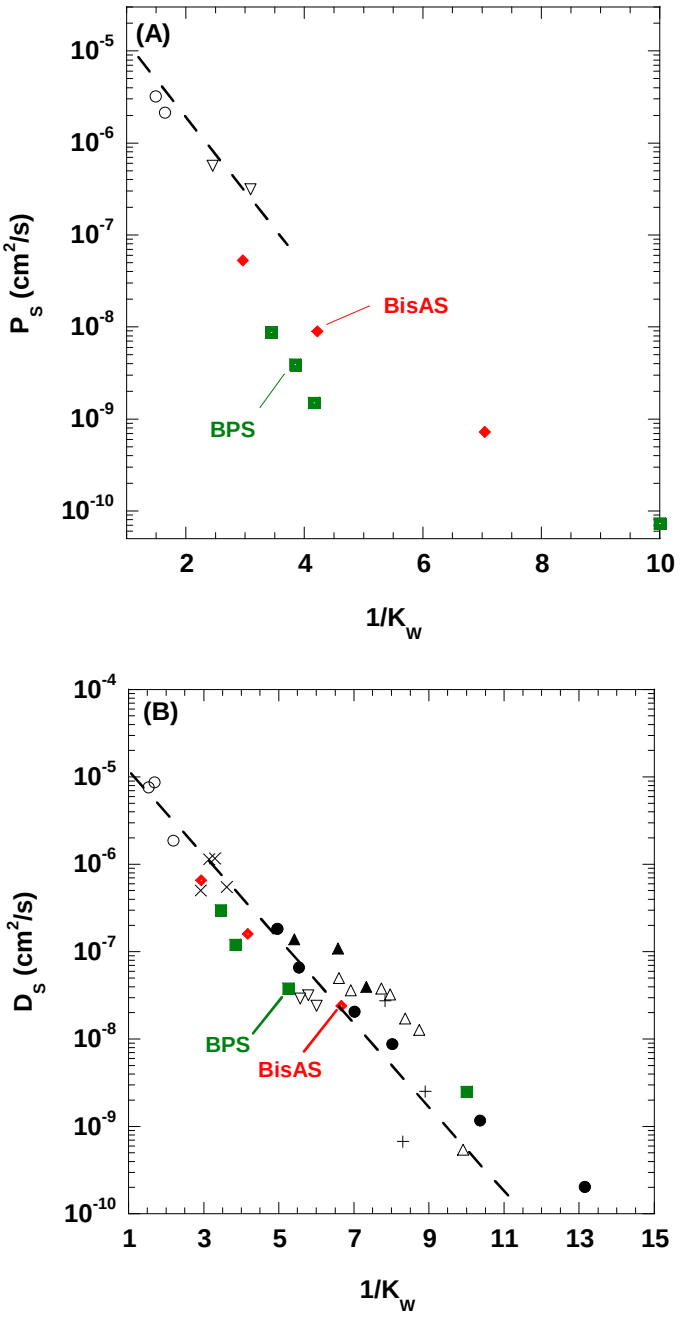

Figure 4.10. Salt permeability (A) and diffusivity (B) as a function of $1/K_W$. (♦) = BisAS cast at 60 °C, (■) = BPS cast at 60 °C then 110 °C with vacuum,[1] (●) = MMA/GMA,[30] (△) = HPMA/MMA, [30] (◣) = HPMA, [30] (▽) = HPMA/GdMA,[30] (+) = Cellulose Acetate,[30] (▲) = HEMA/MMA, [30] (×) = HEMA, [30] (○) = HPMA/GMA. [30] The dashed lines represent a fit of literature data to Equation 2.2.[1,32]

The water permeability/salt permeability selectivity values of the BisAS and BPS materials are plotted against water permeability and compared to different desalination materials from the literature[2,31,36–39] in Figure 4.11. The hydraulic permeability presented in Figure 4.3 (A) was converted to units of cm^2/s using Equation 3.8 with the term $(1-K_W)^2(1-2\chi \cdot K_W)$ set equal to 1; the diffusive water permeability has not been determined for all materials presented from the literature, and the hydraulic water permeability is a more relevant comparison. All materials lie below the empirically determined upper bound from the literature.[37] It is commercially desirable for materials to have high salt rejection along with high water permeability, driving the optimum relationship between selectivity and water permeability to the upper-right corner of the figure, towards or even beyond the upper bound.[37] Additionally, when the salt rejection, a common metric of desalination performance, is derived from the mass transport equations for water and salt, it is found to be dependent on hydraulic water permeability/salt permeability selectivity as follows:[40]

$$R(\%) = \frac{\frac{P_{W,H}}{P_S}\frac{\overline{V}}{RT}(\Delta p - \Delta \pi)}{1+\frac{P_{W,H}}{P_S}\frac{\overline{V}}{RT}(\Delta p - \Delta \pi)} \tag{4.1}$$

Figure 4.12 shows the water diffusivity/salt diffusivity selectivity as a function of salt diffusivity. The water diffusivity values in this figure are calculated from the hydraulic water permeability shown in Figure 4.11; thus while these values do not represent the true molecular diffusivity of water in the hydrated polymer, they serve as a comparison to the historic data from the literature. Figure 4.13 shows the tradeoff relationship between water sorption/salt sorption selectivity vs. water sorption coefficient. While salt content in the polymer does increase along with water content in

the polymer, the salt sorption is not as strongly affected by the water content as the salt diffusivity, and the BisAS and BPS[1] materials do not show a strong tradeoff in sorption selectivity as water sorption increases.

It has been demonstrated in this work that the changes in permeability over the range of degree of sulfonation in the BisAS polymers is driven strongly, though not solely, by the changes in diffusivity. Thus it is to be expected that there is similar trend in the diffusivity selectivity relationship (cf., Figure 4.12) as in the permeability selectivity relationship (cf., Figure 4.11), where the selectivity decreases as the water diffusivity or permeability increases. It has also been demonstrated that the salt diffusivity and salt permeability are more sensitive to the changes in water content in the polymer than are the water diffusivity and water permeability. This effect is responsible for the tradeoff relationships, whereby increasing water content allows for increasing water permeability, but to a greater extent increasing salt permeability. The increase of salt permeability drives down the water/salt permeability selectivity, and thus drives down salt rejection. It is also apparent from Figures 4.11 and 4.12 that the BisAS materials share qualitatively similar trends in selectivity with the reported BPS[1] materials, and are in line with the salt form and acid form (BPSH) in both tradeoff plots, though further towards the lower-right corner. This suggests that the BisAS materials (cast at 60 °C) perform similarly to hypothetical BPS materials (cast at 110 °C) of higher water uptake, and demonstrates the degree to which differences in water content drive differences in performance within the two polymer systems.

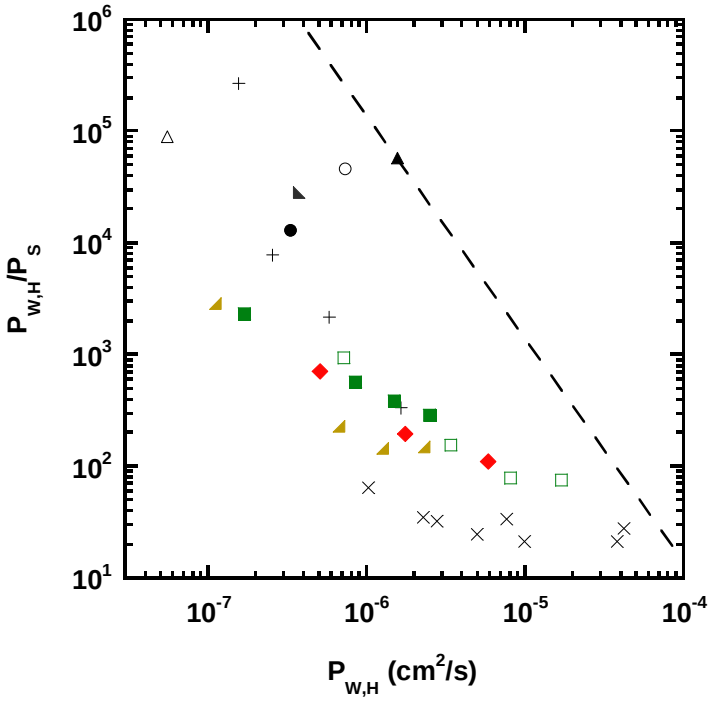

Figure 4.11. Water/Salt permeability selectivity tradeoff. (♦) = BisAS cast at 60 °C, (■) = BPS cast at 60 °C then 110 °C with vacuum,[1] (□) = BPSH cast at 60 °C then 110 °C with vacuum,[1] (◢) = BPS cast under IR lamp then 120 °C with vacuum,[2] (●) = Aromatic Polyamide,[36] (△) = Polyimide,[36] (◣) = PAH, [36] (+) = Cellulose Acetate,[38] (▲) = PBP,[36] (×) = PEG,[31] (○) = Aromatic Polyamide.[39] The dashed line represents the tradeoff upper bound from the literature.[37]

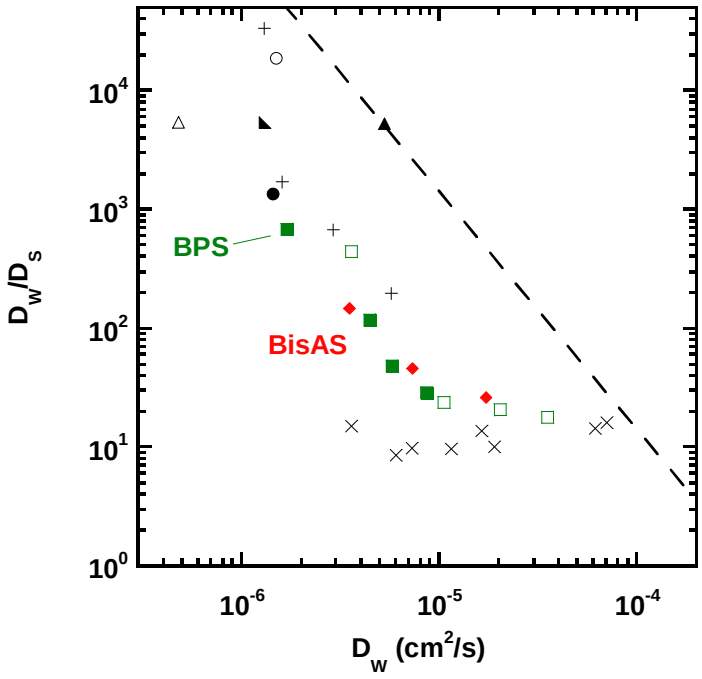

Figure 4.12. Water/salt diffusivity selectivity tradeoff. . (♦) = BisAS cast at 60 °C, (■) = BPS cast at 60 °C then 110 °C with vacuum,[1] (□) = BPSH cast at 60 °C then 110 °C with vacuum,[1] (●) = Aromatic Polyamide,[36] (△) = Polyimide,[36] (◣) = PAH, [36] (+) = Cellulose Acetate,[38] (▲) = PBP,[36] (×) = PEG,[31] (○) = Aromatic Polyamide.[39] The dashed line represents the tradeoff upper bound from the literature.[37]

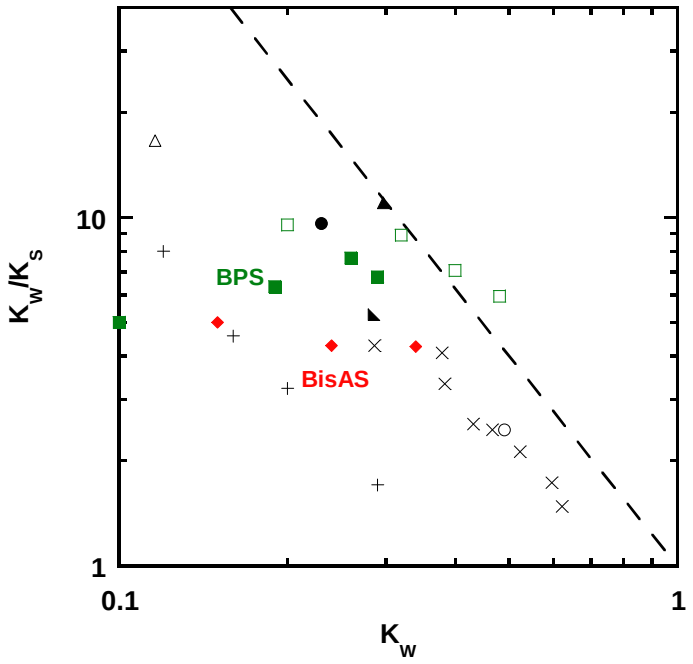

Figure 4.13. Water/Salt solubility selectivity tradeoff. (♦) = BisAS cast at 60 °C, (■) = BPS cast at 60 °C then 110 °C with vacuum, (□) = BPSH cast at 60 °C then 110 °C with vacuum, (●) = Aromatic Polyamide, (△) = Polyimide, (◣) = PAH, (+) = Cellulose Acetate, (▲) = PBP, (×) = PEG, (○) = Aromatic Polyamide. The dashed line represents the tradeoff upper bound from the literature.[37]

REFERENCES

1. W. Xie, J. Cook, H.B. Park, B.D. Freeman, C.H. Lee, J.E. McGrath. Fundamental salt and water transport properties in directly copolymerized disulfonated poly(arylene ether sulfone) random copolymers. *Polymer*. 52 (2011) 2032–2043.

2. H.B. Park, B.D. Freeman, Z.-B. Zhang, M. Sankir, J.E. McGrath. Highly chlorine-tolerant polymers for desalination. *Angewandte Chemie (International Ed in English)*. 47 (2008) 6019–6024.

3. J. Glater, S.K. Hong, M. Elimelech. The search for a chlorine-resistant reverse osmosis membrane. *Desalination*. 95 (1994) 325–345.

4. A. Noshay, L. Robeson. Sulfonated polysulfone. *Journal of Applied Polymer Science*. 20 (1976) 1885–1903.

5. C. Brousse, R. Chapurlat, J.P. Quentin. New membranes for reverse osmosis I. Characteristics of the base polymer: sulphonated polysulphones. *Desalination*. 18 (1976) 137–153.

6. P.L. Parise, A.E. Allegrezza Jr., B.S. Parekh. Reverse osmosis: Chlorine-resistant polysulfone reverse osmosis membrane and module. *Ultrapure Water*. (1987) 54–65.

7. A.E. Allegrezza Jr., B.S. Parekh, P.L. Parise, E.J. Swiniarski, J.L. White. Chlorine resistant polysulfone reverse osmosis modules. *Desalination*. 64 (1987) 285–304.

8. M. Padaki, A.M. Isloor, P. Wanichapichart, A.F. Ismail. Preparation and characterization of sulfonated polysulfone and N-phthloyl chitosan blend composite cation-exchange membrane for desalination. *Desalination*. 298 (2012) 42–48.

9. W. Xie, G.M. Geise, B.D. Freeman, C.H. Lee, J.E. McGrath. Influence of processing history on water and salt transport properties of disulfonated polysulfone random copolymers. *Polymer*. 53 (2012) 1581–1592.

10. C.H. Lee, D. VanHouten, O. Lane, J.E. McGrath, J. Hou, L.A. Madsen, J. Spano, S. Wi, J. Cook, W. Xie, H.J. Oh, G.M. Geise, B.D. Freeman. Disulfonated poly(arylene ether sulfone) random copolymer blends tuned for rapid water permeation via cation complexation with poly(ethylene glycol) oligomers. *Chemistry of Materials*. 23 (2011) 1039–1049.

11. S.G. Kimura. Reverse osmosis performance of sulfonated poly(2,6-dimethylphenylene ether) ion exchange membranes. *Industrial & Engineering Chemistry Product Research and Development*. 10 (1971) 335–339.

12. C. Friedrich, A. Driancourt, C. Noel, L. Monnerie. Asymmetric reverse osmosis and ultrafiltration membranes prepared from sulfonated polysulfone. *Desalination*. 36 (1981) 39–62.

13. J. Quentin. Sulfonated polyarylethersulfones. U.S. Patent Number 3,709,841. 1973.

14. A.F. Graefe, C.W. Saltonstall, W.J. Schell. Process for the preparation of a stable salt form of a sulfonated polyarylether sulfone. U.S. Patent Number 3,875,096. 1975.

15. A. Hamza, G. Chowdhury, T. Matsuura, S. Sourirajan. Sulphonated poly(2,6-dimethyl-1,4-phenylene oxide)-polyethersulphone composite membranes. Effects of composition of solvent system, used for preparing casting solution, on membrane-surface structure and reverse-osmosis performance. *Journal of Membrane Science*. 129 (1997) 55–64.

16. F. Wang, M. Hickner, Y.S. Kim, T.A. Zawodzinski, J.E. McGrath. Direct polymerization of sulfonated poly(arylene ether sulfone) random (statistical) copolymers: candidates for new proton exchange membranes. *Journal of Membrane Science*. 197 (2002) 231–242.

17. M.A. Hickner, H. Ghassemi, Y.S. Kim, B.R. Einsla, J.E. McGrath. Alternative polymer systems for proton exchange membranes (PEMs). *Chemical Reviews*. 104 (2004) 4587–4612.

18. W.L. Harrison, F. Wang, J.B. Mecham, V.A. Bhanu, M. Hill, Y.S. Kim, J.E. McGrath. Influence of the bisphenol structure on the direct synthesis of sulfonated poly(arylene ether) copolymers. I. *Journal of Polymer Science Part A: Polymer Chemistry*. 41 (2003) 2264–2276.

19. T. E. Long, Y. Li, F. Wang, J. Yang, D. Liu, A. Roy, S. Case, J. Lesko, J.E. McGrath. Synthesis and characterization of controlled molecular weight disulfonated poly(arylene ether sulfone) copolymers and their applications to proton exchange membranes. *Polymer*. 47 (2006) 4210–4217.

20. B. Kosmala, J. Schauer. Ion-exchange membranes prepared by blending sulfonated poly(2,6-dimethyl-1,4-phenylene oxide) with polybenzimidazole. *Journal of Applied Polymer Science*. 85 (2002) 1118–1127.

21. Agarwal, A.K., R.Y.M. Huang. Studies on the enhancement of separation characteristics of sulfonated poly(phenylene oxide)/polysulfone thin film composite membranes for reverse osmosis applications. I. Effect of chemical treatment. *Die Angewandte Makromolekulare Chemie*. 163 (1988) 1–13.

22. K.-J. Kim, G. Chowdhury, T. Matsuura. Low pressure reverse osmosis performances of sulfonated poly(2,6-dimethyl-1,4-phenylene oxide) thin film composite membranes: effect of coating conditions and molecular weight of polymer. *Journal of Membrane Science*. 179 (2000) 43–52.

23. A.K. Agarwal, R.Y.M. Huang. Studies on the enhancement of separation characteristics of sulfonated poly (phenylene oxide)/polysulfone thin film composite membranes for reverse osmosis applications II. Effects of nitromethane

and the chemical treatment combined with gamma-ray irradia. *Die Angewandte Makromolekulare Chemie*. 163 (1988) 15–21.

24. P. Chludzinski, J.F. Austin, J. Enos. Development of polyphenylene oxide membranes. *Office of Saline Water Research and Development Progress Report No 697*. (1971).

25. K. Ikeda, T. Nakano, H. Ito, T. Kubota, S. Yamamoto. New composite charged reverse osmosis membrane. *Desalination*. 68 (1988) 109–119.

26. R.J. Petersen. Composite reverse osmosis and nanofiltration membranes. *Journal of Membrane Science*. 83 (1993) 81–150.

27. C. Plummer, G. Kimura, A. LaConti. *Office of Saline Water Research and Development Progress Report No. 551*. 1970.

28. W. Xie, H. Ju, G.M. Geise, B.D. Freeman, J.I. Mardel, A.J. Hill, J.E. McGrath. Effect of free volume on water and salt transport properties in directly copolymerized disulfonated poly(arylene ether sulfone) random copolymers. *Macromolecules*. 44 (2011) 4428–4438.

29. H. Yasuda, C.E. Lamaze, A. Peterlin. Diffusive and hydraulic permeabilities of water in water-swollen polymer membranes. *Journal of Polymer Science Part A: Polymer Chemistry*. 9 (1971) 1117–1131.

30. H. Yasuda, C.E. Lamaze, L.D. Ikenberry. Permeability of solutes through hydrated polymer membranes, Part 1. Diffusion of sodium chloride. *Die Makromolekulare Chemie*. 118 (1968) 19–35.

31. H. Ju, A.C. Sagle, B.D. Freeman, J.I. Mardel, A.J. Hill. Characterization of sodium chloride and water transport in crosslinked poly(ethylene oxide) hydrogels. *Journal of Membrane Science*. 358 (2010) 131–141.

32. G.M. Geise, B.D. Freeman, D.R. Paul. Characterization of a sulfonated pentablock copolymer for desalination applications. *Polymer*. 51 (2010) 5815–5822.

33. G.M. Geise, L.P. Falcon, B.D. Freeman, D.R. Paul. Sodium chloride sorption in sulfonated polymers for membrane applications. *Journal of Membrane Science*. 423-424 (2012) 195–208.

34. F.G. Donnan. The theory of membrane equilibria. *Chemical Reviews*. 1 (1924) 73–90.

35. F.G. Donnan. Theory of membrane equilibria and membrane potentials in the presence of non-dialysing electrolytes. A contribution to physical-chemical physiology. *Journal of Membrane Science*. 100 (1995) 45–55.

36. W.J. Koros, G.K. Fleming, S.M. Jordan, T.H. Kim, H.H. Hoehn. Polymeric membrane materials for solution-diffusion based permeation separations. *Progress in Polymer Science*. 13 (1988) 339–401.

37. G.M. Geise, H.B. Park, A.C. Sagle, B.D. Freeman, J.E. McGrath. Water permeability and water/salt selectivity tradeoff in polymers for desalination. *Journal of Membrane Science*. 369 (2011) 130–138.

38. H.K. Lonsdale, U. Merten, R.L. Riley. Transport properties of cellulose acetate osmotic membranes. *Journal of Applied Polymer Science*. 9 (1965) 1341–1362.

39. M.A. Frommer, J.S. Murday, R.M. Messalem. Solubility and diffusivity of water and of salts in an aromatic polyamide film. *European Polymer Journal*. 9 (1973) 367–373.

40. G.M. Geise, H.-S. Lee, D.J. Miller, B.D. Freeman, J.E. McGrath, D.R. Paul. Water purification by membranes: the role of polymer science. *Journal of Polymer Science Part B: Polymer Physics*. 48 (2010) 1685–1718.

5. Effect of Mixed Valence Ionic Feeds on Water and Ion Permeability of Sulfonated Polysulfones

ABSTRACT

Sulfonated polysulfone films were subjected to reverse osmosis permeability measurements by crossflow filtration. Feed compositions consisted of aqueous solutions containing increasing concentrations of NaCl, as well as binary mixtures of NaCl and salts such as $CaCl_2$, $MgCl_2$, or Na_2SO_4. Water and ion permeability coefficients were determined as a function of feed composition. The presence of multivalent cations in the feed reduced the water permeability of the sulfonated polysulfones, possibly due to ionic crosslinking. Additionally, in the presence of multivalent cations, NaCl permeability in the polymers was higher, possibly due to the shielding of the fixed sulfonate charges on the polymer backbone.

RESULTS AND DISCUSSION

In order to provide some material comparison between the two sulfonated polysulfones, the water uptake of BPS-32 (cast at 60 °C for 8 h in air, followed by drying under vacuum at 120 °C for 12 h) and BisAS-35 (from Akron Polymer Systems, cast at 60 °C for 48 h in air) were measured, and are displayed in Table 5.1. Note that the water uptake and charge concentration for BPS-32 are similar to those of the BPS-32 sample cast at 60 °C in air presented in Chapter 4, which is consistent with the lack of significant change in density as a function of casting conditions reported in Figure 4.1.

Polymer (Potassium Form)	IEC (meq/g of dry polymer)	Water uptake (wt% of water in hydrated polymer)	Dry density (g/cm^3)	Hydrated charge concentration (meq/cm^3 hydrated polymer)
BPS-32	133	21 %	1.35	1.41
BisAS-35	1.30	28 %	1.29	1.23

Table 5.1. Material properties of random copolymers used in this study.

Salt permeability with a mixed anion feed

Since the polymers used in this study (cf., Figure 3.1) are cation exchange materials, their transport properties should be less affected by the presence of different species of anions in the feed solution than by the presence of multivalent cations that can undergo strong ionic interaction with the sulfonate groups on the polymer backbone. A control test was performed to verify this notion. Permeability measurements were undertaken using BPS-32 and BisAS-35 samples (Figure 5.1 (A) and (B), respectively) with a 34 mM sodium chloride feed solution. Sodium sulfate was added to this initial solution, at concentrations from 0.4 mM to 6.9 mM (i.e., 60 to 1000 ppm Na_2SO_4) as described in Chapter 3. These values are compared to the sodium permeability measured in the 16 mM to 48 mM (i.e., 940 to 2800 ppm NaCl) crossflow tests described above, though Figure 5.1 only shows the range of sodium concentrations present in the mixed $NaCl/Na_2SO_4$ feed solutions for comparison. In Figure 5.1, the sodium chloride permeabilities (P_{NaCl}) from both the NaCl only and mixed $NaCl/Na_2SO_4$ feed tests are presented as a function of the concentration of the common cation, Na^+. For both polymers, P_{NaCl} values were very similar with both the feed solution containing only NaCl and the mixed anion feed, increasingly slightly with total cation concentration. Thus, the presence of a divalent anion in the feed solution to this cation exchange membrane has a modest effect on salt permeability, similar to that observed when the anion is monovalent chloride. Presumably, this result is due to the lack of favorable

interactions of the divalent anion with the negatively charged sulfonate groups on the polymer backbone. As will be demonstrated below, the situation is quite different when a divalent cation is introduced into the feed.

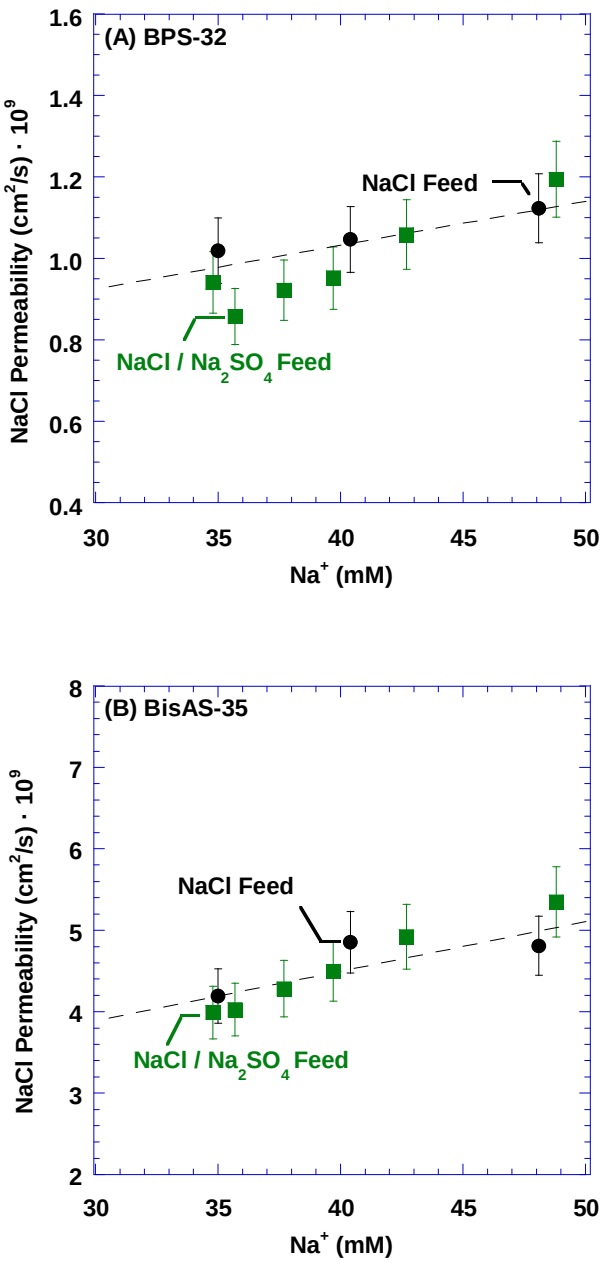

Figure 5.1. Permeability of sodium chloride in the presence of divalent anions in: (A) BPS-32 and (B) BisAS-35. (●) = NaCl permeability of the polymers with a feed solution containing only NaCl , (■) = NaCl permeability with a feed solution having a fixed NaCl concentration of 34 mM and an increasing Na_2SO_4 concentration.

Water permeability with a mixed cation feed

Water permeability was measured from the crossflow tests using a nominally 34 mM sodium chloride feed with calcium chloride added in increasing amounts, a 34 mM sodium chloride feed with an increasing concentration of magnesium chloride, and a feed solution containing only sodium chloride at various concentrations (the experimental feed concentration of NaCl varied slightly and is indicated on the following figures). The data from these tests are presented in Figure 5.2 as a function of the total concentration of chloride anions in the feed solution; the chloride anion is used as the abscissa since it is the common ion shared among all of the salts considered (i.e., $CaCl_2$, $MgCl_2$, and NaCl), and salt transport in cation exchange materials is often strongly influenced by the rate of transport of anions through the membrane.[1,2] With only sodium chloride in the feed solution, both polymers show little change in water permeability over the concentration range investigated. However, when a divalent cation was introduced to the feed mixture, water permeability decreased at even low concentrations of the divalent cation, and the water permeability decrease appears to plateau at higher concentrations of divalent cation concentrations considered. Previous studies suggest that charged polymers can experience ionic crosslinking in the presence of multivalent counterions, where the two charges on a divalent ion may interact with charged sulfonate groups bound to two different polymer chains or to two charged groups on the same chain.[3–7] This phenomenon effectively decreases the free volume available for water sorption,[8–11] which can decrease water permeability, qualitatively consistent with the trends observed in the BPS-32 and BisAS-35 data in Figure 5.2.

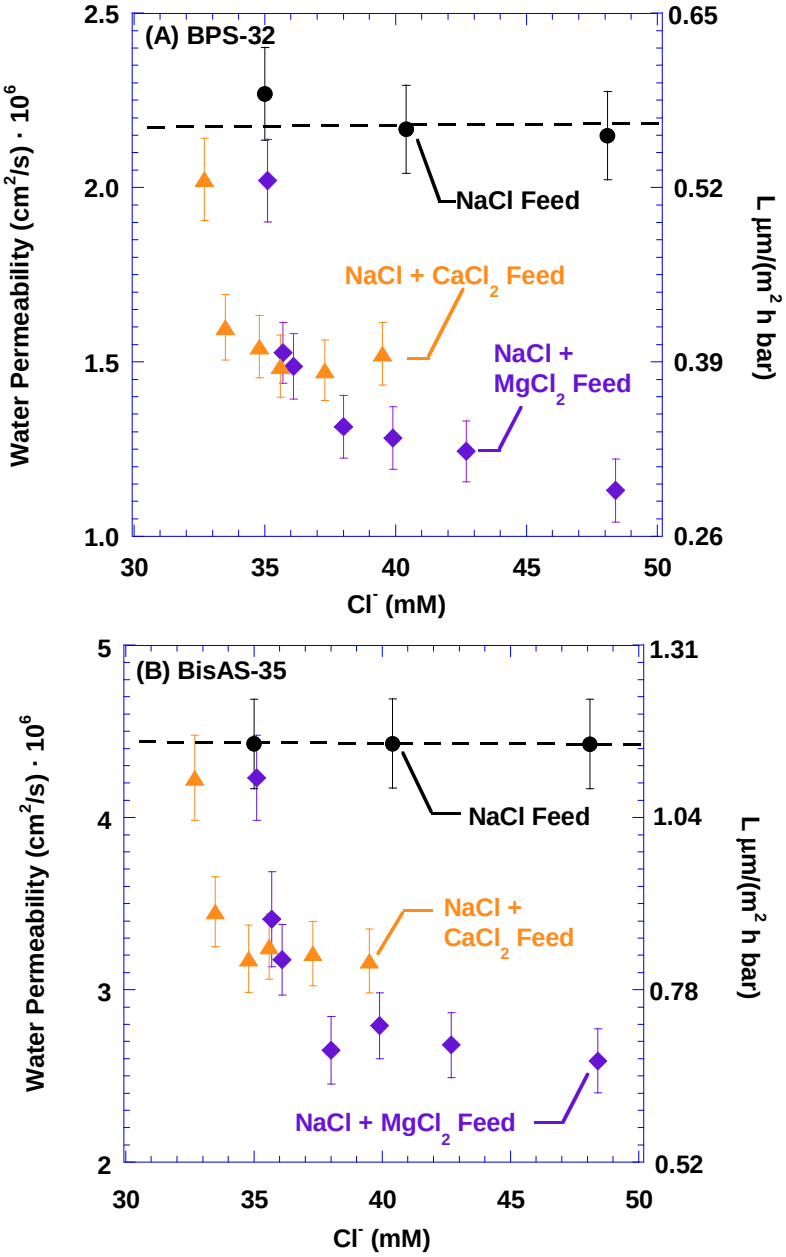

Figure 5.2. Water permeability in: (A) BPS-32 and (B) BisAS-35 in the presence of divalent cations. (●) = water permeability with an aqueous feed solution containing only NaCl, (▲) = water permeability with a mixed NaCl/$CaCl_2$ feed solution, (◆) = water permeability with a mixed NaCl/$MgCl_2$ feed solution. The first point of the mixed ion feed curves are measured using the initial NaCl only feed solution from those runs. The dashed lines represent a linear fit of the P_W values in the NaCl only tests.

Salt permeability with a mixed cation feed

From the crossflow tests in Figure 5.2, the cation permeability values for Na^+, Ca^{++}, and Mg^{++} may be determined using Equation 3.20. The permeability values of Na^+ and Ca^{++} using a mixed $NaCl/CaCl_2$ feed are presented in Figure 5.3 (A) as a function of the calcium ion concentration in the feed mixture. Similarly, the permeability values for Na^+ and Mg^{++} using a mixed $NaCl/MgCl_2$ feed are presented in Figure 5.3 (B) as a function of the magnesium ion concentration in the feed mixture. In both polymers, sodium permeability (and, therefore, sodium chloride permeability) increases as the feed concentration of divalent cation increases. In previous studies of BPS-32,[12] as well as other charged polymers,[13,14] sodium chloride permeability was found to increase at higher feed concentrations of sodium chloride. This increase in permeability has been ascribed to an increase salt sorption, K_S, perhaps due at least in part to screening of the Donnan effect,[1,15–17] as well as increasing salt diffusivity, D_S.[2] The effect of increasing salt permeability with increasing divalent salt content in the feed appears qualitatively consistent with the salt permeability rise resulting from increasing monovalent salt content.

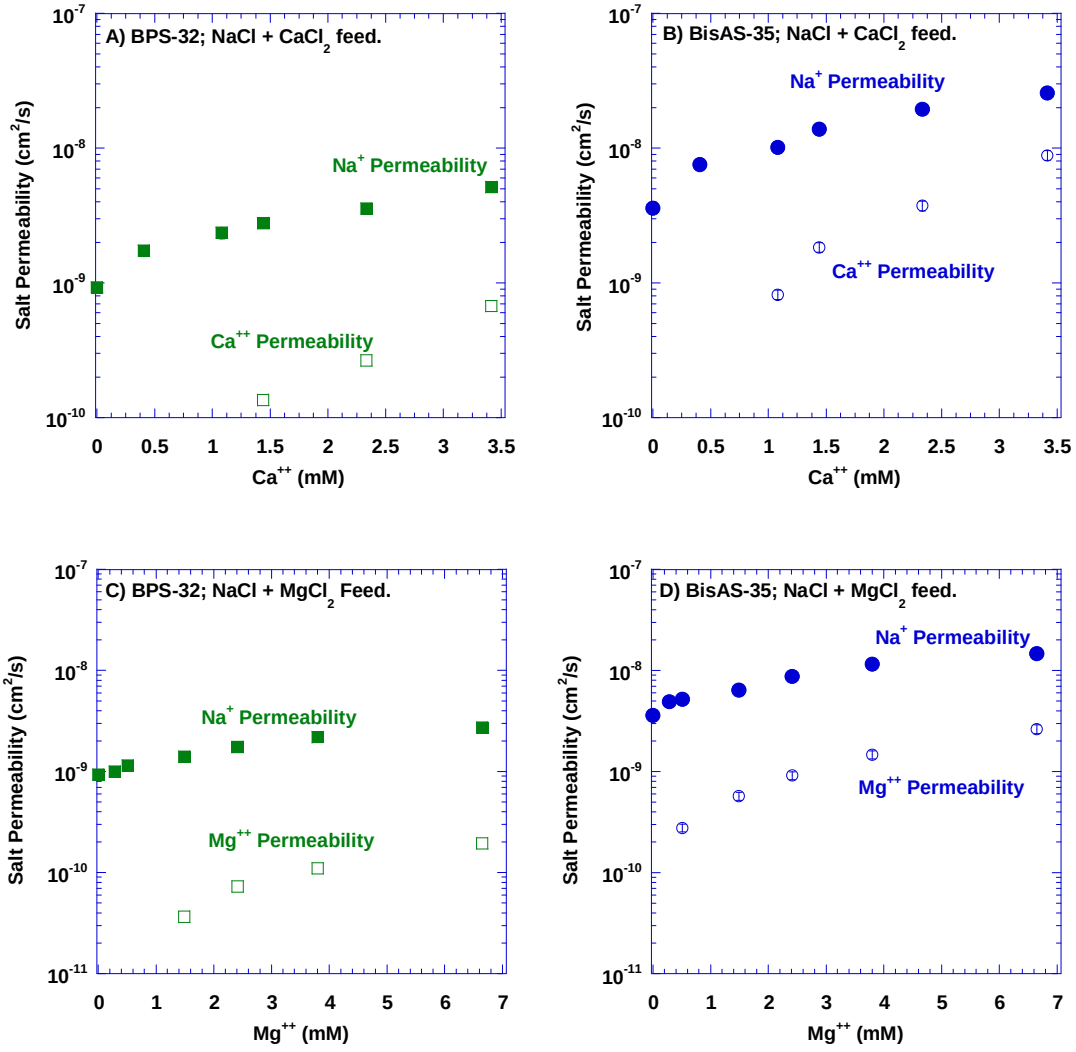

Figure 5.3. Cation permeabilities of sulfonated polysulfones with a: (A and B) mixed sodium chloride/calcium chloride feed, or (C and D) mixed sodium chloride/magnesium chloride feed. (■) = Na^+ permeability in BPS-32, (□) = divalent cation permeability in BPS-32, (●) = Na^+ permeability in BisAS-35, (○) = divalent cation permeability in BisAS-35.

Parise et al. reported salt passage test results on a bisphenol-A based polysulfone that was sulfonated after polymerization, and their results are presented in Figure 5.4 (A).[18] In these studies, the passage of calcium with a feed solution consisting of increasing concentrations of only calcium chloride is recorded (see the data labeled Ca^{++} (Pure Feed) in Figure 5.4 (A)). This calcium chloride only feed test is then compared to the passage of calcium and sodium using a feed solution consisting of 130 ppm sodium chloride and increasing concentrations of calcium chloride (see the data labeled Ca^{++} (Mixed Feed) in Figure 5.4 (A)).[18] Figure 5.4 (B) presents sodium and calcium passage values in a BPS-32 sample calculated from the tests using a 34 mM NaCl (2000 ppm NaCl, or 780 ppm Na^{+}) aqueous feed with increasing concentration of $CaCl_2$ shown in Figure 5.2 (A) and Figure 5.3 (A). Additionally, crossflow testing was performed on samples of BPS-32 using a feed solution containing only $CaCl_2$, and the passage values from these experiments are also shown in Figure 5.4 (B).

The polysulfone samples from the Parise et al. study[18] and this study demonstrate similar trends, where both sodium and calcium passage increase as increasing amounts of calcium are added to a feed solution containing sodium chloride, consistent with the previously discussed effects of Donnan exclusion screening and charge neutralization. However, a comparison of the calcium passage values reveals that in both materials, the divalent ion passage is higher in a calcium chloride only solution than in a solution containing mixtures of calcium and sodium chloride. Thus, while the presence of both monovalent and divalent cations in the feed solution increases the monovalent ion transport, such a mixed feed appears to inhibit the transport of the divalent cation since, for both materials, the calcium passage in the mixed feed is considerably lower than that in a feed solution containing only calcium chloride (i.e., with no NaCl present). However,

a fundamental explanation for this phenomenon and a detailed model to predict it is not available at this time.

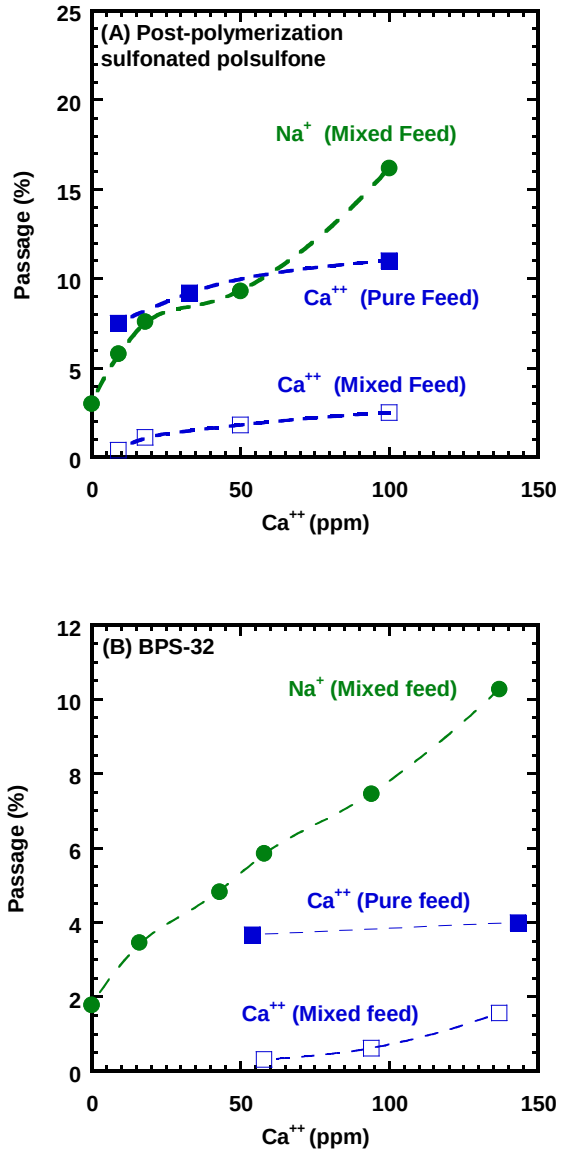

Figure 5.4. Comparison of cation passage with a mixed sodium/calcium feed in a post-polymerization sulfonated polysulfone (A)[18] and in BPS-32 (B). (●) = sodium passage with a mixed sodium/calcium feed, (■) = calcium passage with a feed solution containing only $CaCl_2$, (□) = calcium passage with a mixed sodium/calcium feed. The lines are drawn to guide the eye.

Figure 5.5 shows NaCl permeability coefficients as a function of feed chloride concentration for BPS-32 and BisAS-35 using NaCl only, mixtures of NaCl and $CaCl_2$, and mixtures of NaCl and $MgCl_2$ in the feed solution from the same crossflow tests whose results are reported in Figure 5.2 and Figure 5.3. Focusing first on the feed solution containing only NaCl, both polymers display an increase in NaCl permeability similar to that reported previously for sulfonated polymers.[5,13] However, when a divalent cation is added to the feed in similar amounts (based on the concentration of cation charges), both sulfonated polysulfones show a much greater increase in NaCl permeability than when the only salt in the feed solution is NaCl. Multivalent ions may bind more strongly with sulfonate groups on the polymer backbone and effectively shield or neutralize those charges, reducing the ability of the negative sulfonate groups to impede salt transport through the polymer.[5,6,18–21] This will be discussed in greater detail in Chapter 6. Additionally, salt permeability in these materials is also influenced by free volume effects, where increases in water uptake in a polymer typically increases water permeability, and increases salt permeability even more than that of water.[12,22,23] If the decreases in water permeability shown in Figure 5.2 result from decreasing water uptake in the polymers due to, for example, ionic crosslinking and osmotic deswelling, then presumably these effects would act to lower the salt permeabilities. However, because the salt permeabilities increase rather than decrease as divalent salt concentration increases, the charge shielding and other ionic effects acting on salt permeabilities may be even stronger than is apparent from these measurements.

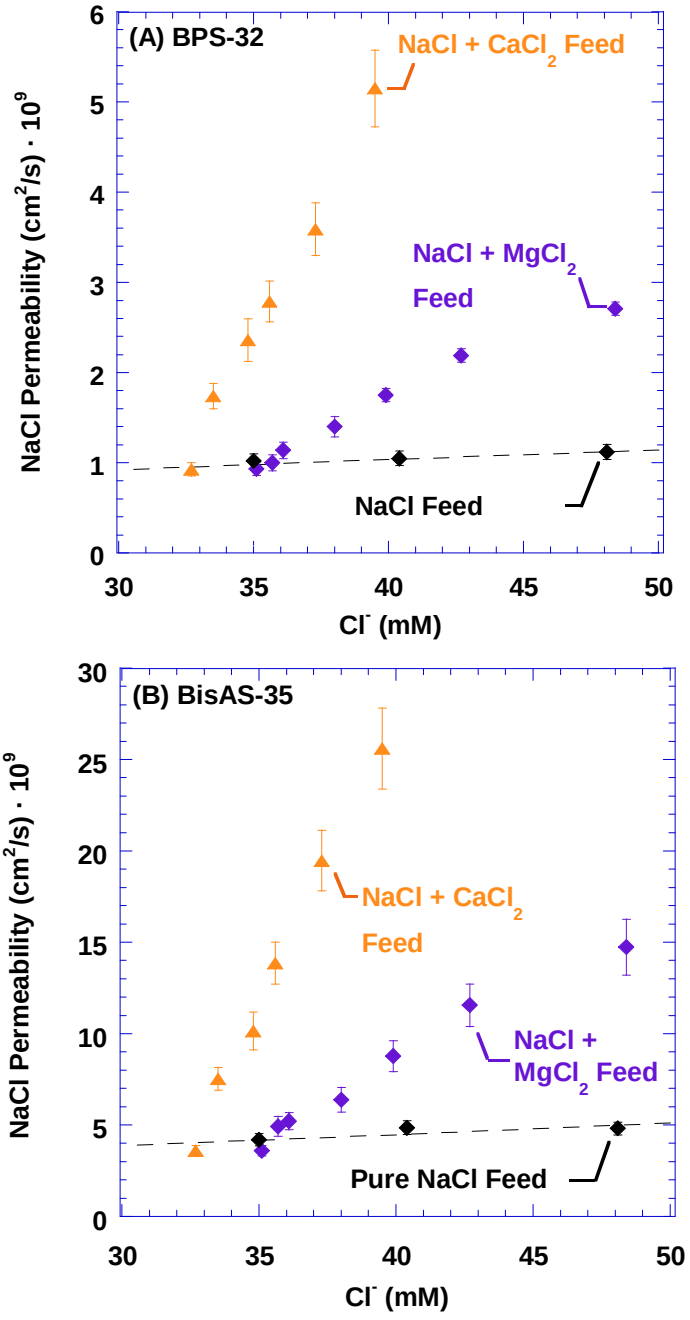

Figure 5.5. Sodium chloride permeability in BPS and BisA in mixed ion and NaCl only feeds. (●) = NaCl permeability with a feed solution containing only NaCl, (▲) = NaCl permeability with a mixed NaCl/$CaCl_2$ feed, (◆) = NaCl permeability with a mixed NaCl/$MgCl_2$ feed. The first point of each mixed ion feed curve is the permeability value for the initial NaCl only feed.

Both polymers exhibit higher NaCl permeability in the presence of calcium than in the presence of magnesium. Based upon ion sorption equilibrium studies conducted on Dowex 50 crosslinked sulfonated polystyrene ion exchange resins, calcium has a greater affinity than magnesium for sulfonate groups.[24] Thus, at equal concentrations of $CaCl_2$ and $MgCl_2$ in the feed, the calcium cations should sorb into the polymer at greater concentrations than magnesium cations, more effectively shielding the sulfonate anions, and thus increasing the NaCl permeability more. Chapter 6 will evaluate the ion and water sorption of the BPS-32 polymer when equilibrated in salt solutions of the same compositions as the feed solutions used in this chapter.

Figure 5.6 presents the NaCl permeabilities from Figure 5.5 relative to the NaCl permeability in the feed solution containing only NaCl used at the beginning of each mixed ion experiment. NaCl permeability increases approximately 2 times in BPS-32 and 3 times in BisAS-35 in the presence of 4 mM of Mg^{++}, while the NaCl permeability increases about 5.5 times for BPS-32 and 7 times for BisAS-35 in the presence of similar concentrations of Ca^{++}. Thus, there is also an effect of polymer backbone structure on the magnitude of the NaCl permeability increase in these mixed ion environments. As discussed above, decreasing water content often has the effect of reducing salt permeability. Since the BisAS-35 has higher water uptake and a lower concentration of sulfonate groups in the hydrated polymer than BPS-32 (cf., Table 5.1), the BisAS-35 may experience less dampening of the divalent cation-driven increases in NaCl permeability due to free volume effects. However, a complete, molecular level understanding of the differences in the influences of these divalent ions on polymers of various backbone structures is not currently available.

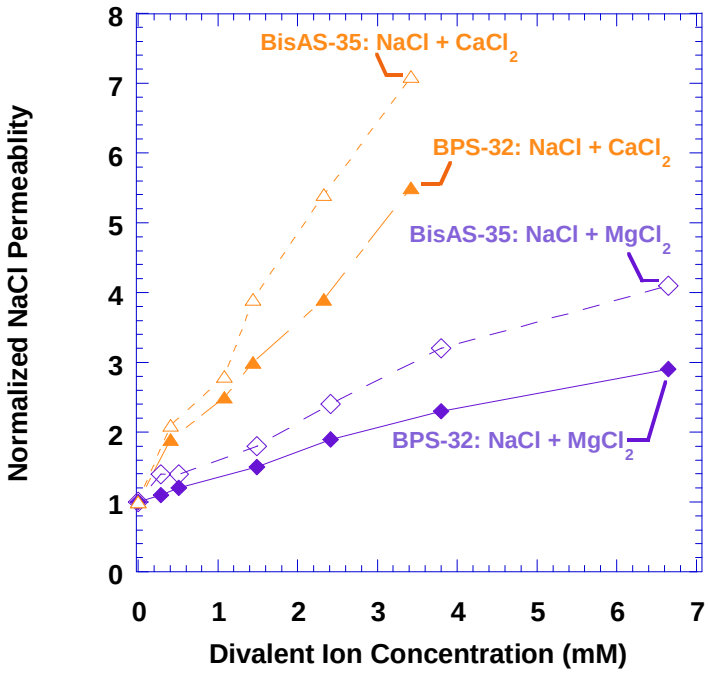

Figure 5.6. NaCl permeability of BPS-32 and BisAS-35 in mixed ion feeds normalized by the initial permeability of sodium chloride in a feed solution containing only NaCl. (▲) = normalized NaCl permeability of BPS-32 in a mixed NaCl/$CaCl_2$ feed, (△) = normalized NaCl permeability of BPS-32 in a mixed NaCl/$CaCl_2$ feed, (◆) = normalized NaCl permeability of BPS-32 in a mixed NaCl/$MgCl_2$ feed, (◇) = normalized NaCl permeability of BisAS-35 in a mixed NaCl/$MgCl_2$ feed.

To confirm that these effects are in fact due to interactions between the ions and the charged polymers rather than any non-ideal thermodynamic effects on the driving force for ion transport, the mean activity coefficients of NaCl in NaCl-$CaCl_2$ and NaCl-$MgCl_2$ mixtures were calculated using the Pitzer model for mixed electrolyte solutions.[25] The activity coefficients were calculated for solutions containing only NaCl, mixtures of NaCl and $CaCl_2$ and mixtures of NaCl and $MgCl_2$. The results of these calculations are displayed in Figure 5.7. The activity coefficients are less than unity and decrease with

increasing salt concentration, as expected.[25] The addition of the divalent cation salts used in this study to a 34 mM (i.e., 2000 ppm) NaCl feed solution has only a small effect on the NaCl activity coefficient.

To provide an example of the impact of this effect on permeation properties, NaCl permeability was recalculated using salt activity difference across the polymer sample as the driving force for ion transport (rather than salt concentration difference) in Equation 3.20 for BPS-32, as shown below:

$$P_{Na} = \frac{J_{Na} \cdot l}{a_{Na,f} - a_{Na,p}} \tag{5.1}$$

The example calculation was undertaken at conditions where the feed solution contained 34 mM NaCl and 3.4 mM $CaCl_2$, which is the feed solution composition at which the most significant increase in NaCl permeability was observed. The results are recorded in Table 1. For the feed solution containing only NaCl, the NaCl permeability coefficient calculated based on activity is higher than that based on concentration, as expected since the activity coefficient is less than unity. The NaCl permeability coefficient calculated based on activity in the feed solution containing only NaCl is practically the same as that calculated based on activity when the feed solution contained a mixture of NaCl and $CaCl_2$ since the activity coefficient of NaCl is practically the same in these two solutions. Thus, at the relevant concentrations, the change in NaCl activity due to presence of $CaCl_2$ cannot account for strong increase in NaCl permeability observed when $CaCl_2$ was added to the feed solution; similar principles apply for mixtures of NaCl and $MgCl_2$.

Permeability (P_{NaCl} (cm^2/s) · 10^9) calculated based on:		
Concentration difference for solution containing only NaCl	Activity difference for solution containing only NaCl	Activity difference for a solution containing a mixture of NaCl and $CaCl_2$
4.74	6.24	6.25

Table 5.2. Effect thermodynamic activity correction on the calculated NaCl permeability of BPS-32.

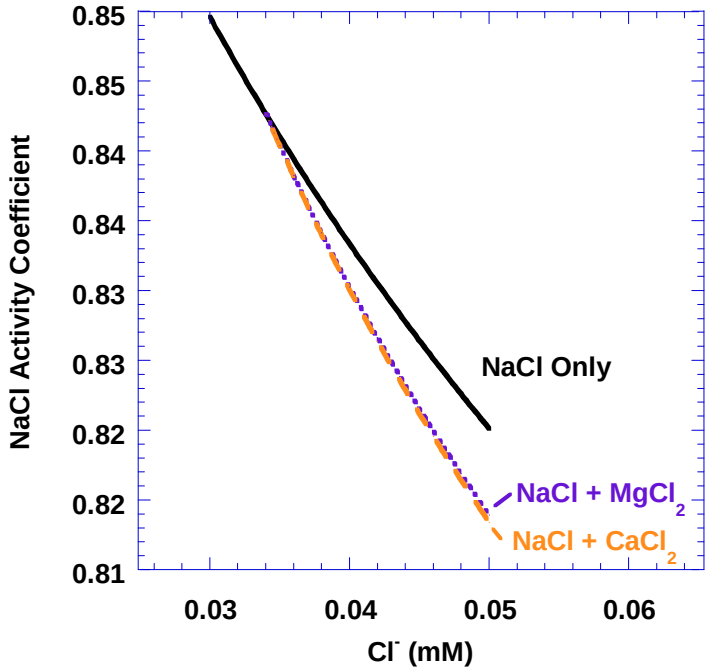

Figure 5.7. Activity coefficients for NaCl in solutions containing: (a) only 34mM NaCl, (b) 34 mM NaCl with increasing $CaCl_2$ concentration, and (c) 34 mM NaCl with increasing $MgCl_2$ concentration.

Water/salt permeability selectivity

Another fundamental property of desalination materials is the water/salt permeability selectivity, $P_{W,H}/P_S$. As discussed in Chapter 4, salt rejection depends on permeability selectivity; all other factors being equal, as selectivity increases, due to

either increasing water permeability or decreasing salt permeability, salt rejection increases, from Equation 4.1:[14]

$$R(\%) = \frac{\frac{P_{W,H}}{P_S}\frac{\overline{V}}{RT}(\Delta p - \Delta\pi)}{1 + \frac{P_{W,H}}{P_S}\frac{\overline{V}}{RT}(\Delta p - \Delta\pi)} \tag{4.1}$$

The permeability selectivity also serves as another marker for the effects of divalent cations on polymer transport properties.

Values for water/NaCl permeability selectivity were calculated from the water and salt permeability values in Figures 5.2 and 5.3, and they are presented as a function of divalent ion concentration in Figure 5.8. The initial values for selectivity are those of the BPS-32 and BisAS-35 films using a feed solution containing approximately 34 mM NaCl. Both increasing NaCl permeability and decreasing water permeability act to decrease selectivity. As shown in Figure 5.4, the decreasing selectivity also manifests itself as increasing NaCl passage as $CaCl_2$ feed concentration increases.

In many desalination materials, increasing water content increases both salt and water permeability, with salt permeability increasing more than that of water due to the transport of the larger hydrated ions benefiting more from the increases in free volume brought about by increased water uptake.[12,22,23,26] This phenomenon results in a tradeoff where increasing water permeability is often accompanied with decreasing water/salt permeability selectivity.[26] The selectivity values from Figure 5.8 are plotted against the empirically derived upper bound[26] as a function of $P_{W,H}$ in Figure 5.9. As the divalent ion concentration increases, decreasing selectivity and decreasing water permeability move the transport properties away from the upper bound.

Developing a better fundamental understanding of phenomena such as the influence of divalent ion sorption and diffusion on monovalent ion transport would be an

important step in understanding the molecular basis for such phenomena and learning how to control them via rational polymer design.

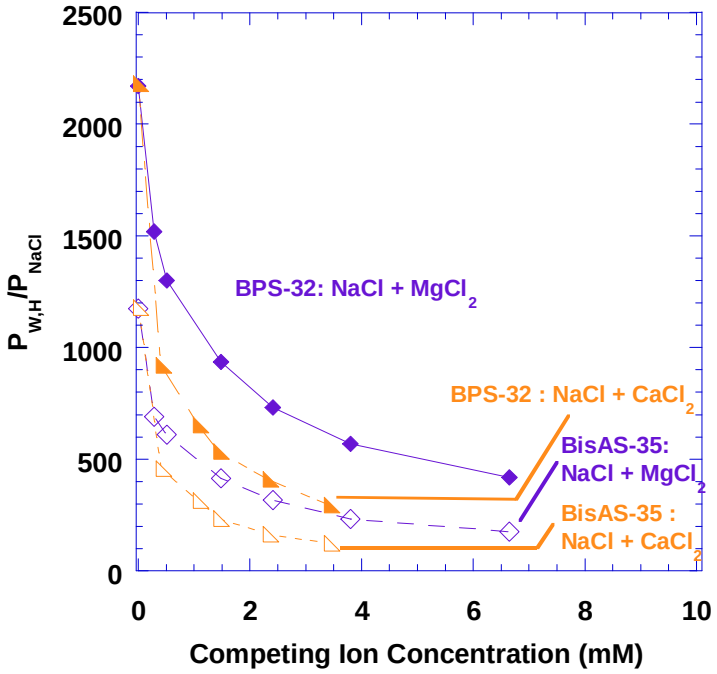

Figure 5.8. Water/sodium chloride permeability selectivity in BPS-32 and BisAS-35 in the presence of divalent cations. (▲) = selectivity of BPS-32 in a mixed NaCl/$CaCl_2$ feed, (△) = selectivity of BPS-32 in a mixed NaCl/$CaCl_2$ feed, (◆) = selectivity of BPS-32 in a mixed NaCl/$MgCl_2$ feed, (◇) = selectivity of BisAS-35 in a mixed NaCl/$MgCl_2$ feed. The first selectivity value is from the feed solution containing only NaCl recorded at the beginning of each mixed ion set of experiments.

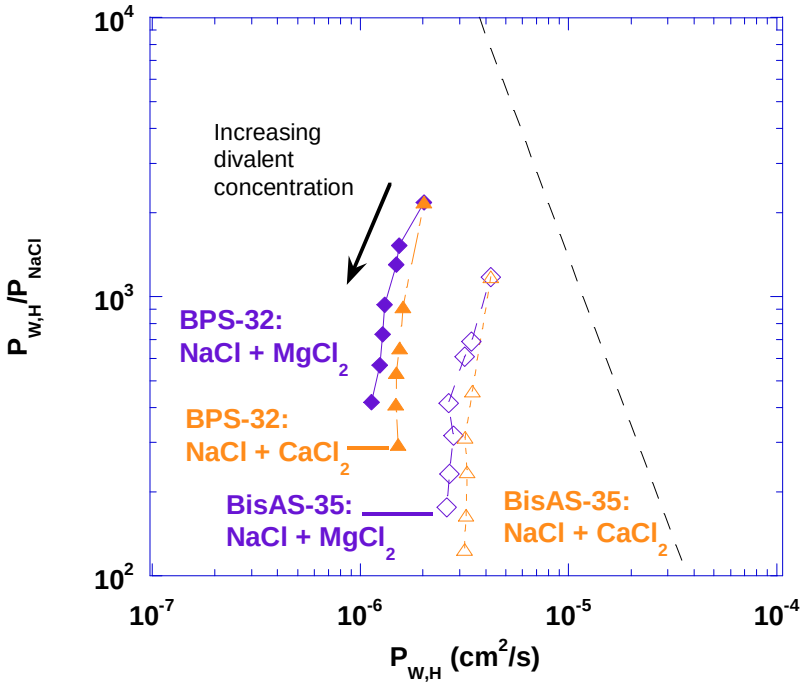

Figure 5.9. Water/sodium chloride permeability selectivity vs. water permeability of BPS-32 (filled symbols) and BisAS-35 (hollow symbols). (▲) = selectivity of BPS-32 in a mixed NaCl/$CaCl_2$ feed, (△) = selectivity of BPS-32 in a mixed NaCl/$CaCl_2$ feed, (◆) = selectivity of BPS-32 in a mixed NaCl/$MgCl_2$ feed, (◇) = selectivity of BisAS-35 in a mixed NaCl/$MgCl_2$ feed. The first selectivity value is from the feed solution containing only NaCl recorded at the beginning of each mixed ion set of experiments. The tradeoff upper bound (i.e., the straight dashed line on this figure) is from Geise et al.[26]

REFERENCES

1. G.M. Geise, L.P. Falcon, B.D. Freeman, D.R. Paul. Sodium chloride sorption in sulfonated polymers for membrane applications. *Journal of Membrane Science*. 423-424 (2012) 195–208.

2. G.M. Geise, B.D. Freeman, D.R. Paul. Sodium chloride diffusion in sulfonated polymers for membrane applications. *Journal of Membrane Science*. 427 (2013) 186–196.

3. K. Inui, T. Noguchi, T. Miyata, T. Uragami. Pervaporation characteristics of methyl methacrylate – methacrylic acid copolymer membranes ionically crosslinked with metal ions for a benzene / cyclohexane mixture. *Journal of Applied Polymer Science*. 71 (1998) 233–241.

4. C.K. Park, B. Oh, M.J. Choi, Y.M. Lee. Separation of benzene/cyclohexane by pervaporation through chelate poly(vinyl alcohol)/poly(allyl amine) blend membrane. *Polymer Bulletin*. 598 (1994) 591–598.

5. G. Geise, B. Freeman, D. Paul. Comparison of the permeation of $MgCl_2$ versus NaCl in highly-charged sulfonated polymer membranes, in: I.C. Escobar, B. Van der Bruggen (Eds.), *Modern Applications in Membrane Science*. American Chemical Society, 2011: pp. 239–245.

6. G. Geise, C. Willis, C. Doherty, A.J. Hill, T.J. Bastow, J. Ford, K.I. Winey, B.D. Freeman, D.R. Paul. Characterization of aluminum-neutralized sulfonated styrenic pentablock copolymer films. *Industrial & Engineering Chemistry Research*. 52 (2012) 1056–1068.

7. R.W. Rees. Ionic Hydrocarbon Polymers. U.S. Patent Number 3,264,272. 1966.

8. A.C. Sagle, H. Ju, B.D. Freeman, M.M. Sharma. PEG-based hydrogel membrane coatings. *Polymer*. 50 (2009) 756–766.

9. H. Ju, A.C. Sagle, B.D. Freeman, J.I. Mardel, A.J. Hill. Characterization of sodium chloride and water transport in crosslinked poly(ethylene oxide) hydrogels. *Journal of Membrane Science*. 358 (2010) 131–141.

10. M. Paul, H.B. Park, B.D. Freeman, A. Roy, J.E. McGrath, J.S. Riffle. Synthesis and crosslinking of partially disulfonated poly(arylene ether sulfone) random copolymers as candidates for chlorine resistant reverse osmosis membranes. *Polymer*. 49 (2008) 2243–2252.

11. Y.-J. Kim, K.-S. Lee, M.-H. Jeong, J.-S. Lee. Highly chlorine-resistant end-group crosslinked sulfonated-fluorinated poly(arylene ether) for reverse osmosis membrane. *Journal of Membrane Science*. 378 (2011) 512–519.

12. W. Xie, J. Cook, H.B. Park, B.D. Freeman, C.H. Lee, J.E. McGrath. Fundamental salt and water transport properties in directly copolymerized disulfonated poly(arylene ether sulfone) random copolymers. *Polymer*. 52 (2011) 2032–2043.

13. G.M. Geise, B.D. Freeman, D.R. Paul. Characterization of a sulfonated pentablock copolymer for desalination applications. *Polymer*. 51 (2010) 5815–5822.

14. G.M. Geise, H.-S. Lee, D.J. Miller, B.D. Freeman, J.E. McGrath, D.R. Paul. Water purification by membranes: the role of polymer science. *Journal of Polymer Science Part B: Polymer Physics*. 48 (2010) 1685–1718.

15. F. Helfferich. *Ion exchange*. Dover Publications, New York, 1962.

16. F.G. Donnan. The theory of membrane equilibria. *Chemical Reviews*. 1 (1924) 73–90.

17. H.K. Lonsdale. Donnan-membrane effects in hyperfiltration of ternary systems. *Journal of the Chemical Society, Faraday Transactions 1: Physical Chemistry in Condensed Phases*. 71 (1975) 501–514.

18. P.L. Parise, A.E. Allegrezza Jr., B.S. Parekh. Reverse osmosis: Chlorine-resistant polysulfone reverse osmosis membrane and module. *Ultrapure Water*. (1987) 54–65.

19. K.K. Pushpa, D. Nandan, R.M. Iyer. Thermodynamics of water sorption by perfluorosulphonate (Nafion-117) and polystyrene-divinylbenzene sulphonate (Dowex 50W) ion-exchange resins at 298±1 K. *Journal of the Chemical Society, Faraday Transactions 1: Physical Chemistry in Condensed Phases*. 84 (1988) 2047–2056.

20. K.P. Lee, T.C. Arnot, D. Mattia. A review of reverse osmosis membrane materials for desalination—Development to date and future potential. *Journal of Membrane Science*. 370 (2011) 1–22.

21. R.J. Petersen. Composite reverse osmosis and nanofiltration membranes. *Journal of Membrane Science*. 83 (1993) 81–150.

22. H. Yasuda, C.E. Lamaze, L.D. Ikenberry. Permeability of solutes through hydrated polymer membranes, Part 1. Diffusion of sodium chloride. *Die Makromolekulare Chemie*. 118 (1968) 19–35.

23. H. Yasuda, C.E. Lamaze, A. Peterlin. Diffusive and hydraulic permeabilities of water in water-swollen polymer membranes. *Journal of Polymer Science Part A: Polymer Chemistry*. 9 (1971) 1117–1131.

24. O.D. Bonner, L.L. Smith. A selectivity scale for some divalent cations on Dowex 50. *The Journal of Physical Chemistry*. 61 (1957) 326–329.

25. K.S. Pitzer, J.J. Kim. Thermodynamics of electrolytes. IV. Activity and osmotic coefficients for mixed electrolytes. *Journal of the American Chemical Society*. 1426 (1974) 5701–5707.

26. G.M. Geise, H.B. Park, A.C. Sagle, B.D. Freeman, J.E. McGrath. Water permeability and water/salt selectivity tradeoff in polymers for desalination. *Journal of Membrane Science*. 369 (2011) 130–138.

6. Sorption of Mixtures of Monovalent and Divalent Salts in Sulfonated Polysulfone

ABSTRACT

Equilibrium cation, anion, and water solubility coefficients were determined in a sulfonated polysulfone (BPS-32) at room temperature using dilute aqueous solutions containing only NaCl, mixtures of NaCl and $CaCl_2$, and mixtures of NaCl and $MgCl_2$. Both divalent cations were more strongly sorbed in the sulfonated polysulfone than the monovalent sodium; the divalent cations comprised the majority of the positive counterion charges in the polymer even at external solutions concentrations that were an order of magnitude or more lower than the external solution sodium concentration. The presence of divalent cations decreased the water content of the polymer. Experimental results suggest nearly complete ion exchange of the divalent cations in the polymer upon equilibration with even low concentrations of divalent cations, relative to sodium, in the external solution.

RESULTS

Water Sorption

Samples of BPS-32 were equilibrated in the salt solutions described in Chapter 3, and their water uptake values are presented in Figure 6.1. To investigate the extent to which the decrease in water content observed in Figure 6.1 is caused by thermodynamic effects (i.e., osmotic deswelling), the activity of water in the external salt solutions was calculated using the Pitzer model.[1] The water activity in the solution containing 34 mM NaCl was 0.9989, while the water activity was 0.9985 in the solution containing 34 mM NaCl and 3.4 mM $CaCl_2$ (this solution was chosen as the example of the highest concentration of $CaCl_2$ used in the permeability tests in Chapter 5). Flory-Huggins theory

was used to calculate that the decrease in the polymer water content (K_W) due to such a change in water activity would be 0.04%,[2–4] while the experimentally observed water uptake decreases from an average value of 26 wt% in the NaCl solution to a value of 21 wt% in the NaCl/$CaCl_2$ solution, a difference of approximately 20%. Thus, the change in water content observed when $CaCl_2$ is introduced to the external solution is not explained by thermodynamic effects alone.

Water uptake decreases in the presence of either magnesium or calcium chloride. However, over the concentration range considered, there is little change in water content with increasing NaCl concentration. This decrease in water content is consistent with similar effects observed in ionomers equilibrated with multivalent counterions[5–9] (for example, a roughly 80% decrease in sulfonated polystyrene block copolymers when exposed to aluminum).[6] In these materials, the divalent counterions (Mg^{++} or Ca^{++} in this study) and sulfonate groups of the polymer provide potential opportunities for ionic crosslinking, which has been suggested to reduce water uptake.[5–10] Similarly, covalent crosslinking in hydrophilic polymers has shown to lead to a reduction in water content and water permeability[6,11–13] consistent with the water permeability decrease discussed in Chapter 5 in BPS-32 when divalent cations were introduced into the feed. Additionally, Dowex sulfonated ion exchange resins, described in more detail below, have shown a dependence upon the counterion form (both monovalent and divalent counterions), where exchange with ions that displayed greater sorption in the material resulted in lower water uptake of the material, and sorption of either magnesium and calcium resulted in lower water uptake than sodium.[14–16]

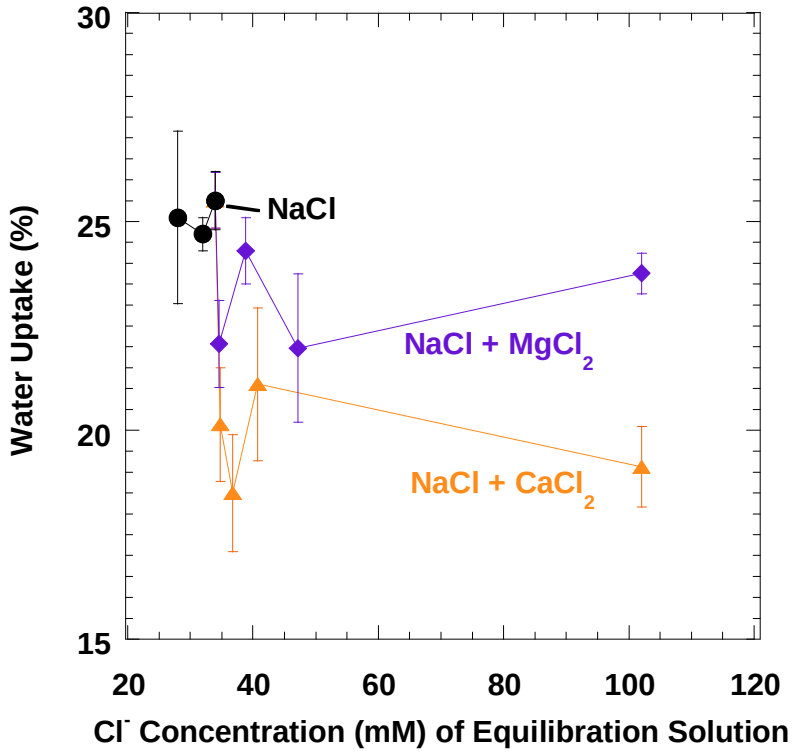

Figure 6.1. Water uptake of BPS-32 equilibrated in aqueous solutions of: NaCl (●), a mixture of NaCl and $CaCl_2$ (▲), and a mixture of NaCl and $MgCl_2$ (◆). The Cl^- concentration is equal to the molar concentration of NaCl plus twice the molar concentration of the divalent cation salt. Equilibrations were performed at room temperature.

Additionally, the water uptake measurements reported in Chapter 5 on potassium-form BPS-32 in deionized water gave values of 20.6% ± 1.4% water, as opposed to the 24-26% range of water uptake in low-concentration NaCl only conditions shown in Figure 6.1; this is consistent with the sensitivity of the water uptake of other sulfonated materials to their counterion form.[14,15] Due to differences in the molecular weight of various ions, the calculation in Equation 3.1 will result in slightly different values of IEC for BPS-32 in different counterion forms. The values of IEC, water uptake, and hydrated charge concentration of BPS-32 in the potassium and sodium forms are listed in Table 6.1.

Polymer	IEC (meq/g of dry polymer)		Water uptake (%)		Hydrated charge concentration (meq/mL of hydrated polymer)	
	K^+ form	Na^+ form	K^+ form	Na^+ form	K^+ form	Na^+ form
BPS-32	1.34	1.37	21	26	1.41	1.37

Table 6.1. Properties of BPS-32.

Cation Sorption

The cation content, C_{meq} (cf., Equation 3.18) of BPS-32 samples equilibrated in solutions of 34 mM NaCl containing increasing $CaCl_2$ concentration is presented in Figure 6.2 (A) as a function of calcium concentration, the cation content from sorption experiments involving mixtures of NaCl and $MgCl_2$ is presented in Figure 6.2 (B) as a function of magnesium concentration, and the data from these tests are represented in Figure 6.2 (C) and (D) as the mol fraction of sulfonate groups associated with each ionic species, assuming 1.25 milliequivalents sulfonate groups per gram of dry polymer are available for transport based on the pure NaCl sorption data from this study and previous studies.[17,18] The initial point in both graphs was determined from equilibration in a solution containing only 34 mM NaCl. When equilibrated in a solution of 34 mM NaCl, the BPS-32 polymer exhibits a Na^+ concentration of 1.25 meq/gram of dry polymer, which is within the range of IEC values that have been reported previously by sodium sorption (1.2 to 1.3 meq/g dry polymer) on BPS-32 (initially the acid form BPSH-32, though equilibration in NaCl results in ion exchange to the sodium form).[17] While there will be some mobile sodium ions present in the polymer that are not associated with sulfonate groups, at the IEC ranges considered in these materials, the majority of the sodium ions are associated with the sulfonate groups on the polymer chains and, as such,

the total sodium ion concentration in the polymer serves as a reasonable proxy for the IEC of the material.[17]

When equilibrated in solutions containing a divalent cation, the sodium content of BPS-32 decreases, while the divalent cation concentration increases. Even at low concentrations of divalent cations in the external solution, the divalent cation concentration in the polymer is greater than that of sodium. Similar phenomena have been found in sulfonated ion exchange resins: Bonner et al. have measured equilibrium sorption values of aqueous binary cation mixtures in Dowex sulfonated polystyrene ion exchange resins, and developed a selectivity scale of cations in the resin by normalizing the thermodynamic equilibrium constants against those of lithium.[15,19–22] For example, the thermodynamic equilibrium constant in one resin for the Cs^+/Li^+ exchange was experimentally found to be 4.15, and thus the selectivity scale was set at 4.15 for Cs^+ and arbitrarily assigned to 1 for Li^+;[22] for the Cs^+/H^+ exchange in the same resin the thermodynamic equilibrium constant was measured as 2.86, and thus the selectivity scale for hydrogen relative to lithium was calculated as 1.45 using the equilibrium constant of the Cs^+/Li^+ exchange, i.e., 4.15/2.86 = 1.45.[22] In these selectivity studies, the selectivity scale of the 16% divinylbenzene (DVB, a crosslinking agent in the resin) samples showed a selectivity scale of 7.27 for Ca^{++}, 3.51 for Mg^{++}, and 2.37 for Na^+ (the 16% DVB resin was chosen as a comparison because though its water uptake is roughly five times higher than the BPS-32 material, depending on the counterion form, it has the closest water uptake to BPS-32 of the resins investigated).[15] For comparison, Table 6.2 lists the water sorption data for the 16% DVB Dowex resin (IEC in hydrogen form = 5.10 meq/g dry polymer)[14] in selected counterion forms, while Table 6.3 lists the relevant monovalent and divalent cation selectivity scales and chemical information.

Counterion Form	Water uptake (%) of sulfonated Dowex 50 at 16% DVB[14,15]
Li^+	130
Na^+	113
K^+	106
Mg^{++}	129
Ca^{++}	115
Sr^{++}	113

Table 6.2. Water uptake for Dowex ion exchange resin.[14,15]

Ion	Selectivity scale in sulfonated Dowex 50 at 16% DVB[15]	Ionic radius (Å)[23]	Electronegativity[23]
Li^+	1	0.76	0.98
Na^+	2.37	1.02	0.93
K^+	4.5	1.38	0.82
Cs^+	4.66	1.67	0.79
Mg^{++}	3.51	0.72	1.31
Ca^{++}	7.27	1.00	1.00
Sr^{++}	10.1	1.18	0.95

Table 6.3. Properties of selected ions.

The effect of greater Ca^{++} sorption than Mg^{++} or Na^+ observed in the Dowex materials is also seen in this study, as calcium sorbs in the polymer at higher concentrations than magnesium at similar equilibration solution compositions; the magnesium and calcium cations appear to be displacing sodium cations that would be in equilibrium with sulfonate groups in the absence of a competing species of ion, based on the higher sodium sorption found in the initial point in each plot of Figure 6.1, where the membrane was equilibrated in a 34 mM NaCl only solution.

As the concentration of Ca^{++} in the external solution increases from 0.4 mM to 3.4 mM, the concentration of Ca^{++} in the BPS-32 membrane increases such that calcium occupies a large majority of sulfonate sites as compared to the sodium ion. Over this

same range of feed compositions, the NaCl permeability of the BPS-32 material has been shown to increase by a factor of roughly 5 in Chapter 5. A similar effect is seen in the mixed NaCl/$MgCl_2$ sorption and permeability data over the available range of 0.3 mM Mg^{++} to 6.6 mM Mg^{++}, where the NaCl permeability increased by a factor of roughly 2. The increase of salt permeability or passage in charged materials as a result of the presence of multivalent cations has been investigated in the literature, and has typically been attributed to the neutralization of the fixed charges in the membrane (and thus, the subsequent reduction of the Donnan forces that inhibit salt transport).[6,13,24–26] The neutralization of the charge of an anion suggests ion pairing with a cation,[27,28] and it is possible that the greater electrostatic attraction between the divalent cations and the sulfonate groups, as opposed to the monovalent sodium, results in more contact ion pairing with the sulfonate groups (that is, the cation and sulfonate anion make contact and form an electrically neutral species, as opposed to solvent-shared ion pairing where the two ions are separated by a layer of solvent molecules, or dissociation where the two ions interact negligibly).[29,30] Ion pairing in a solution may be expressed in terms of a time average equilibrium constant: ions will associate in pairs then dissociate after a period of time that is dependent upon the electrostatic forces between the ions and the forces of the surrounding solvent acting upon the associated pair.[27] Thus, all other factors being equal, ions that interact more strongly with the surrounding solvent may be less likely to form ion pairs; similarly, ions with greater Coulombic attraction to the fixed anion may be more likely to form ion pairs. It has been found in the literature that, in general, larger cations of the same charge value have weaker interactions with polar solvent molecules such as water or ammonia.[27,29–31] It is possible that, within some sulfonated polymers, the generally higher affinity of divalent cations than monovalent cations for sulfonate groups is driven by the greater charge of the divalent cation, while the higher sulfonate affinity

of larger species of either monovalent or divalent cations may be due to their possession of more weakly bound hydration shells with increasing ionic radius. Thus, the divalent cations could be forming contact ion pairs with the sulfonate groups, leading to the neutralization of the sulfonate charges and observed increasing of NaCl permeability. This hypothesis has been investigated quantitatively by Bontha, Pintauro, and Tandon, by means of the Gibbs free energy of hydration.[32–34] They found that ions of greater size (and thus lower charge density at equal valencies) had a smaller free energy change associated with transfer from the external solution to the pore fluid in sulfonated Nafion 117 membranes due to the weaker water-ion interactions as ion radius increased.[32–34] This trend in hydration energy was correlated with greater sorption in the Nafion material of larger monovalent ions (e.g., $Cs^+ > K^+ > Li^+$); however the same size trend was not repeated amongst the divalent cations, unlike the trends found by Bonner and this study, which was attributed to a sharp decrease of solution dielectric constant as the ion approached the wall of the pore from the center radius, thus more effectively repelling the hydrated divalent cations.[34] Additionally, these studies on Nafion 117 were able to measure the ion pairing of divalent cations to the polymer sulfonate sites through both NMR measurements as well as the fitting of ion sorption data for the polymer to a thermodynamic model.[33,34]

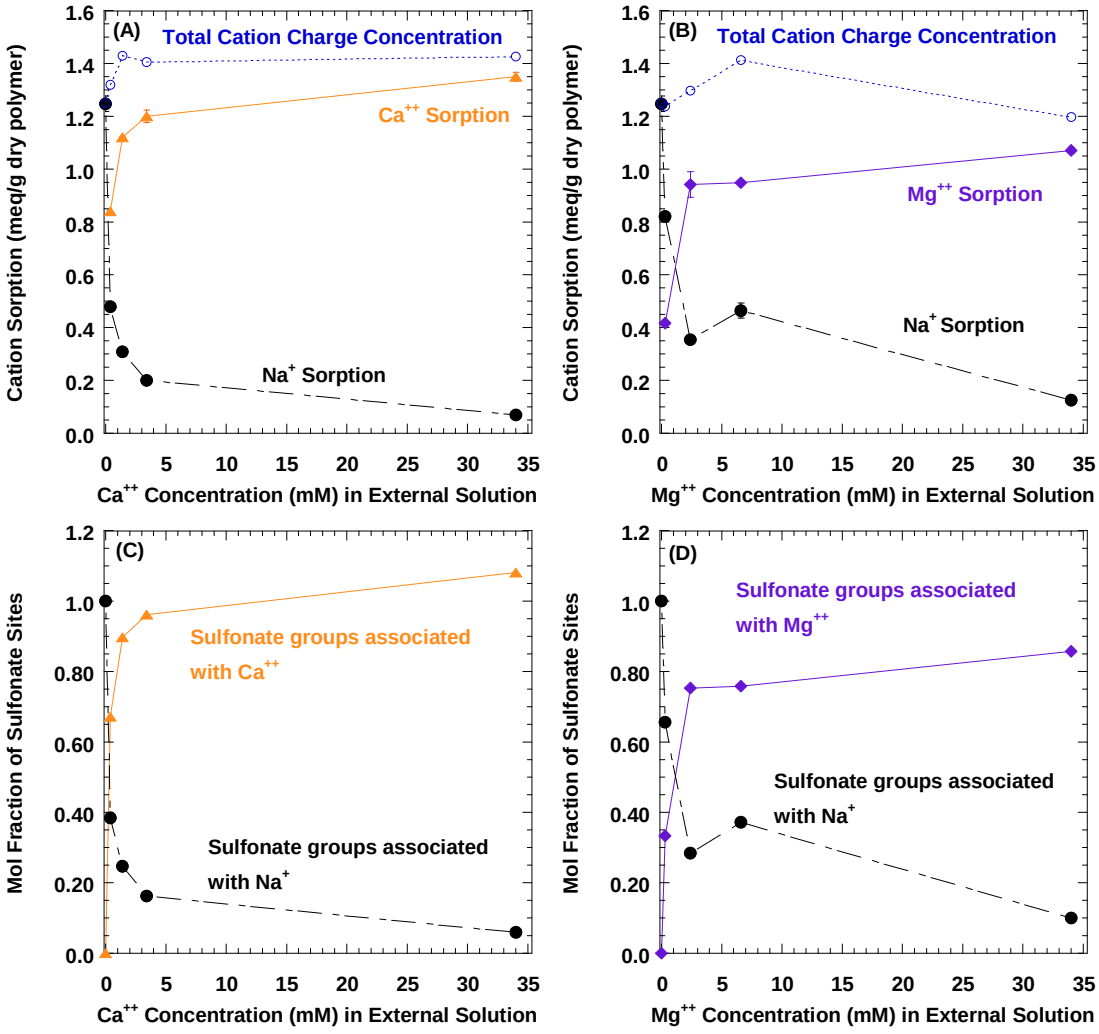

Figure 6.2. Cation sorption into BPS-32 when equilibrated in: (A) a mixed NaCl and $CaCl_2$ solution and (B) a mixed NaCl and $MgCl_2$ solution measured by cation charges per gram of dry polymer, and (C) a mixed NaCl and $CaCl_2$ solution and (D) a mixed NaCl and $MgCl_2$ solution measured by fraction of sulfonate groups occupied by each cation species . (●) = sodium, (▲) = calcium, (◆) = magnesium, (○) = total number of cationic charges. Testing performed at 25 °C; the lines are drawn to guide the eye.

The sorption of ions into polymer materials containing covalently bound charged groups is often described in terms of Donnan sorption effects,[17,35–41] where the electrostatic interactions between the fixed charged groups (e.g., sulfonate groups in

BPS-32) and the co-ions present in the external salt solution (e.g., Cl^- in the case of sulfonated polymers) impede co-ion sorption. The Donnan model also includes a dependence of counterion sorption on the valency of the counterions, discussed in Chapter 2, such that sorption of monovalent and divalent counterions would be described generally as follows:[36]

$$\left(\frac{C_{M+,S}}{C_{M+,P}}\right)^2 = \left(\frac{C_{M++,S}}{C_{M++,P}}\right) \tag{6.1}$$

where $C_{M+,S}$ and $C_{M+,P}$ are the monovalent ion (M^+) concentration of the equilibration solution and polymer, respectively, and $C_{M++,S}$ and $C_{M++,P}$ are the respective equilibration solution and polymer divalent ion (M^{++}) concentrations.

Higa et al. have performed ion sorption measurements on a sulfonated poly(vinyl alcohol) (PVA; hydrated charge concentration = 0.05 meq/g), and derived from Donnan theory the following expression for the divalent cation concentration in the membrane phase:[40]

$$C_{M++,P} = C_{M++,S}\left[\frac{-C_{M+,S}/C_{M++,S}}{4} + \left(\left(\frac{C_{M+,S}/C_{M++,S}}{4}\right)^2 - \frac{z_A C_A}{2C_{M++,S}}\right)^{1/2}\right]^2 \tag{6.2}$$

where C_A is the concentration of fixed anions (i.e., the sulfonate group), and z_A is fixed anion charge (i.e., -1 for sulfonate). Equation 6.2 makes several assumptions. First, the model assumes that the ion activity coefficients and standard chemical potentials do not change between the polymer phase and the solution phase, due in part to the high water content and low charge density of the PVA membrane studied; the validity of this assumption on BPS-32 is not clear at this time and is the subject of ongoing investigations in our laboratories. Second, the model assumes that all ions are fully dissociated; as discussed above, this may not be the case for divalent cations in the BPS-

32 material. Finally, Equation 6.2 assumes that the concentrations of divalent cations in the solution is less than 0.1× the concentration of sulfonate groups in the membrane; in this study that assumption is valid, as the maximum solution concentration of divalent cations is 0.034 M, and as shown in Table 6.1 the concentration of sulfonate groups in the sodium form is 1.41 meq/mL of hydrated polymer (equivalent to 1.41 Molar).

Figure 6.3 presents the influence of external solution divalent ion concentration on the sorption of Ca^{++} and Mg^{++} into BPS-32 when it is equilibrated with mixtures of NaCl and $CaCl_2$ or NaCl and $MgCl_2$. These concentrations were determined from the ashing data and Equation 3.16, and are compared to the divalent cation sorption predicted using the simplified Donnan model in Equation 6.2 (note that there are no adjustable parameters in this equation – divalent cation content is calculated directly from the experimental data of solution concentration and membrane properties). The sorption values of Mg^{++} are relatively close to the values expected from Equation 6.2, while the Ca^{++} sorption values qualitatively follow the same trend, though they show much higher sorption than theoretically calculated. The model assumes the same ion activity coefficients in the polymer as in the external solution, however it is not clear that this is so, and changes in the activity coefficients between the two ions would result in differences in their calculated sorption when the effect of activity is not ignored.[15,40] Also, as stated, this model does not account for ion association, which may be occurring between the divalent cations and the sulfonate groups. For comparison, Pintauro et al. developed a model, discussed above, to predict the sorption concentrations of monovalent and divalent salts into a charged material when ion pairing is taken into account (this model assumes that the charged groups are concentrated along pore walls of known radius, and that the solution dielectric properties in such pores differ from that of the external solution, and thus is not directly applicable to the materials in this study).[33] The

predictions of this model were compared to sorption values of mixtures of Pb^{++} and monovalent cations in Nafion 117 (the K^+ form hydrated charge concentration has been calculated as 1.37 meq/mL hydrated polymer, from the reported data).[32,33] When the model was not corrected for the presence of contact ion pairing between the lead and sulfonate groups, it consistently predicted lower divalent cation sorption than was found experimentally, while the pairing-corrected model developed accurate predictions of monovalent and divalent cation sorption.[33] The trend of greater experimental divalent cation sorption values than predicted values in Figure 6.3 is qualitatively consistent with this effect of ion pairing on the porous membrane model from the literature,[33] though at this time more data is needed to determine the parameters necessary to quantitatively evaluate the Donnan behavior of the dense sulfonated BPS-32.

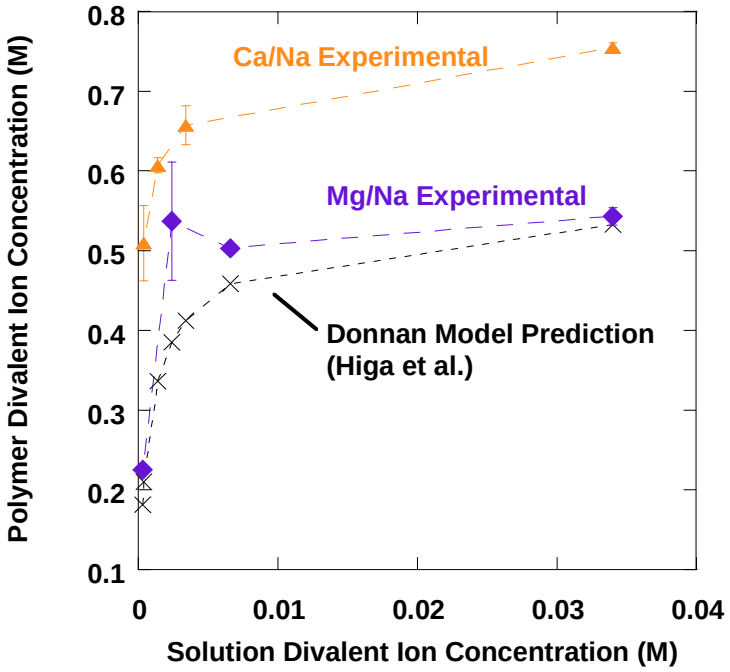

Figure 6.3. Divalent ion concentration in BPS-32 in a 34 mM NaCl solution with increasing divalent ion concentration. (▲) = calcium sorption, (◆) = magnesium sorption, (×) = divalent cation sorption predicted by Equation 6.2.[40]

If the divalent cations effectively neutralize the sulfonate group charges through ion pairing, then the transport properties of the sulfonated polysulfone could appear to be more similar to those of an uncharged material as divalent cation sorption increases. A study has been performed previously to characterize the water and salt transport properties of uncharged crosslinked polyethylene glycol (PEG) hydrogels, and sodium chloride permeability in those materials increased with increasing water partition coefficient.[11] The relationship between P_{NaCl} and K_W is presented in Figure 6.4 for the previously reported PEG materials along with P_{NaCl} values for BPS-32 as a function of

divalent ion feed concentration reported in Chapter 5, and the K_W values calculated from the water uptake shown in Figure 6.1. This figure shows that as the calcium or magnesium concentration of the external solution increases, the P_{NaCl}/K_W relationship of BPS-32 approaches that of the uncharged PEG hydrogels, suggesting that the charge effects which retard salt permeability are being screened out by the presence of the divalent cations.

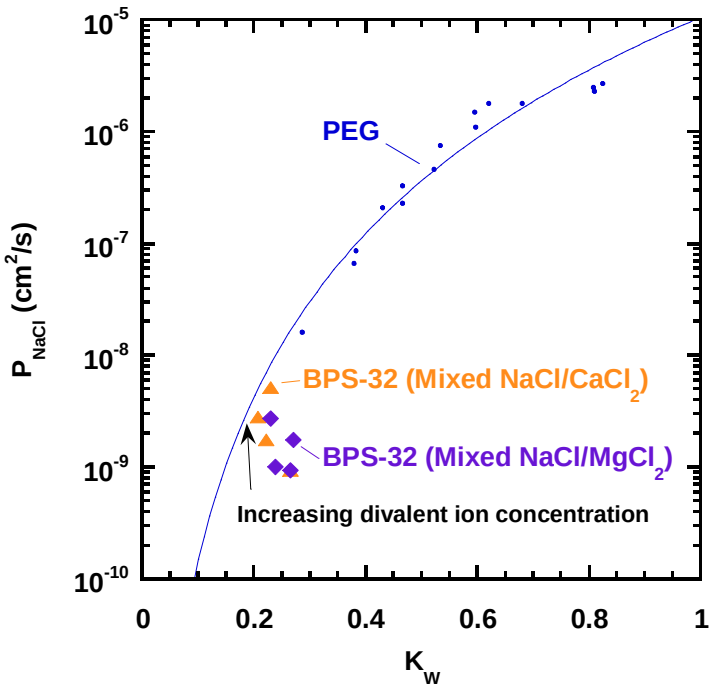

Figure 6.4. NaCl permeability versus water partition coefficient for charged and uncharged polymers. (•) = PEG,[11] (▲) = BPS-32 with a mixed NaCl/$CaCl_2$ external solution, (◆) = BPS-32 with a mixed NaCl/$MgCl_2$ external solution. Permeability values were determined at 25°C. The blue line is a power law curve fit of the PEG data.

Anion Transport Effects

Chloride sorption values were measured by desorption tests on BPS-32 after equilibration in salt solutions, and the results are presented in Table 6.4. Within the range of salt concentrations for which permeability data is available, the chloride sorption coefficient, K_{Cl}, did not exhibit consistent systematic changes. For comparison, the molar concentrations of chloride of BPS-32 when equilibrated in mixed ion solutions calculated from Equation 3.15 are compared to those reported for BPSH-32 previously in Figure 6.5 (the BPSH-32 values were originally reported as a function of external molar NaCl concentration, which is equivalent to molar Cl^- concentration).[17] These concentrations are not normalized by the external salt concentration as the K_{Cl} values are, and can be seen to increase with external salt concentration similarly to the BPSH-32 values over the same range.

(A) K_{Cl} of BPS-32 equilibrated in aqueous solutions containing only NaCl.			
NaCl Concentration	28 mM	34 mM	40 mM
K_{Cl}	0.025 ± 0.005	0.027 ± 0.001	0.020 ± 0.001

(B) K_{Cl} of BPS-32 equilibrated in aqueous solutions containing 34 mM NaCl and $CaCl_2$.				
$CaCl_2$ concentration	0.4 mM	1.4 mM	3.4 mM	34 mM
K_{Cl}	0.032 ± 0.003	0.032 ± 0.001	0.029 ± 0.001	0.045 ± 0.005

(C) K_{Cl} of BPS-32 equilibrated in aqueous solutions containing 34 mM NaCl and $MgCl_2$.				
$MgCl_2$ concentration	0.3 mM	2.4 mM	6.6 mM	34 mM
K_{Cl}	0.023 ± 0.002	0.027 ± 0.003	0.031 ± 0.003	0.031 ± 0.002

Table 6.4. Chloride partition coefficients of BPS-32 equilibrated in aqueous solutions containing only NaCl, mixtures of NaCl and $CaCl_2$, and mixtures of NaCl and $MgCl_2$.

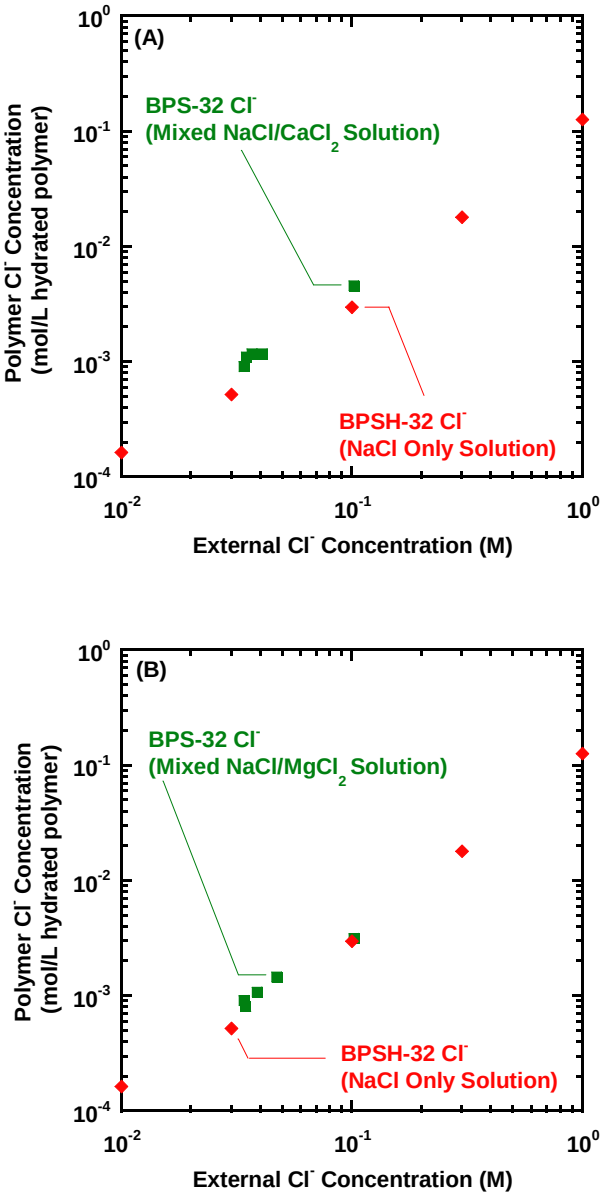

Figure 6.5. Anion concentration of BPSH-32[17] compared to (A) BPS-32 equilibrated in a mixed $NaCl/CaCl_2$ external solution, (B) BPS-32 equilibrated in a mixed $NaCl/MgCl_2$ external solution. The initial point of the BPS-32 mixed ion samples is from the 34 mM NaCl only solution.

The chloride permeability (P_{Cl}) was calculated from mixed ion crossflow permeation tests in Chapter 5, and they are shown in Figure 6.6. The chloride permeability is very close in value to the sodium permeability, which is expected since NaCl is the most highly concentrated salt species in the feed and permeate. In this case, it is the chloride anion whose concentration in the polymer is restricted due to electrostatic interactions with the sulfonate groups and which forms the key ion in the mobile salt. So as the electrostatic screening of chloride is reduced at higher concentrations of divalent cations, the polymer exhibits more rapid chloride transport and, therefore, more rapid cation transport as well.[17,36,37,42]

From the values of P_{Cl} in Figure 6.6 and K_{Cl} in Table 6.4, D_{Cl} values were calculated from the solution-diffusion model, represented in Equation 3.13, and are presented in Figure 6.7. In Figure 6.7, the D_{Cl} values of BPS-32 increase more in the presence of calcium than magnesium, which is consistent with the higher sorption of calcium and higher hypothesized sulfonate charge neutralization by calcium, at similar concentrations. In the case of both feed mixtures, the increase in the calculated D_{Cl} values tracks closely with that of the P_{Cl} values: as calcium is added to the 34mM external solution/feed in the concentrations shown, P_{Cl} increases by a factor of 5.1 while D_{Cl} increases by a factor of 5.2. Similarly, in the case of the mixed magnesium sodium solutions, P_{Cl} increases by a factor of 2.1 while D_{Cl} increases by a factor of 1.8. The similarity in the trends of chloride diffusivity and chloride permeability indicate that the increase in NaCl permeability in BPS-32 in mixed valence cation environments is primarily driven by diffusivity phenomena. The observed rise in D_{Cl} in Figure 6.7, which may be related to increased neutralization of the BPS-32 sulfonate groups at higher divalent cation concentrations, supports the observations that fixed charged groups serve to retard salt diffusion in such charged polymers.[6,13,24–26] However, a complete

fundamental understanding of all of the phenomenon at play is not available, so further studies of this type will be needed to understand if this proposed explanation represents a dominant contribution to the observed phenomena or not.

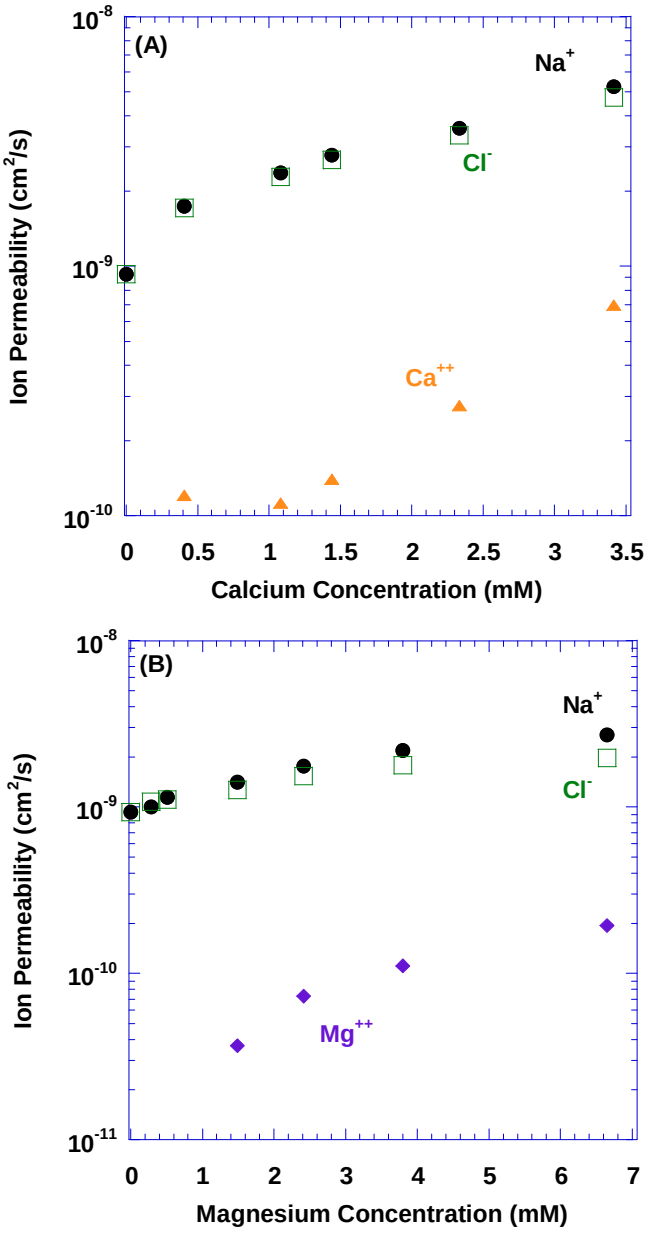

Figure 6.6. Ion permeability in BPS-32 with (A) a feed of 34 mM NaCl with increasing feed of $CaCl_2$, and (B) feed of 34 mM NaCl with increasing feed of $MgCl_2$. (●) = Na^+ permeability, (□) = Cl^- permeability, (▲) = Ca^{++} permeability, (◆) = Mg^{++} permeability. Testing performed at 25 °C.

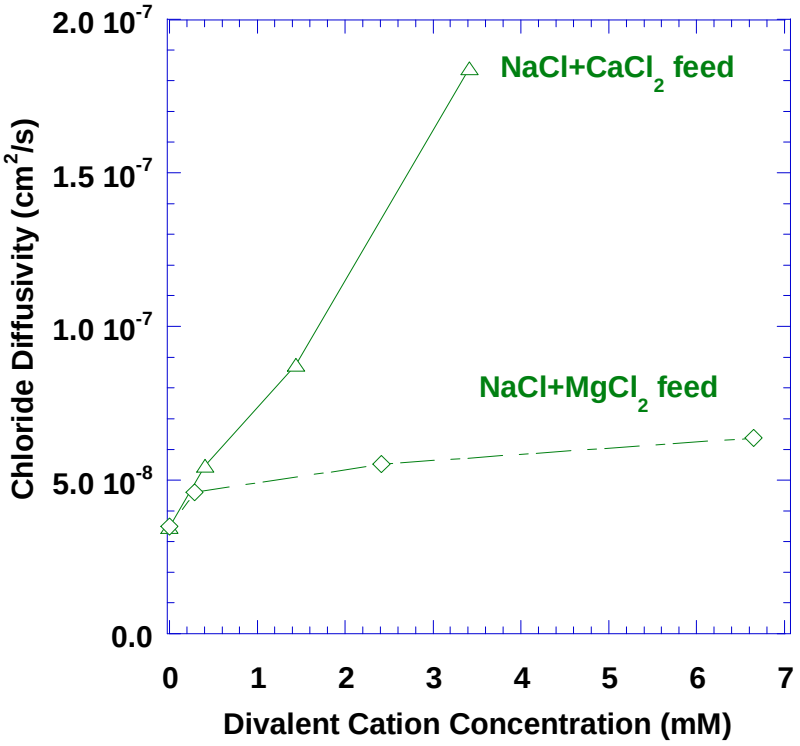

Figure 6.7. Chloride diffusivity in BPS-32 with mixed ion feeds. (△) = D_{Cl} in a mixed $NaCl/CaCl_2$ feed, (◇) = D_{Cl} in a mixed $NaCl/MgCl_2$ feed. The lines are drawn to guide the eye.

REFERENCES

1. K.S. Pitzer, J.J. Kim. Thermodynamics of electrolytes. IV. Activity and osmotic coefficients for mixed electrolytes. *Journal of the American Chemical Society*. 1426 (1974) 5701–5707.

2. P. Flory. Thermodynamics of high polymer solutions. *The Journal of Chemical Physics*. 9 (1941) 660.

3. M.L. Huggins. Solutions of long chain compounds. *The Journal of Chemical Physics*. 9 (1941) 440.

4. D.R. Paul. Relation between hydraulic permeability and diffusion in homogeneous swollen membranes. *Journal of Polymer Science Part B: Polymer Physics*. 11 (1973) 289–296.

5. R.W. Rees. Ionic Hydrocarbon Polymers. U.S. Patent Number 3,264,272. 1966.

6. G. Geise, C. Willis, C. Doherty, A.J. Hill, T.J. Bastow, J. Ford, K.I. Winey, B.D. Freeman, D.R. Paul. Characterization of aluminum-neutralized sulfonated styrenic pentablock copolymer films. *Industrial & Engineering Chemistry Research*. 52 (2012) 1056–1068.

7. K. Inui, T. Noguchi, T. Miyata, T. Uragami. Pervaporation characteristics of methyl methacrylate – methacrylic acid copolymer membranes ionically crosslinked with metal ions for a benzene / cyclohexane mixture. *Journal of Applied Polymer Science*. 71 (1998) 233–241.

8. C.K. Park, B. Oh, M.J. Choi, Y.M. Lee. Separation of benzene/cyclohexane by pervaporation through chelate poly(vinyl alcohol)/poly(allyl amine) blend membrane. *Polymer Bulletin*. 598 (1994) 591–598.

9. S.-T. Lee, F.-L. Mi, Y.-J. Shen, S.-S. Shyu. Equilibrium and kinetic studies of copper(II) ion uptake by chitosan-tripolyphosphate chelating resin. *Polymer*. 42 (2001) 1879–1892.

10. S.K. Bajpai, S. Sharma. Investigation of swelling/degradation behaviour of alginate beads crosslinked with Ca^{2+} and Ba^{2+} ions. *Reactive and Functional Polymers*. 59 (2004) 129–140.

11. H. Ju, A.C. Sagle, B.D. Freeman, J.I. Mardel, A.J. Hill. Characterization of sodium chloride and water transport in crosslinked poly(ethylene oxide) hydrogels. *Journal of Membrane Science*. 358 (2010) 131–141.

12. A.C. Sagle, H. Ju, B.D. Freeman, M.M. Sharma. PEG-based hydrogel membrane coatings. *Polymer*. 50 (2009) 756–766.

13. G. Geise, B. Freeman, D. Paul. Comparison of the permeation of $MgCl_2$ versus NaCl in highly-charged sulfonated polymer membranes, in: I.C. Escobar, B. Van der Bruggen (Eds.), *Modern Applications in Membrane Science*. American Chemical Society, 2011: pp. 239–245.

14. O.D. Bonner. A selectivity scale for some monovalent cations on Dowex 50. *The Journal of Physical Chemistry*. 58 (1954) 318–320.

15. O.D. Bonner, L.L. Smith. A selectivity scale for some divalent cations on Dowex 50. *The Journal of Physical Chemistry*. 61 (1957) 326–329.

16. G.M. Geise, D.R. Paul, B.D. Freeman. Fundamental water and salt transport properties of polymeric materials. *Progress in Polymer Science*. 39 (2014) 1–42.

17. G.M. Geise, L.P. Falcon, B.D. Freeman, D.R. Paul. Sodium chloride sorption in sulfonated polymers for membrane applications. *Journal of Membrane Science*. 423-424 (2012) 195–208.

18. L.K.R. Passaniti. *Solubility measurements in partially disulfonated poly (arylene ether sulfone) for reverse osmosis water purification applications*. M.S. Thesis. The University of Texas, Austin, TX, 2010.

19. O.D. Bonner, W.H. Payne. Equilibrium studies of some monovalent ions on Dowex 50. *The Journal of Physical Chemistry*. 58 (1954) 183–185.

20. O.D. Bonner, F.L. Livingston. Cation-exchange equilibria involving some divalent ions. *The Journal of Physical Chemistry*. 60 (1956) 530–532.

21. O.D. Bonner, V. Rhett. Equilibrium studies of the silver-sodium-hydrogen system on Dowex 50. *The Journal of Physical Chemistry*. 57 (1953) 254–256.

22. O.D. Bonner. Ion-exchange equilibria involving rubidium, cesium and thallous ions. *The Journal of Physical Chemistry*. 59 (1955) 719–721.

23. D.R. Lide, ed. *The CRC Handbook of Chemistry and Physics*. 85th ed. CRC Press, Boca Raton, 2004.

24. A.E. Allegrezza Jr., B.S. Parekh, P.L. Parise, E.J. Swiniarski, J.L. White. Chlorine resistant polysulfone reverse osmosis modules. *Desalination*. 64 (1987) 285–304.

25. P.L. Parise, A.E. Allegrezza Jr., B.S. Parekh. Reverse osmosis: Chlorine-resistant polysulfone reverse osmosis membrane and module. *Ultrapure Water*. (1987) 54–65.

26. R.J. Petersen. Composite reverse osmosis and nanofiltration membranes. *Journal of Membrane Science*. 83 (1993) 81–150.

27. R.M. Fuoss, C.A. Kraus. Properties of electrolytic solutions. III. The dissociation constant. *Journal of the American Chemical Society*. 55 (1933) 1019–1028.

28. R.M. Fuoss. Ionic association. III. The equilibrium between ion pairs and free ions. *Journal of the American Chemical Society*. 80 (1958) 5059–5061.

29. D.E. Irish. Interactions in aqueous alkali metal nitrate solutions. *Canadian Journal of Chemistry*. 46 (1968) 943–951.

30. J.B. Gill. Solute-solute interaction in liquid ammonia solutions: A vibrational spectroscopic view. *Pure and Applied Chemistry*. 53 (1981) 1365–1381.

31. L. V. Coulter. The thermochemistry of the alkali and alkaline earth metals and halides in liquid ammonia at -33C. *The Journal of Physical Chemistry*. 57 (1953) 553–558.

32. J.R. Bontha, P.N. Pintauro. Water orientation and ion solvation effects during multicomponent salt partitioning in a Nafion cation exchange membrane. *Chemical Engineering Science*. 49 (1994) 3835–3851.

33. P.N. Pintauro, R. Tandon, L. Chao, W. Xu, R. Evilia. Equilbrium partitioning of monovalent/divalent cation-salt mixtures in Nafion cation-exchange membranes. *Journal of Physical Chemistry*. 99 (1995) 12915–12924.

34. R. Tandon, P.N. Pintauro. Divalent / monovalent cation uptake selectivity in a Nation cation-exchange membrane : Experimental and modeling studies. *Journal of Membrane Science*. 136 (1997) 207–219.

35. H.K. Lonsdale. Donnan-membrane effects in hyperfiltration of ternary systems. *Journal of the Chemical Society, Faraday Transactions 1: Physical Chemistry in Condensed Phases*. 71 (1975) 501–514.

36. F.G. Donnan. The theory of membrane equilibria. *Chemical Reviews*. 1 (1924) 73–90.

37. F.G. Donnan. Theory of membrane equilibria and membrane potentials in the presence of non-dialysing electrolytes. A contribution to physical-chemical physiology. *Journal of Membrane Science*. 100 (1995) 45–55.

38. K.P. Lee, T.C. Arnot, D. Mattia. A review of reverse osmosis membrane materials for desalination—Development to date and future potential. *Journal of Membrane Science*. 370 (2011) 1–22.

39. P. Mukherjee, A.K. Sengupta. Ion exchange selectivity as a surrogate indicator of relative permeability of ions in reverse osmosis processes. *Environmental Science & Technology*. 37 (2003) 1432–1440.

40. M. Higa, A. Kira, A. Tanioka, K. Miyasaka. Ionic partition equilibrium in a charged membrane immersed in a mixed ionic solution. *Journal of the Chemical Society, Faraday Transactions*. 89 (1993) 3433–3435.

41. F. Helfferich. *Ion exchange*. Dover Publications, New York, 1962.

42. G.M. Geise, B.D. Freeman, D.R. Paul. Sodium chloride diffusion in sulfonated polymers for membrane applications. *Journal of Membrane Science*. 427 (2013) 186–196.

7. Conclusions and Recommendations

CONCLUSIONS

Bisphenol-A Based Sulfonated Polysulfone

BisAS series polymers were synthesized by our collaborators at Virginia Tech with controlled degrees of sulfonation. The water and salt transport properties of these polymers were measured and reported, and it has been demonstrated that the water and salt permeability, diffusivity, and sorption coefficients increase as a function of increasing degree of sulfonation, while the water/salt permeability selectivity and diffusivity selectivity decrease with degree of sulfonation. Thus, although these are charged materials with Donnan properties, as more charged groups are added to the polymer backbone the increased water content induces higher salt content and salt diffusivity, in a similar fashion to uncharged materials. The differences in the transport properties of the BisAS materials and BPS materials reported in the literature have shown evidence of sensitivity to casting conditions, as BPS-32 displayed water and salt permeability properties closer to those of BisAS polymers when cast at the same conditions (60 °C with no vacuum for 48 h); however when these properties are viewed on the basis of hydrated charge concentration, the BisAS materials show comparably higher water and salt permeability due to their greater water content. It is possible that the isopropylidene unit in the backbone structure allows for greater water uptake in the BisAS series materials than in the BPS series materials, resulting in higher water permeability but lower selectivity in the BisAS polymers at similar charge concentrations. However, a more thorough characterization of the effect of casting conditions is needed to differentiate between the effects of thermal history and polymer chemistry.

Effect of Mixed Valence Ionic Feeds on the Permeability of Sulfonated Polysulfones

Monovalent and divalent ion permeabilities, was well as water permeabilities of two sulfonated polysulfones were characterized using feed solutions of increasing NaCl concentration and feed solutions containing a fixed NaCl concentration and increasing concentrations of $CaCl_2$, $MgCl_2$, or Na_2SO_4. The presence of a competing anion, sulfate, in the feed did not result in significant changes in sodium chloride transport properties, as expected for cation exchange materials. However, introduction of a divalent cation to the feed solution resulted in stronger increases in sodium ion permeability than when an equivalent amount (based on number of positively charged groups on the salts in the feed solution) of NaCl was added, which may be attributed to neutralization of the sulfonated ion charges by the more highly charged divalent cations, though direct confirmation of this sulfonate neutralization is needed. Additionally, lower water permeability in the sulfonated polysulfones was observed in the presence of divalent cations, potentially due to ionic crosslinking reducing the free volume available for ion transport. Both of these effects decrease the water/NaCl permeability selectivity with increasing divalent ion concentration in the feed solution.

Sorption Behavior of Mixtures of Monovalent and Divalent Cations in Sulfonated Polysulfone

BPS-32 sulfonated polysulfone samples were equilibrated in aqueous solutions containing NaCl, mixtures of NaCl and $CaCl_2$, and mixtures of NaCl and $MgCl_2$ in similar concentrations to those used in the permeability tests reported in Chapter 5. BPS-32 exhibited lower water sorption in the mixed valence salt solutions than in the solution containing only NaCl, which is consistent with the observed lower water permeability in such mixed salt solutions. This decrease in water content is consistent with behavior in other sulfonated materials, and may show evidence of ionic crosslinking of the charged

polymer in the presence of a divalent cation. The cation sorption of Na^{+}, Ca^{++}, and Mg^{++} in the BPS-32 was measured, and increasing divalent cation sorption correlated with increasing NaCl permeability, supporting the hypothesis that ion pairing between the more highly charged divalent cations and the sulfonate groups may contribute to neutralization of at least some of the sulfonate groups. Chloride sorption was shown to increase as a function of divalent ion concentration in a fashion similar to that of BPSH-32 as a function of increasing NaCl concentration. The calculated effective chloride diffusivity increased over the investigated concentration range in magnitudes roughly matching that of the chloride permeability, suggesting that chloride permeability effects are largely driven by the chloride diffusivity effects over the range of external solution compositions investigated.

RECOMMENDATIONS

New material development and characterization

The synthesis and systematic characterization of new polymers has allowed the field of gas transport and separations to build a foundation of knowledge of relationships between chemical structure and transport properties.[1] Such a foundation is just as important in the water purification field, and the systematic characterization of water and salt transport properties of new materials is crucial to the development of more effective desalination membranes. Since polysulfones have shown such strong chemical stability, the characterization of new hydrophilic polysulfones, as well as development of a more detailed correlation of casting conditions and transport properties, would aid in the would be beneficial towards the development of chlorine-tolerant desalination materials.[2–6]

Polymer crosslinking is an effective method of controlling water uptake and thus controlling polymer water and salt permeability,[7–10] and work has already begun towards

the development of crosslinkable sulfonated polysulfones.[11] It is not known if the crosslinking of sulfonated polysulfone would alter the decrease of water permeability/uptake in the presence of divalent cations shown in Chapters 5 and 6 or not, and this topic should be the subject of future work. Additionally, the application of an anionic moiety with less attraction to magnesium or calcium might demonstrate less sensitivity to the presence of these cations; for example, polysulfones with carboxylate groups would be of interest for this reason (such weaker acidic groups would likely introduce complex dependences of degree of ionization on pH, for example, that would need to be carefully controlled).[12] However, the propensity of charged polymers to demonstrate higher NaCl permeability at higher NaCl concentrations, or with relatively low concentrations of divalent cations in the feed, is believed to be due to the fixed charged groups in their backbone.[13–16] The presence of charged moieties are useful to induce hydrophilicity in otherwise hydrophilic materials such as polysulfone,[17–19] but it may be possible to copolymerize chlorine-resistant sulfone monomers with uncharged hydrophilic groups to introduce the hydrophilicity necessary for water transport. For example, block copolymers have been prepared with hydrophilic, uncharged polyethylene glycol.[20] Such materials might be of use to help separate the effects of water content on transport properties from the effect of charge per se.

Ion-polymer interaction measurements

It is common in the desalination field to describe the sorption of salt in charged polymers through Donnan effects.[14–16,21,22] However, the sorption work in Chapter 6 was not able to demonstrate full compliance Donnan theory under the stated assumptions. Therefore it would be beneficial to the field to perform detailed, systematic salt sorption and salt transport studies on charged and develop fundamental molecular relationships for

these phenomena, and compare these data to existing models of ion-polymer interaction. Such a study could begin by determining the sorption relationships of alkaline metal-chloride salts (again, maintaining chloride as the common anion to isolate the cation effects), where the sorption of several such salt species (e.g., LiCl, KCl, NaCl) are determined as a function of concentration of single-salt solutions, followed by sorption relationships of mixtures of such salts. With a full range of sorption data between pairs of all salt species of interest, correlation of sorption equilibria with ion properties such as electronegativity, solvation thermodynamics, and ionic size, and polymer properties such as dielectric constant, IEC, and water uptake, may be used to derive more thorough models for the sorption of ions in charged polymers. Further studies could be performed using ternary mixtures, or divalent or trivalent cation salts.

REFERENCES

1. W.J. Koros, G.K. Fleming, S.M. Jordan, T.H. Kim, H.H. Hoehn. Polymeric membrane materials for solution-diffusion based permeation separations. *Progress in Polymer Science*. 13 (1988) 339–401.

2. H.B. Park, B.D. Freeman, Z.-B. Zhang, M. Sankir, J.E. McGrath. Highly chlorine-tolerant polymers for desalination. *Angewandte Chemie (International Ed in English)*. 47 (2008) 6019–6024.

3. J. Glater, S.K. Hong, M. Elimelech. The search for a chlorine-resistant reverse osmosis membrane. *Desalination*. 95 (1994) 325–345.

4. R.J. Petersen. Composite reverse osmosis and nanofiltration membranes. *Journal of Membrane Science*. 83 (1993) 81–150.

5. A.E. Allegrezza Jr., B.S. Parekh, P.L. Parise, E.J. Swiniarski, J.L. White. Chlorine resistant polysulfone reverse osmosis modules. *Desalination*. 64 (1987) 285–304.

6. P.L. Parise, A.E. Allegrezza Jr., B.S. Parekh. Reverse osmosis: Chlorine-resistant polysulfone reverse osmosis membrane and module. *Ultrapure Water*. (1987) 54–65.

7. H. Ju, B.D. McCloskey, A.C. Sagle, V. a. Kusuma, B.D. Freeman. Preparation and characterization of crosslinked poly(ethylene glycol) diacrylate hydrogels as fouling-resistant membrane coating materials. *Journal of Membrane Science*. 330 (2009) 180–188.

8. Y.-J. Kim, K.-S. Lee, M.-H. Jeong, J.-S. Lee. Highly chlorine-resistant end-group crosslinked sulfonated-fluorinated poly(arylene ether) for reverse osmosis membrane. *Journal of Membrane Science*. 378 (2011) 512–519.

9. M. Paul, H.B. Park, B.D. Freeman, A. Roy, J.E. McGrath, J.S. Riffle. Synthesis and crosslinking of partially disulfonated poly(arylene ether sulfone) random copolymers as candidates for chlorine resistant reverse osmosis membranes. *Polymer*. 49 (2008) 2243–2252.

10. H. Ju, A.C. Sagle, B.D. Freeman, J.I. Mardel, A.J. Hill. Characterization of sodium chloride and water transport in crosslinked poly(ethylene oxide) hydrogels. *Journal of Membrane Science*. 358 (2010) 131–141.

11. B. Sundell, K.-S. Lee, A. Nebipasagil, A. Shaver, J.R. Cook, E.S. Jang, B.D. Freeman, J.E. McGrath. Crosslinking disulfonated poly(arylene ether sulfone) telechelic oligomers part 1: Synthesis, characterization and membrane preparation. *Industrial and Engineering Chemistry Research*. 53 (2014) 2583–2593

12. M.D. Guiver, S. Croteau, J.D. Hazlett, O. Kutowy. Synthesis and characterization of carboxylated polysulfones. *British Polymer Journal*. 23 (1990) 29–39.

13. H.K. Lonsdale. Donnan-membrane effects in hyperfiltration of ternary systems. *Journal of the Chemical Society, Faraday Transactions 1: Physical Chemistry in Condensed Phases*. 71 (1975) 501–514.

14. F.G. Donnan. The theory of membrane equilibria. *Chemical Reviews*. 1 (1924) 73–90.

15. F.G. Donnan. Theory of membrane equilibria and membrane potentials in the presence of non-dialysing electrolytes. A contribution to physical-chemical physiology. *Journal of Membrane Science*. 100 (1995) 45–55.

16. F. Helfferich. *Ion exchange*. Dover Publications, New York, 1962.

17. W. Harrison, M. Hickner, Y. Kim, J. McGrath. Poly (arylene ether sulfone) copolymers and related systems from disulfonated monomer building blocks: synthesis, characterization, and performance–a topical review. *Fuel Cells*. 5 (2005) 201–212.

18. W.L. Harrison, F. Wang, J.B. Mecham, V.A. Bhanu, M. Hill, Y.S. Kim, J.E. McGrath. Influence of the bisphenol structure on the direct synthesis of sulfonated poly(arylene ether) copolymers. I. *Journal of Polymer Science Part A: Polymer Chemistry*. 41 (2003) 2264–2276.

19. F. Wang, M. Hickner, Y.S. Kim, T.A. Zawodzinski, J.E. McGrath. Direct polymerization of sulfonated poly(arylene ether sulfone) random (statistical) copolymers: candidates for new proton exchange membranes. *Journal of Membrane Science*. 197 (2002) 231–242.

20. N. Tirelli, M.P. Lutolf, A. Napoli, J. Hubbell. Poly(ethylene glycol) block copolymers. *Journal of Biotechnology*. 90 (2002) 3–15.

21. G.M. Geise, L.P. Falcon, B.D. Freeman, D.R. Paul. Sodium chloride sorption in sulfonated polymers for membrane applications. *Journal of Membrane Science*. 423-424 (2012) 195–208.

22. G. Geise, B. Freeman, D. Paul. Comparison of the permeation of $MgCl_2$ versus NaCl in highly-charged sulfonated polymer membranes, in: I.C. Escobar, B. Van der Bruggen (Eds.), *Modern Applications in Membrane Science*. American Chemical Society, 2011: pp. 239–245.

Appendix A. Permeability of Sulfonated Polysulfones with Mixed Monovalent Salt Feeds

Water and ion permeability values were recorded for BPS-32 and BisAS-35 using feed solutions consisting of nominally 34 mM NaCl and increasing concentrations of LiCl, KCl, and CsCl as described in Chapter 3 (with BPS-32 again dried in air at 60 °C for 8 h followed by vacuum drying at 120 °C for 12 h, and BisAS-35 dried in air at 60 °C for 48 h). The NaCl permeability values from these tests are presented in Figure A.1. When lithium chloride is added to the feed, there is very little effect on the NaCl permeability trend. When K^+ is present in the feed, Na^+ permeability increases to a lesser degree than when divalent cations were introduced to the feed; for example, in BPS-32, as the presence of cation charges from added K^+ increases by 7.3 meq/L, P_{Na} increases by a factor of 1.7, while P_{Na} increases by a factor of 2.3 with similar additions of Mg^{++} based on charge concentration. The addition of Cs^+ increases Na^+ permeability similarly to the addition of an equivalent number of cationic charges from Mg^{++}, for example an increase of P_{Na} in BPS-32 by 2 times was observed when 4.5 meq/L of Cs^+ was added to the feed, compared to a 1.8 times increase in P_{Na} with a similar addition of Mg^{++}; however, the effect of Cs^+ on film selectivity is not as great as the effect of Mg^{++}, with water/NaCl permeability selectivity decreasing from 2031 to 1070 with the 4.5 meq/L feed concentration increase of Cs^+, while similar concentrations of Mg^{++} resulted in a much greater selectivity decrease from 2170 to 418. Over the concentration range investigated, the addition of monovalent salts to the feed had little effect on the water permeability (among the monovalent mixed salt tests, only the NaCl/KCl feed test showed a change in water permeability outside the margin of error, with a P_W increase of 9.9% over the concentration range investigated). As shown in Table 6.1, both potassium and cesium have greater affinity for sulfonate ions than magnesium in the Dowex 50 16% DVB

material. It is possible, following the discussion in Chapter 6, that the potassium and cesium ions, being larger than sodium, have less strongly bound hydration shells than sodium, resulting in their higher sulfonate affinity. The evidence presented in Chapter 6 indicates that both ion size and ion charge play a role in the transport properties of cation exchange materials.

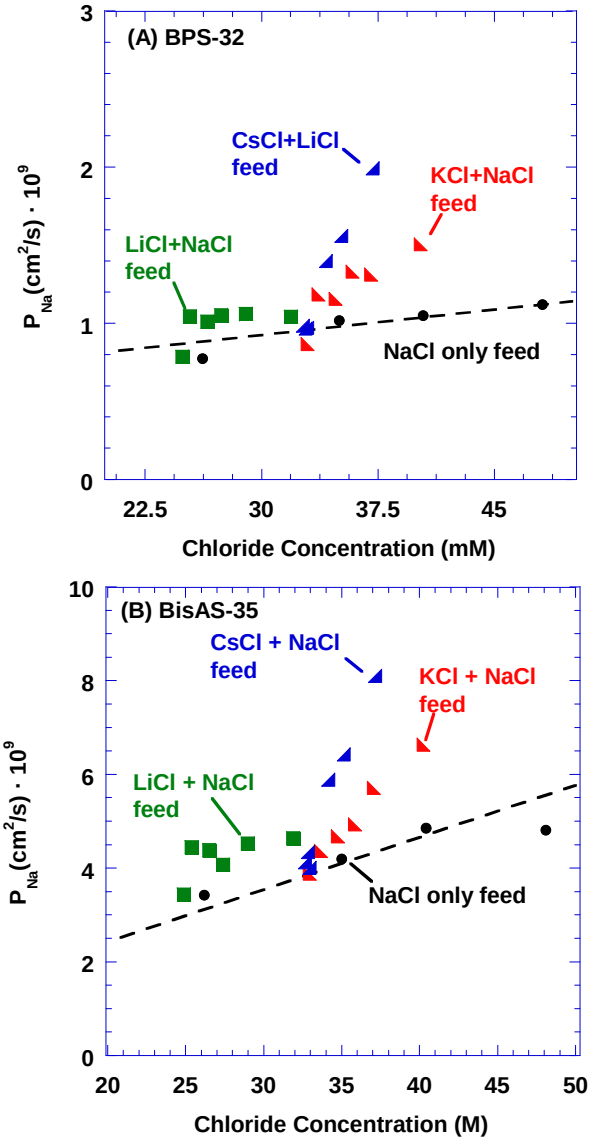

Figure A.1. Sodium chloride permeability in BPS and BisA in mixed ion and NaCl only feeds. (●) = pure NaCl feed, (■) = mixed NaCl/LiCl feed, (◣) = mixed NaCl/KCl feed, (◢) = mixed NaCl/CsCl feed. The first point of each mixed ion feed curve is the permeability value for the initial NaCl only feed.

Appendix B. Comparison of Salt Permeability Values determined by Crossflow and Direct Permeation

EXPERIMENTAL PROCEDURE

In order to compare the values of P_S as determined by crossflow and diffusion cell measurements, samples of BPS-32 were cast into dense films of 25 – 55 micron thickness following the vacuum casting methods described in Chapter 3, with the oven conditions set at 60 °C at partial vacuum (-0.2 barg) for 8 h, followed by 120 °C at full vacuum for 12 h (all other steps are the same as those described in Chapter 3). In order to ensure that the results were as consistent as possible, two sheets of BPS-32 (referred to as Cast A and Cast B) were cast at the same time in the oven. Samples for crossflow testing and direct permeation cell testing were cut from each membrane sheet, and any samples with thickness variations, based on standard deviation of thickness measurements, above 15% were discarded (all crossflow samples from Cast A were found to violate this standard, and are not included).

Salt permeability was determined in diffusion cells at concentrations of 0.034 M (2000 ppm) NaCl as described in Chapter 3 (this method is referred to as the "direct permeation" method below). After this the cells were rinsed with DI water while the samples remained clamped into the cells, and the donor and receiver cells were filled with DI water solutions and monitored for any increase in salt concentration indicating the desorption of mobile salt. If conductivity increases in the donor or receiver solutions were detected, the cells were rinsed, and this process was repeated until solution conductivity increases were not detected. Then the salt permeability measurements were performed on the polymer samples at a donor cell concentration of 1 M NaCl.

In order to determine if any conductivity rise in the lower concentration 0.034 M direct permeation tests were due to absorption of atmospheric CO_2 into the receiver cell solution, direct permeation tests on fresh samples cut from Cast A and Cast B films were performed using donor cell solutions of 0.034 M (2000 ppm) NaCl and receiver cell solutions of DI water that had been equilibrated in air. These receiver cell solutions were prepared from DI water poured into clean glass Erlenmeyer flasks, covered with Kimwipes to prevent dust contamination but allow air flow, and stirred at ambient conditions for 3 days.

Crossflow measurements of permeability were carried out a feed pressure of 800 psig in order to overcome the high osmotic pressure difference in the one 1 M NaCl test (around 35 bar, or 500 psi, depending on the salt rejection of the material). Crossflow permeability was determined first at 0.034 M (2000 ppm) NaCl, then NaCl was added to the feed to increase the concentration 1 M. The crossflow testing was allowed to come to steady state and the feed permeate samples were collected at each concentration as described in Chapter 3. Salt concentration of the feed and permeate samples were determined by ion chromatography as described in Chapter 3.

RESULTS.

The values of salt permeability for each sample tested are listed in Table 1, with each row indicating a discrete sample. Overall, the values of the Cast A and Cast B samples, where both are available, are within the same range. As discussed in Chapter 4, these polymers are glassy non-equilibrium materials and are sensitive to processing history; this may contribute to the variation seen in salt permeability in Table 1, where values can be observed to change by as much as a factor of 3 within the same material (this was part of the motivation for performing mixed ion permeability tests of varying

feed compositions on the same samples in series in Chapter 5). However, a complete understanding of the wide scatter in the data was never obtained in this work. The average values of each set of tests shown in Table B.1 and their standard deviations are displayed in Figure B.1. The P_S values determined in the 0.034 M NaCl diffusion cell tests with donor solutions that were equilibrated in air are nearly identical to those of the 0.034 M NaCl diffusion cell tests using DI water as the donor solution, indicating that, at these conditions, the measured values of salt permeability do not depend on whether or not the donor cell solution was equilibrated in air. This result may suggest a limited influence of atmospheric CO_2 on the results. However, no control was performed on solutions that were rigorously CO_2-free, so a complete answer to whether CO_2 influences the results and, if so, to what extent, is not known. There is generally good agreement between the salt permeabilities reported by crossflow tests and diffusion cell tests at 1M where the error bars overlap, though at the concentration of 0.034 molar the crossflow permeabilities are slightly lower than the diffusion cell permeabilities; a greater number of samples for each test may better indicate the degree of change in salt permeability between samples. Future testing on a large sample size of equilibrium-state materials between the two testing methods would be valuable in determining more accurately any discrepancies between the two testing methods.

Sample Set	Thickness (μm)	P_S (cm^2/s) 10^9 At 0.034 M	P_S (cm^2/s) 10^9 At 1 M
Crossflow testing at 800 psig			
Cast A	43 ± 5%	0.37	6.4
	41 ± 12%	0.43	7.8
Diffusion cell testing, DI water in the donor cell			
Cast A	25 ± 3%	0.46	4.0
	55 ± 2%	1.2	6.6
	52 ± 2%		7.3
Cast B	41 ± 3%	0.72	5.0
	27 ± 11%	0.71	6.6
	30 ± 6%		5.7
Diffusion cell testing, Air-equilibrated water in the donor cell			
Cast A	46 ± 7%	0.46	
	46 ± 2%	1.12	
	21 ± 10%	0.51	
Cast B	36 ± 2%	0.71	
	31 ± 6%	0.83	
	43 ± 2%	0.94	

Table B.1. Thicknesses and salt permeabilities of BPS-32 samples. Each line represents one sample.

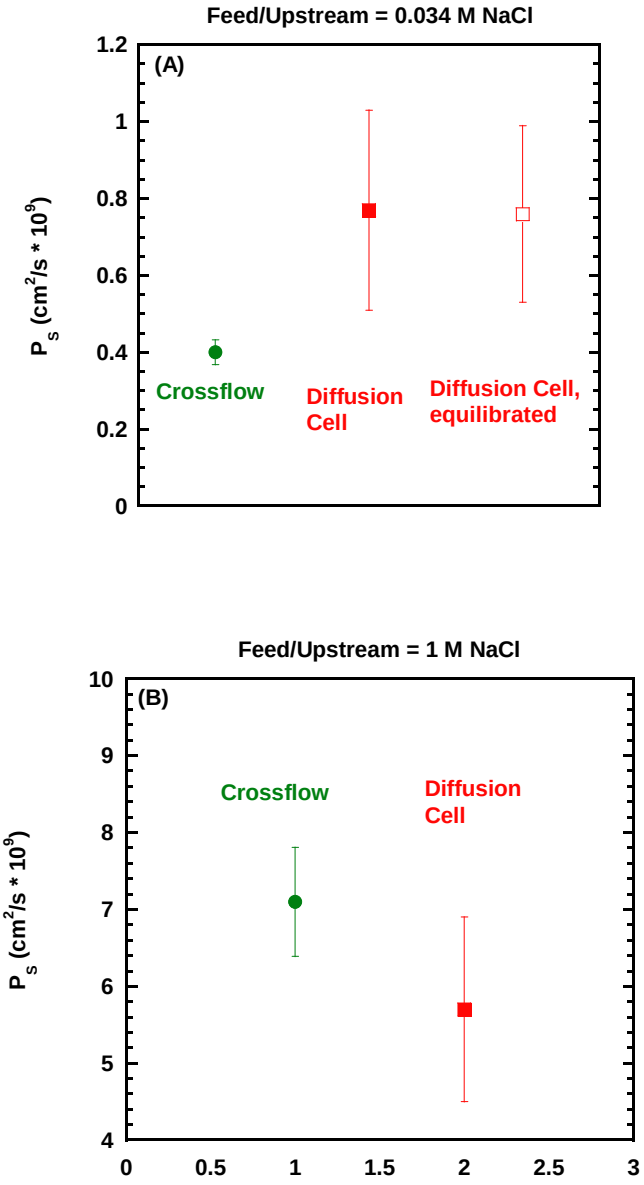

Figure B.1. Average values of crossflow and diffusion cell tests of BPS-32 at (A) 0.034 M NaCl and (B) 1 M NaCl.

Bibliography

Agarwal, A.K., R.Y.M. Huang. Studies on the enhancement of separation characteristics of sulfonated poly(phenylene oxide)/polysulfone thin film composite membranes for reverse osmosis applications. I. Effect of chemical treatment. *Die Angewandte Makromolekulare Chemie*. 163 (1988) 1–13.

Agarwal, A.K., R.Y.M. Huang. Studies on the enhancement of separation characteristics of sulfonated poly(phenylene oxide)/polysulfone thin film composite membranes for reverse osmosis applications II. Effects of nitromethane and the chemical treatment combined with gamma-ray irradia. *Die Angewandte Makromolekulare Chemie*. 163 (1988) 15–21.

Allegrezza Jr., A.E., B.S. Parekh, P.L. Parise, E.J. Swiniarski, J.L. White. Chlorine resistant polysulfone reverse osmosis modules. *Desalination*. 64 (1987) 285–304.

Analysis of water from four wells at the Brackish Groundwater National Desalination Research Facility. Tetra Tech, Inc. for the Bureau of Reclamation, Alamogordo, Contract No. R10PC40009, 2011.

Bajpai, S.K., S. Sharma. Investigation of swelling/degradation behaviour of alginate beads crosslinked with Ca^{2+} and Ba^{2+} ions. *Reactive and Functional Polymers*. 59 (2004) 129–140.

Baker, R. *Membrane technology and applications*. 1st ed. John Wiley & Sons, 1995.

Bonner, O.D. A selectivity scale for some monovalent cations on Dowex 50. *The Journal of Physical Chemistry*. 58 (1954) 318–320.

Bonner, O.D. Ion-exchange equilibria involving rubidium, cesium and thallous ions. *The Journal of Physical Chemistry*. 59 (1955) 719–721.

Bonner, O.D., F.L. Livingston. Cation-exchange equilibria involving some divalent ions. *The Journal of Physical Chemistry*. 60 (1956) 530–532.

Bonner, O.D., L.L. Smith. A selectivity scale for some divalent cations on Dowex 50. *The Journal of Physical Chemistry*. 61 (1957) 326–329.

Bonner, O.D., V. Rhett. Equilibrium studies of the silver-sodium-hydrogen system on Dowex 50. *The Journal of Physical Chemistry*. 57 (1953) 254–256.

Bonner, O.D., W.H. Payne. Equilibrium studies of some monovalent ions on Dowex 50. *The Journal of Physical Chemistry*. 58 (1954) 183–185.

Bontha, J.R., P.N. Pintauro. Water orientation and ion solvation effects during multicomponent salt partitioning in a Nafion cation exchange membrane. *Chemical Engineering Science*. 49 (1994)

3835–3851.

Borsani, R., S. Rebagliati. Fundamentals and costing of MSF desalination plants and comparison with other technologies. *Desalination*. 182 (2005) 29–37.

Brousse, C., R. Chapurlat, J.P. Quentin. New membranes for reverse osmosis I. Characteristics of the base polymer: sulphonated polysulphones. *Desalination*. 18 (1976) 137–153.

Burbano, A. The state of full-scale RO/NF desalination: Results from a worldwide survey. *Journal - American Waterworks Association*. 99 (2007) 116.

Cadotte, J.E. Interfacially synthesized reverse osmosis membrane. U.S. Patent Number 4,277,344. 1981.

Cai, X. Water stress, water transfer and social equity in northern China—implications for policy reforms. *Journal of Environmental Management*. 87 (2008) 14–25.

Chludzinski, P., J.F. Austin, J. Enos. Development of polyphenylene oxide membranes. *Office of Saline Water Research and Development Progress Report No 697*. (1971).

Coulter, L. V. The thermochemistry of the alkali and alkaline earth metals and halides in liquid ammonia at -33C. *The Journal of Physical Chemistry*. 57 (1953) 553–558.

Donnan, F.G. The theory of membrane equilibria. *Chemical Reviews*. 1 (1924) 73–90.

Donnan, F.G. Theory of membrane equilibria and membrane potentials in the presence of non-dialysing electrolytes. A contribution to physical-chemical physiology. *Journal of Membrane Science*. 100 (1995) 45–55.

E. Long, T., Y. Li, F. Wang, J. Yang, D. Liu, A. Roy, S. Case, J. Lesko, J.E. McGrath. Synthesis and characterization of controlled molecular weight disulfonated poly(arylene ether sulfone) copolymers and their applications to proton exchange membranes. *Polymer*. 47 (2006) 4210–4217.

Flory, P. Thermodynamics of high polymer solutions. *The Journal of Chemical Physics*. 9 (1941) 660.

Franklin, K.R., R.P. Townsend. Multicomponent ion exchange in zeolites. *Journal of the Chemical Society, Faraday Transactions 1: Physical Chemistry in Condensed Phases*. 81 (1985) 1071–1086.

Freeman, B.D. Osmosis, in: *Encyclopedia of Applied Polymer Physics*. 1995: pp. 59–71.

Friedrich, C., A. Driancourt, C. Noel, L. Monnerie. Asymmetric reverse osmosis and ultrafiltration membranes prepared from sulfonated polysulfone. *Desalination*. 36 (1981) 39–62.

Fritzmann, C., J. Löwenberg, T. Wintgens, T. Melin. State-of-the-art of reverse osmosis

desalination. *Desalination*. 216 (2007) 1–76.

Frommer, M.A., J.S. Murday, R.M. Messalem. Solubility and diffusivity of water and of salts in an aromatic polyamide film. *European Polymer Journal*. 9 (1973) 367–373.

Fuoss, R.M. Ionic association. III. The equilibrium between ion pairs and free ions. *Journal of the American Chemical Society*. 80 (1958) 5059–5061.

Fuoss, R.M., C.A. Kraus. Properties of electrolytic solutions. III. The dissociation constant. *Journal of the American Chemical Society*. 55 (1933) 1019–1028.

Geise, G., B. Freeman, D. Paul. Comparison of the permeation of $MgCl_2$ versus NaCl in highly-charged sulfonated polymer membranes, in: Escobar, I.C., B. Van der Bruggen (Eds.), *Modern Applications in Membrane Science*. American Chemical Society, 2011: pp. 239–245.

Geise, G., C. Willis, C. Doherty, A.J. Hill, T.J. Bastow, J. Ford, K.I. Winey, B.D. Freeman, D.R. Paul. Characterization of aluminum-neutralized sulfonated styrenic pentablock copolymer films. *Industrial & Engineering Chemistry Research*. 52 (2012) 1056–1068.

Geise, G.M., B.D. Freeman, D.R. Paul. Characterization of a sulfonated pentablock copolymer for desalination applications. *Polymer*. 51 (2010) 5815–5822.

Geise, G.M., B.D. Freeman, D.R. Paul. Sodium chloride diffusion in sulfonated polymers for membrane applications. *Journal of Membrane Science*. 427 (2013) 186–196.

Geise, G.M., D.R. Paul, B.D. Freeman. Fundamental water and salt transport properties of polymeric materials. *Progress in Polymer Science*. 39 (2014) 1–42.

Geise, G.M., H.B. Park, A.C. Sagle, B.D. Freeman, J.E. McGrath. Water permeability and water/salt selectivity tradeoff in polymers for desalination. *Journal of Membrane Science*. 369 (2011) 130–138.

Geise, G.M., H.-S. Lee, D.J. Miller, B.D. Freeman, J.E. McGrath, D.R. Paul. Water purification by membranes: the role of polymer science. *Journal of Polymer Science Part B: Polymer Physics*. 48 (2010) 1685–1718.

Geise, G.M., L.P. Falcon, B.D. Freeman, D.R. Paul. Sodium chloride sorption in sulfonated polymers for membrane applications. *Journal of Membrane Science*. 423-424 (2012) 195–208.

Gill, J.B. Solute-solute interaction in liquid ammonia solutions: A vibrational spectroscopic view. *Pure and Applied Chemistry*. 53 (1981) 1365–1381.

Glater, J., S.K. Hong, M. Elimelech. The search for a chlorine-resistant reverse osmosis membrane. *Desalination*. 95 (1994) 325–345.

Glueckauf, E. A new approach to ion exchange polymers. *Proceedings of the Royal Society A: Mathematical, Physical and Engineering Sciences*. 268 (1962) 350–370.

Graefe, A.F., C.W. Saltonstall, W.J. Schell. Process for the preparation of a stable salt form of a sulfonated polyarylether sulfone. U.S. Patent Number 3,875,096. 1975.

Greenlee, L.F., D.F. Lawler, B.D. Freeman, B. Marrot, P. Moulin. Reverse osmosis desalination: water sources, technology, and today's challenges. *Water Research*. 43 (2009) 2317–48.

Guiver, M.D., S. Croteau, J.D. Hazlett, O. Kutowy. Synthesis and characterization of carboxylated polysulfones. *British Polymer Journal*. 23 (1990) 29–39.

Hamza, A., G. Chowdhury, T. Matsuura, S. Sourirajan. Sulphonated poly(2,6-dimethyl-1,4-phenylene oxide)-polyethersulphone composite membranes. Effects of composition of solvent system, used for preparing casting solution, on membrane-surface structure and reverse-osmosis performance. *Journal of Membrane Science*. 129 (1997) 55–64.

Harrison, W., M. Hickner, Y. Kim, J. McGrath. Poly (arylene ether sulfone) copolymers and related systems from disulfonated monomer building blocks: synthesis, characterization, and performance–a topical review. *Fuel Cells*. 5 (2005) 201–212.

Harrison, W.L., F. Wang, J.B. Mecham, V.A. Bhanu, M. Hill, Y.S. Kim, J.E. McGrath. Influence of the bisphenol structure on the direct synthesis of sulfonated poly(arylene ether) copolymers. I. *Journal of Polymer Science Part A: Polymer Chemistry*. 41 (2003) 2264–2276.

Helfferich, F. *Ion exchange*. Dover Publications, New York, 1962.

Hickner, M.A., H. Ghassemi, Y.S. Kim, B.R. Einsla, J.E. McGrath. Alternative polymer systems for proton exchange membranes (PEMs). *Chemical Reviews*. 104 (2004) 4587–4612.

Higa, M., A. Kira, A. Tanioka, K. Miyasaka. Ionic partition equilibrium in a charged membrane immersed in a mixed ionic solution. *Journal of the Chemical Society, Faraday Transactions*. 89 (1993) 3433–3435.

Huggins, M.L. Solutions of long chain compounds. *The Journal of Chemical Physics*. 9 (1941) 440.

Ikeda, K., T. Nakano, H. Ito, T. Kubota, S. Yamamoto. New composite charged reverse osmosis membrane. *Desalination*. 68 (1988) 109–119.

Inui, K., T. Noguchi, T. Miyata, T. Uragami. Pervaporation characteristics of methyl methacrylate – methacrylic acid copolymer membranes ionically crosslinked with metal ions for a benzene / cyclohexane mixture. *Journal of Applied Polymer Science*. 71 (1998) 233–241.

Irish, D.E. Interactions in aqueous alkali metal nitrate solutions. *Canadian Journal of Chemistry*. 46

(1968) 943–951.

Ju, H., A.C. Sagle, B.D. Freeman, J.I. Mardel, A.J. Hill. Characterization of sodium chloride and water transport in crosslinked poly(ethylene oxide) hydrogels. *Journal of Membrane Science*. 358 (2010) 131–141.

Ju, H., B.D. McCloskey, A.C. Sagle, V. a. Kusuma, B.D. Freeman. Preparation and characterization of crosslinked poly(ethylene glycol) diacrylate hydrogels as fouling-resistant membrane coating materials. *Journal of Membrane Science*. 330 (2009) 180–188.

Kim, K.-J., G. Chowdhury, T. Matsuura. Low pressure reverse osmosis performances of sulfonated poly(2,6-dimethyl-1,4-phenylene oxide) thin film composite membranes: effect of coating conditions and molecular weight of polymer. *Journal of Membrane Science*. 179 (2000) 43–52.

Kim, Y.-J., K.-S. Lee, M.-H. Jeong, J.-S. Lee. Highly chlorine-resistant end-group crosslinked sulfonated-fluorinated poly(arylene ether) for reverse osmosis membrane. *Journal of Membrane Science*. 378 (2011) 512–519.

Kim, Y.S., F. Wang, M. Hickner, S. McCartney, Y.T. Hong, W. Harrison, T.A. Zawodzinski, J.E. Mcgrath. Effect of acidification treatment and morphological stability of sulfonated poly(arylene ether sulfone) copolymer proton-exchange membranes for fuel-cell use above 100 °C. *Journal of Polymer Science Part B: Polymer Physics*. 41 (2003) 2816–2828.

Kimura, S.G. Reverse osmosis performance of sulfonated poly(2,6-dimethylphenylene ether) ion exchange membranes. *Industrial & Engineering Chemistry Product Research and Development*. 10 (1971) 335–339.

Koros, W.J., G.K. Fleming, S.M. Jordan, T.H. Kim, H.H. Hoehn. Polymeric membrane materials for solution-diffusion based permeation separations. *Progress in Polymer Science*. 13 (1988) 339–401.

Kosmala, B., J. Schauer. Ion-exchange membranes prepared by blending sulfonated poly(2,6-dimethyl-1,4-phenylene oxide) with polybenzimidazole. *Journal of Applied Polymer Science*. 85 (2002) 1118–1127.

Lee, C.H., D. VanHouten, O. Lane, J.E. McGrath, J. Hou, L.A. Madsen, J. Spano, S. Wi, J. Cook, W. Xie, H.J. Oh, G.M. Geise, B.D. Freeman. Disulfonated poly(arylene ether sulfone) random copolymer blends tuned for rapid water permeation via cation complexation with poly(ethylene glycol) oligomers. *Chemistry of Materials*. 23 (2011) 1039–1049.

Lee, K.P., T.C. Arnot, D. Mattia. A review of reverse osmosis membrane materials for desalination—Development to date and future potential. *Journal of Membrane Science*. 370 (2011) 1–22.

Lee, S.-T., F.-L. Mi, Y.-J. Shen, S.-S. Shyu. Equilibrium and kinetic studies of copper(II) ion uptake

by chitosan-tripolyphosphate chelating resin. *Polymer*. 42 (2001) 1879–1892.

Li, D., H. Wang. Recent developments in reverse osmosis desalination membranes. *Journal of Materials Chemistry*. 20 (2010) 4551–4566.

Lide, D.R., ed. *The CRC Handbook of Chemistry and Physics*. 85th ed. CRC Press, Boca Raton, 2004.

Lonsdale, H.K. Donnan-membrane effects in hyperfiltration of ternary systems. *Journal of the Chemical Society, Faraday Transactions 1: Physical Chemistry in Condensed Phases*. 71 (1975) 501–514.

Lonsdale, H.K., U. Merten, R.L. Riley. Transport properties of cellulose acetate osmotic membranes. *Journal of Applied Polymer Science*. 9 (1965) 1341–1362.

Merten, U., ed. *Desalination by Reverse Osmosis*. MIT Press, Cambridge, Massachusetts, 1966.

Mukherjee, P., A.K. Sengupta. Ion exchange selectivity as a surrogate indicator of relative permeability of ions in reverse osmosis processes. *Environmental Science & Technology*. 37 (2003) 1432–1440.

Noshay, A., L. Robeson. Sulfonated polysulfone. *Journal of Applied Polymer Science*. 20 (1976) 1885–1903.

Nunes, S.P., K. V. Peinemann, eds. *Membrane Technology in the Chemical Industry.* Wiley-VCH, Weinheim, 2006.

Padaki, M., A.M. Isloor, P. Wanichapichart, A.F. Ismail. Preparation and characterization of sulfonated polysulfone and N-phthloyl chitosan blend composite cation-exchange membrane for desalination. *Desalination*. 298 (2012) 42–48.

Parise, P.L., A.E. Allegrezza Jr., B.S. Parekh. Reverse osmosis: Chlorine-resistant polysulfone reverse osmosis membrane and module. *Ultrapure Water*. (1987) 54–65.

Park, C.K., B. Oh, M.J. Choi, Y.M. Lee. Separation of benzene/cyclohexane by pervaporation through chelate poly(vinyl alcohol)/poly(allyl amine) blend membrane. *Polymer Bulletin*. 598 (1994) 591–598.

Park, H.B., B.D. Freeman, Z.-B. Zhang, M. Sankir, J.E. McGrath. Highly chlorine-tolerant polymers for desalination. *Angewandte Chemie (International Ed in English)*. 47 (2008) 6019–6024.

Passaniti, L.K.R. *Solubility measurements in partially disulfonated poly (arylene ether sulfone) for reverse osmosis water purification applications*. M.S. Thesis, The University of Texas, Austin, TX, 2010.

Paul, D.R. Reformulation of the solution-diffusion theory of reverse osmosis. *Journal of Membrane Science*. 241 (2004) 371–386.

Paul, D.R. Relation between hydraulic permeability and diffusion in homogeneous swollen membranes. *Journal of Polymer Science Part B: Polymer Physics*. 11 (1973) 289–296.

Paul, M., H.B. Park, B.D. Freeman, A. Roy, J.E. McGrath, J.S. Riffle. Synthesis and crosslinking of partially disulfonated poly(arylene ether sulfone) random copolymers as candidates for chlorine resistant reverse osmosis membranes. *Polymer*. 49 (2008) 2243–2252.

Petersen, R.J. Composite reverse osmosis and nanofiltration membranes. *Journal of Membrane Science*. 83 (1993) 81–150.

Pintauro, P.N., R. Tandon, L. Chao, W. Xu, R. Evilia. Equilbrium partitioning of monovalent/divalent cation-salt mixtures in Nafion cation-exchange membranes. *Journal of Physical Chemistry*. 99 (1995) 12915–12924.

Pitzer, K.S., J.J. Kim. Thermodynamics of electrolytes. IV. Activity and osmotic coefficients for mixed electrolytes. *Journal of the American Chemical Society*. 1426 (1974) 5701–5707.

Plummer, C., G. Kimura, A. LaConti. *Office of Saline Water Research and Development Progress Report No. 551*. 1970.

Pusch, W. Measurement techniques of transport through membranes. *Desalination*. 59 (1986) 105–198.

Pushpa, K.K., D. Nandan, R.M. Iyer. Thermodynamics of water sorption by perfluorosulphonate (Nafion-117) and polystyrene-divinylbenzene sulphonate (Dowex 50W) ion-exchange resins at 298±1 K. *Journal of the Chemical Society, Faraday Transactions 1: Physical Chemistry in Condensed Phases*. 84 (1988) 2047–2056.

Quentin, J. Sulfonated polyarylethersulfones. U.S. Patent Number 3,709,841. 1973.

Rees, R.W. Ionic Hydrocarbon Polymers. U.S. Patent Number 3,264,272. 1966.

Sagle, A.C., H. Ju, B.D. Freeman, M.M. Sharma. PEG-based hydrogel membrane coatings. *Polymer*. 50 (2009) 756–766.

Service, R.F. Desalination freshens up. *Science*. 313 (2006) 1099–1090.

Shih, W.-Y., A. Rahardianto, R.-W. Lee, Y. Cohen. Morphometric characterization of calcium sulfate dihydrate (gypsum) scale on reverse osmosis membranes. *Journal of Membrane Science*. 252 (2005) 253–263.

Sundell, B., K.-S. Lee, A. Nebipasagil, A. Shaver, J.R. Cook, E.S. Jang, B.D. Freeman, J.E.

McGrath. Crosslinking disulfonated poly(arylene ether sulfone) telechelic oligomers part 1: Synthesis, characterization and membrane preparation. *Industrial and Engineering Chemistry Research*. 53 (2014) 2583–2593.

Tandon, R., P.N. Pintauro. Divalent / monovalent cation uptake selectivity in a Nation cation-exchange membrane: Experimental and modeling studies. *Journal of Membrane Science*. 136 (1997) 207–219.

Tirelli, N., M.P. Lutolf, A. Napoli, J. Hubbell. Poly(ethylene glycol) block copolymers. *Journal of Biotechnology*. 90 (2002) 3–15.

Turekian, K.K. *Oceans*. First Ed. Prentice Hall, Englewood Cliffs, 1968.

Van Wagner, E.M., A.C. Sagle, M.M. Sharma, B.D. Freeman. Effect of crossflow testing conditions, including feed pH and continuous feed filtration, on commercial reverse osmosis membrane performance. *Journal of Membrane Science*. 345 (2009) 97–109.

Wang, F., M. Hickner, Y.S. Kim, T.A. Zawodzinski, J.E. McGrath. Direct polymerization of sulfonated poly(arylene ether sulfone) random (statistical) copolymers: candidates for new proton exchange membranes. *Journal of Membrane Science*. 197 (2002) 231–242.

Watkins, K., L. Carvajal, D. Coppard, R. Fuentes. *Human development report 2006*. Prepared for the United Nations Development Programme, New York, 2006.

Wijmans, J.G., R.W. Baker. The solution-diffusion model: a review. *Journal of Membrane Science*. 107 (1995) 1–21.

Xie, W., G.M. Geise, B.D. Freeman, C.H. Lee, J.E. McGrath. Influence of processing history on water and salt transport properties of disulfonated polysulfone random copolymers. *Polymer*. 53 (2012) 1581–1592.

Xie, W., G.M. Geise, B.D. Freeman, H.-S. Lee, G. Byun, J.E. McGrath. Polyamide interfacial composite membranes prepared from m-phenylene diamine, trimesoyl chloride and a new disulfonated diamine. *Journal of Membrane Science*. 403-404 (2012) 152–161.

Xie, W., H. Ju, G.M. Geise, B.D. Freeman, J.I. Mardel, A.J. Hill, J.E. McGrath. Effect of free volume on water and salt transport properties in directly copolymerized disulfonated poly(arylene ether sulfone) random copolymers. *Macromolecules*. 44 (2011) 4428–4438.

Xie, W., J. Cook, H.B. Park, B.D. Freeman, C.H. Lee, J.E. McGrath. Fundamental salt and water transport properties in directly copolymerized disulfonated poly(arylene ether sulfone) random copolymers. *Polymer*. 52 (2011) 2032–2043.

Yasuda, H., C.E. Lamaze, A. Peterlin. Diffusive and hydraulic permeabilities of water in water-swollen polymer membranes. *Journal of Polymer Science Part A: Polymer Chemistry*. 9 (1971)

1117–1131.

Yasuda, H., C.E. Lamaze, L.D. Ikenberry. Permeability of solutes through hydrated polymer membranes, Part 1. Diffusion of sodium chloride. *Die Makromolekulare Chemie*. 118 (1968) 19–35.

Zawodzinski, T.A., T.E. Springer, J. Davey, R. Jestel, C. Lopez, J. Valerio, S. Gottesfeld. A comparative study of water uptake by and transport through ionomeric fuel cell membranes. *Journal of The Electrochemical Society*. 140 (1993) 1981.

Vita

Joseph Cook graduated from Ruston High School in May 2003 in Ruston, Louisiana, and earned his Eagle Scout rank that same year with BSA Troop 45. He then attended Louisiana Tech University, where he earned a B.S. in Chemical Engineering in August of 2007. After completing his undergraduate work, he joined the Chemical Engineering Ph.D. program at the University of Texas in Austin, Texas. Upon completion of this degree he will begin a position in the Process Development Center at Albemarle Corporation in Baton Rouge, Louisiana.

Permanent email: jcook@utexas.edu

This dissertation was typed by the author.